Title
Mechanoresponsive Mechanisms In Hypertrophic Cardiac Remodeling

Author
Kimball, Todd Haswell

Publication Date
2023

Peer reviewed|Thesis/dissertation

UNIVERSITY OF CALIFORINA

Los Angeles

Mechanoresponsive Mechanisms In Hypertrophic Cardiac Remodeling

A dissertation submitted in partial satisfaction of the requirements for the degree Doctor of Philosophy in Molecular, Cellular, and Integrative Physiology

by

Todd Haswell Kimball

2023

ABSTRACT OF THE DISSERTATION

Mechanoresponsive Mechanisms

In Hypertrophic Remodeling

by

Todd Haswell Kimball

Molecular, Cellular, and Integrative Physiology

University of California, Los Angeles, 2023

Professor Thomas M. Vondriska, Chair

All cells of the body are under some form of mechanical load and these forces are part of the factors defining cell type specificity. The mechanical environment influences cellular behavior and is the basis of mechanobiology. The forces acting on cells must be met with a cellular response, as the input signals are transduced to molecular mechanisms that drive gene regulation. In the heart, the distinct roles of cardiomyocytes and fibroblasts, as fibroblasts enforce tissue stiffness homeostasis through extracellular matrix maintenance and cardiomyocyte contraction-relaxation cycles work against this stiffness with every heartbeat, enable each to respond to cardiac stressors through differential gene expression, changing their cellular physical phenotype. At the cellular level, cardiac hypertrophy is a growth of the cardiomyocyte (without proliferation) and increased interstitial fibrosis, and these phenotypes are the result of changes to gene expression. While the gene expression program induced by cardiac hypertrophy is well documented, this dissertation unravels mechanosensitive mechanisms activated by changes to

the myocardial environment and cellular forces driving dysfunctional gene regulation perpetuating cardiac disease.

Gene translation ends in the nucleus; however, it does not always start there. We viewed gene expression as an end point, being influenced by a number of factors outside the nucleus, including metabolism, nucleoskeletal, cytoskeletal, sarcomere organization, sarcolemmal signal transduction pathways, and the tissue environment. In examining transcriptional influence outside the nucleus, we first summarize the bidirectional effect of metabolic and gene regulation dysfunction in heart disease, as metabolic substrates and intermediates impact cardiac epigenetics and chromatin stores information. We report our findings from our pressure overload induced cardiac hypertrophy studies, demonstrating cardiomyocyte cellular remodeling influences nucleoskeletal ultrastructure through the expression of the structural and chromatin binding protein Lamin A/C. We phenotypically characterize an α_1-adrenergic model of cardiac hypertrophy and investigate cell specific mechanism driving tissue remodeling and cellular mechanosensitive pathways underlying pathological stress. Through these studies, we explore the cardiac stressors that remodel the heart tissue during hypertrophy and the cellular mechanisms altering the cellular phenotype through gene regulation.

The dissertation of Todd Haswell Kimball is approved.

Amy Rowat

Tzung Hsiai

Matthew Fischer

Thomas M. Vondriska, Committee Chair

University of California, Los Angeles

2023

TABLE OF CONTENTS

LIST OF FIGURES

LIST OF TABLES

ACKNOWLEDGEMENTS

From what I understand of it, I subscribe to the idea of chaos theory. I do understand the steps that brought me to Los Angeles and UCLA, but of all the labs I could have been hired in, some divine mathematical model landed me with Dr. Thomas Vondriska. We understood each other before I understood what research science was. Over the last decade (plus) he has been there as my mentor, driving me to be a better scientist while allowing me to find my own way in science. I am truly grateful for his guidance and friendship. His dedication to the lab environment, always getting our thoughts on potential new additions and finding the right individuals who are not only extremely talented and thoughtful scientists, but, more importantly, warm and kind and absolute delights as people. It has been a village of individuals who have helped me become the scientist I am today, and I am thankful Tom continues to be mindful of all of us personally, while guiding us to make discoveries we find interesting and important.

Speaking of a village, I am eternally grateful for all the Vondriska lab members, past and present, have all had a hand in our success, and I'd like to thank them all. Dr. Sarah Franklin showed me what research science meant and the dedication required to excel. I will never forget the day the mice we worked on for months showed a phenotype, all the time and troubleshooting to get the conditions right, and when they were, the joy on her face showed me what we were working towards. Dr. Sherise Mitchell-Jorden was stoic, helpful, and wanted no BS, Dr. Michelle Parvatiyar was a glimpse of Ohio representation and kindness, and Dr. Haodong Chen, whose kindness and dedication were inspiring, were all welcoming and helpful to a young research technician learning the ropes. To Dr. Emma Monte, who pushed me to go to graduate school and provided a foil to my unrepentant nonsense. To Dr. Elaheh Karbassi, Dr. Rachel Lopez, Dr. Shanxi Jiang, Mr. Max Cabaj, Ms. Elizabeth Soehalim, and Ms. Ashley Zhu, who made coming to work every day an absolute joy. To Dr. Yixin Ruan, who cannot support for a winning NBA team, no matter how many he tries to root for, I hope our paths cross soon. To the undergraduates who

helped me struggle with being a mentor, that I am not sure if they enjoyed research science, but knew they enjoyed the lab, Mr. Brandon Ho, Ms. Anna Reese, Ms. Lesley Munoz Velazquez, and Ms. Ashley Agubata, I hope you all find your success. Thank you to Dr. Matt Fischer for all his support and kindness as we have worked on projects over the years. My fellow graduate students, Ms. Tanya Gromova and Ms. Natalie Gehred, I think the world of you two and am so thankful we have been on this road together. To Dr. Shuaishuai Hu whose dedication has been a driving force for the lab. To Dr. Adrian Arrieta for his unwavering support and guidance, no matter how small the issue, and for pushing everyone in the lab towards the details before the story. A big thank you to Dr. Douglas Chapski who has helped me in so many ways, you've kept me up to date on World Wars and historical biographies, and contributed so much to me as a scientist and friend. Finally, thank you to Dr. Manuel Rosa-Garrido, my brother from across the sea, you have taught me so much in science, and showed me that my voice in science is valuable, personalities drive culture and science, and to never shy away from that.

I would like to thank my dissertation committee for their guidance and advice: Dr. Amy Rowat, Dr. Tzung Hsiai, Dr. Matthew Fischer, and Dr. Reza Ardehalli. They were there to help me, and I am grateful for their feedback. I hope to continue successful collaborations with our labs.

I'm grateful for the Molecular, Cellular, and Integrative Physiology program and specifically for Dr. Mark Frye and Ms. Yesenia Rayos. I would also like to thank Dr. Rachelle Crosbie for her support over my career and to Dr. Stephanie White, who mentored me during my masters program, taking a fledgling scientist and helping find my voice.

I want to thank the American Heart Association for funding my project by awarding me the Predoctoral Fellowship. I would like to thank the National Institutes of Health and the David Geffen School of Medicine at UCLA for their support to the Vondriska lab.

I am so grateful to have a supportive family. To my mom and dad, who always saw potential in me and pushed me towards it. I know being so far from home is hard, but the distance disappears when I think about your love. To my brother Greg and his growing family, I do not want to write something nice about Greg to ruin the façade we have built, but Thank you, Brother! To my sister Sarah and her family, I am so thankful for your love and support.

I came to Los Angeles because the love of my life was here pursuing her dreams and we have been on this journey together. Blaire, my love, thank you for your patience and kindness and decision making. I would not be in this position if it was not for you, and seeing your growth as an individual and your career have been a true testament to dedication and adaptability. And to our little baby Niko, may she learn to love unconditionally as you do, and I am excited to witness her growth and our growth as a family. May we bloom together.

BIOGRAPHICAL SKETCH

Education

PhD in Molecular, Cellular & Integrative Physiology — Expected Spring 2023
University of California, Los Angeles

Master of Science in Integrative Biology and Physiology — Fall 2018
University of California, Los Angeles

Bachelor of Art in Molecular Biology and Biochemistry — Summer 2006
Wittenberg University

Employment

Clinical Laboratory Technician — 2006-2010
University of Kentucky, Clinical Microbiology Lab

Research Technician — 2010-2016
University of California, Los Angeles

Teaching

University of California, Los Angeles

PS121: Disease Mechanisms and Therapies	Fall 2016, 2017
PS121: Classroom Data Analysis	Winter 2017
PS175: Why Fido Can't Speak: Biological Evolution of Language	Spring 2017, 2018
LS3: Introduction to Molecular Biology	Winter 2018
Summer Institute on Scientific Teaching	Summer 2017
Summer Institute on Scientific Teaching – Facilitator	Summer 2019
Teaching Assistant Coordinator	Summer 2019
LS495: Teaching in Lifescience	Fall 2019
MCDB138: Developmental Biology	Spring 2021

Contributions to Science

Dr. Tom Vondriska Lab (2010-2016)

I. Rosa-Garrido M, Chapski DJ, Schmitt AD, **Kimball TH**, Karbassi E, Monte E, Balderas E, Pellegrini M, Shih TT, Soehalim E, Liem DA, Ping P, Galjart NJ, Ren S, Wang Y, Ren B, Vondriska T. High resolution mapping of chromatin conformation in cardiac myocytes reveals structural remodeling of the epigenome in heart failure. Circulation. Aug 2017. PMID: 28802249. PMCID: PMC5648689.

II. Franklin S, **Kimball T**, Rasmussen TL, Rosa-Garrido M, Chen, H, Tran T, Gray R, Jiang S, MacLellan RM, Ren S, Wang Y, Tucker H, Vondriska TM. A myocyte-specific SET and MYND histone methyl- transferase restricts adult mammalian heart growth through transcriptional repression. Am J Physiol Heart Circ Physiology H1234-H1247. Sept 2016. PMID: 27663768. PMCID: PMC5130490.

III. Monte, E, Mouillesseaux, K, Chen, H, **Kimball, T**, Ren, S, Wang, Y, Chen, J, Vondriska, TM, Franklin, S. Systems proteomics of cardiac chromatin identifies nucleolin as a regulator of growth and cellular plasticity in cardiomyocytes. Am J Physiol Heart Circ Physiology H1624-H1638. Sept. 2013. PMID: 24077883. PMCID: PMC3882469.

Dr. Stephanie White Lab (2016-2018)

I. Burkett Z, Day N, **Kimball TH**, Aamodt C, Heston J, Hilliard A, Xiao X, White SA. FoxP2 isoforms delineate spatiotemporal transcriptional networks for vocal learning in the zebra finch. eLife. Jan 2017. PMID: 29360038. PMCID: PMC5826274.

II. Gedman GL, **Kimball TH**, Factor D, Vojtova G, Wright TG, White SA. Improved zebra finch genome reveals a FOXP2-mediated speech and language-related gene regulatory network. *submitted*

Dr. Tom Vondriska Lab (2019-2022)

I. Fischer MA, Mahajan A, Cabaj M, **Kimball TH**, Morselli M, Soehalim E, Chapski DJ, Montoya D, Farrell CP, Scovotti J, Bueno CT, Mimila NA, Shemin RJ, Elashoff D, Pellegrini M, Monte E, Vondriska TM. DNA methylation-based prediction of post-operative atrial fibrillation. Frontiers in Cardiovascular Medicine. May 2022. PMID: 35620521. PMCID: PMC9127230.

II. Cao Y, Vergnes L, Wang Y, Pan C, Krishnan K, Moore T, Rosa-Garrido M, **Kimball TH**, Zhou, Z, Charugundia S, Rau C, Seldin M, Wang J, Wang Y, Vondriska T, Reue K. Sex differences in heart mitochondria: relationship to diastolic dysfunction. Nature Comms. Jul 2022. PMID: 35787630. PMCID: PMC9253085.

III. **Kimball TH** and Vondriska T. Metabolism, epigenetics, and causal inference in heart failure. Trends in Endocrinology and Metabolism. Mar 2020. PMID: 31866216. PMCID: PMC7035178.

IV. Hu, S, Chapski DJ, Gehred N, **Kimball TH**, Gromova T, Flores A, Rowat AC, Chen J, Packard R, Olszewski E, Davis J, Rau C, McKinsey TA, Rosa Garrido M, Vondriska TM. Histone H1.0 couples cellular mechanical behaviors to chromatin structure. *Submitted*

Research Support

American Heart Association Predoctoral Fellowship 05/2020-04/2022
20PRE35200059

Preface

Heart failure does not have a single cause: rather, it is the convergence of a multitude of cardiac stressors culminating in a failure of the heart to supply the body with enough oxygen and nutrients. Cardiac stressors, including hypertension, excessive adrenergic stimulation, pressure overload, and other stimuli, build upon the physiologic workload of the heart and initially induce left ventricular hypertrophy to ease cardiac wall stress.[1] Pathological hypertrophic remodeling, phenotypically characterized by a thickening of the left ventricular wall and septum and increased interstitial fibrosis, stiffens the heart and induces cell specific responses to the altered environment.[2] Cardiac cell types sense these biophysical and chemical changes and respond accordingly through mechanosensitive molecular mechanisms, to relay these environmental changes for a gene regulatory output. Cardiomyocytes (the post-mitotic, contractile unit of the heart) enlarge to increase contractility, which is facilitated by increased protein synthesis,[3] as part of a beneficial process. However, cardiomyocytes simultaneously exhibit a dysregulated transcriptional response, termed the “fetal gene program,”[4] which involves activating a gene expression profile similar to developing, immature cardiomyocytes, more adaptable to changing environments. Cardiac stress also induces fibroblasts to exit a quiescent state, adapt a proliferative phenotype, and exhibit a heterogenous gene expression profile including myofibroblast differentiation or specialized extracellular matrix secretion, thereby reacting to—while concomitantly promoting—adverse ventricular remodeling[5]. While the gene expression of cardiac cell types under stress has been well characterized, mechanisms underlying these changes are still being uncovered. I hypothesized that by delineating mechanotransduction pathways directly

facilitating gene expression occurring during cardiac hypertrophy, I could uncover insights into the initial cellular sensing and responding processes that drive maladaptive gene expression.

Many studies have focused on single cell gene regulation in different models and phases of heart disease. Epigenetic modifications alter the local spatial organization of chromatin, allowing for transcription factors to facilitate gene regulation, and the aim of my project was to identify a connection between cytoskeletal and sarcomeric dynamics to chromatin biology in cardiac hypertrophy by way of mechanosensitive molecular pathways outside the nucleus that drive changes in gene regulation. My project investigated how mechanisms altering cardiomyocyte and fibroblast physical phenotype are relayed to the nucleus for a chromatin output, or vice versa. Pathological hypertrophy is induced by increased cardiac workload and cardiomyocytes enlarge due to production and organization of sarcomeres to increase force generation, a necessity to ensure proper cardiac output with a stiffened ventricular wall.[6] While sarcomeric proteins are the main contributor to cardiomyocyte stiffness, whole tissue stiffness is largely mediated by cardiac fibrosis,[7] a product of fibroblast proliferation and extracellular matrix remodeling. My study in Chapter 4 characterizes a hypertrophic model for mechanosensitive mediators and responders to hypertrophic stimuli. Cardiomyocytes have mechanosensitive compartments within the sarcomere, and changes in force generation in response to increased demand for work lead to altered gene activation. This process includes the Titin binding protein Ankrd1, which is upregulated in many forms of heart disease, and moves into the nucleus to regulate gene expression. Cardiomyocytes also communicate with fibroblasts through TGFB signaling, which causes fibroblast

proliferation and excess fibrotic deposition and which is mediated by Mrtfa and SRF signaling. These pathways show that changes to the cardiac environment induce cell specific reactions, and these signal transduction pathways are responsive to altered tissue mechanics.

This dissertation begins with a published review on metabolic-epigenetic crosstalk in heart failure. While my projects strayed away from metabolism, this paper was the start of my journey to look outside the nucleus and understand coupling of cardiomyocyte organelles and subcompartments with gene expression in heart disease. In this paper, we proposed a model wherein vital information from the metabolic environment can be stored in the epigenetic memory, either via histone modifying enzymes or the overall architecture of the chromatin itself (Chapter 1). I shifted to focus on coupling of mechanical signals to chromatin in my funded American Heart Association Predoctoral Fellowship (Chapter 2), which served as the foundation for my dissertation research. Through this project, I began identifying factors outside of chromatin, that impact cardiomyocyte cellular biophysics and assessed their involvement in gene regulation and integrated chromatin as a biological responsive suborganelle, responding to differing environmental conditions. Chapter 3 details the findings that came out of the work this grant funded, including methods development for isolation of adult cardiomyocytes and establishment of new approaches to characterize nuclear Lamin A/C ultrastructural changes and their application in the setting of cardiac hypertrophy. Chapter 4 is the culmination of my as-yet unpublished work on mechanosensitive mechanisms involved in an α_1-adrenergic induced model of cardiac hypertrophy. The study characterizes an α_1-adrenergic stimulated hypertrophy model and uses the gene expression profile to identify

mechanosensitive pathways driving cardiomyocyte cell growth, linking these gene expression changes to transcription factor and chromatin remodelers that underpin them. I also identify cardiomyocyte-fibroblast crosstalk and the mechanisms underlying fibroblast extracellular matrix production, proliferation, and morphological alterations inducing the gene profile responsible for the altered phenotype. In the last section of the dissertation, I speculate on future directions of the field of mechnobiology in the heart: while several mechanotransduction pathways have been elucidated in specific tissue types, the constant state of movement cardiac cells experience, poses unique obstacles and tremendous opportunity for examining how mechanosensation is controlled over different time scales, integrated with epigenetic memory and altered during the onset of cardiac disease.

Preface: Bibliography

1. Kehat I, Molkentin JD. Molecular pathways underlying cardiac remodeling during pathophysiological stimulation. Circulation. 2010;122(25):2727-35.

2. Munch J, Abdelilah-Seyfried S. Sensing and Responding of Cardiomyocytes to Changes of Tissue Stiffness in the Diseased Heart. Front Cell Dev Biol. 2021;9:642840.

3. Nakamura M, Sadoshima J. Mechanisms of physiological and pathological cardiac hypertrophy. Nat Rev Cardiol. 2018;15(7):387-407.

4. Rajabi M, Kassiotis C, Razeghi P, Taegtmeyer H. Return to the fetal gene program protects the stressed heart: a strong hypothesis. Heart Fail Rev. 2007;12(3-4):331-43.

5. Tallquist MD, Molkentin JD. Redefining the identity of cardiac fibroblasts. Nat Rev Cardiol. 2017;14(8):484-91.

6. Hieda M, Sarma S, Hearon CM, Jr., Dias KA, Martinez J, Samels M, et al. Increased Myocardial Stiffness in Patients With High-Risk Left Ventricular Hypertrophy: The Hallmark of Stage-B Heart Failure With Preserved Ejection Fraction. Circulation. 2020;141(2):115-23.

7. Yamamoto K, Masuyama T, Sakata Y, Nishikawa N, Mano T, Yoshida J, et al. Myocardial stiffness is determined by ventricular fibrosis, but not by compensatory or excessive hypertrophy in hypertensive heart. Cardiovasc Res. 2002;55(1):76-82.

Chapter 1: Metabolism, Epigenetics and Causal Inference in Heart Failure

Todd H. Kimball and Thomas M. Vondriska

[This research was originally published by Kimball, T.H. and Vondriska T.M. Metabolism, Epigenetics and Causal Inference in Heart Failure. Trends Endocrinol Metab. doi: 10.1016/j.tem.2019.11.009. (2019). PMID: 31866216 © The Authors]

Abstract

Eukaryotes must balance metabolic and cell death actions in mitochondria with control of gene expression and cell fate by chromatin, thereby functionally binding the epigenome and metabolome. This interaction has far reaching implications for chronic disease in humans, the most common of which are those of the cardiovascular system. The most devastating consequence of cardiovascular disease, heart failure, is not a single disease, diagnosis or endpoint. Human and animal studies have revealed that, regardless of etiology and symptoms, heart failure is universally associated with abnormal metabolism and gene expression—to frame as cause or consequence, however, may be to wrongfoot the question. This essay aims to challenge current thinking on metabolic-epigenetic crosstalk in heart failure, presenting hypotheses for how chronic diseases arise, take hold and persist. We unpack assumptions about the order of operations for gene expression and metabolism, exploring recent findings from noncardiac systems linking metabolic intermediates directly to chromatin remodeling. Lastly, we discuss potential mechanisms by which chromatin may serve as a substrate for metabolic memory and how changes in cellular transcriptomes (and hence, cellular behavior) in response to stress correspond to global changes in chromatin accessibility and structure.

Introduction

The clinical syndrome of heart failure is characterized by poor oxygen delivery, exhaustion upon minor physical exertion, fluid retention, shortness of breath and impaired function of the heart itself, presenting as depressed diastolic or systolic function[1]. The central cell and organ level observation in heart failure is a reduction in ATP production and decreased phosphocreatine to ATP ratio, indicative of energy starvation and strongly correlating with cardiovascular mortality [2-4]. Heart failure is often commensurate with other pathophysiological changes, such as fatty liver disease in the case of obesity and metabolic syndrome. Over time these maladies precipitate other serious conditions including renal insufficiency, vascular dementia/Alzheimer's and depression. Management of the heart failure patient relies on modulating fluid balance, vascular tone and cardiomyocyte function, with drugs respectively targeting the renin/angiotensin/aldosterone system to use the kidneys to unload the heart, control of hypertension by modulating vascular tone and improving the work of the heart by β-adrenergic receptor blockade or other modulation of ionotropy. Whereas humans get heart failure from a combination of genetic risk, diet (and accordant BMI), hypertension and atherosclerosis, animal models of heart failure usually arise from a single stress, like high fat diet, infarction, pressure overload or, in many cases, an engineered genetic lesion (i.e. a knockout or transgenic animal). Together these observations present a paradox: the syndrome of heart failure in humans is a spectrum of maladies, unlikely to be treated or cured by a single suite of therapies; yet decades of scientific research has focused on models of heart failure that often times use a set of phenotypes (e.g. myocyte hypertrophy and left ventricular ejection fraction) as a readout that in fact only occur in a portion of the patients suffering from heart failure. One response to this conundrum has been a recent interest in new models of heart failure *with preserved ejection fraction*, with the ostensible goal of identifying therapies for the ~50% of patients with heart failure

that do not exhibit depressed ejection fraction but yet do exhibit diastolic dysfunction and ventricular stiffening.

To understand how chronic diseases develop, we should answer the question of how cells remember what they experience over timescales of seconds, hours or years. A shift in metabolic state can be induced by any number of physiological or experimental factors including substrate availability, physical stress, physiological inputs and energetic demands. These stresses can change gene expression, protein expression, and post-translational modifications, as well as directly alter the substrate pool for metabolic processes, which can themselves store memory in the signaling cascades harboring time delays and feedback loops based on protein and post-translational modification half-lives. Signaling networks and metabolic pathways, due to time delays, post-translational modification and protein lifespans, have the capacity for cellular memory, as do gene expression networks, themselves involving genomic and non-genomic components. But what is the physical substrate of lasting cellular memory and how does this interact with metabolism in a bidirectional manner? We hypothesize that the well characterized cellular bedlam in the failing heart reprograms the epigenome: specifically, it shifts multiple regions of the genome between states of active and inactive conformation—between membraneless suborganelles designed for distinct transcriptional responses—through the actions of chromatin remodelers and transcription factors. In a process of cellular long term memory formation, the entrenching of pathologic metabolism, signaling, calcium handling and myofilament function becomes encoded as a durable substrate via modifications to chromatin structure.

An emerging trend suggests direct coupling of metabolism to chromatin through various molecular means, including substrate availability, enzyme regulation, histone modification, transcription factors and chromatin remodelers (Figure 1) [5,6]. For metabolic-epigenomic coupling to occur, metabolic precursors must interact with cytoplasmic signaling processes or the nucleus

prior to entering the mitochondria or metabolic byproducts of central carbon metabolism (e.g. Kreb's cycle or oxidative phosphorylation products or intermediates) must leave the mitochondria (or trigger a signaling process that leaves the mitochondria) to impinge upon the nucleus. Let us consider the implications of this relationship in the healthy and failing heart.

Metabolic Flexibility

Being born is stressful, and heralds manifold changes for the heart. Vast glycogen stores are depleted, metabolic machinery for fatty acid utilization is mobilized, mitochondria proliferate, oxygen is suddenly available at much higher concentration, and an inchoate muscle protein scaffold organizes into a rigid, regimented network of fibers engineered for the sole purpose of physical work. Adult cardiac muscle is replete with mitochondria engineered to turn carbohydrates, fats and protein into ATP. Fatty acids are imported to cardiac myocytes from the circulation through fatty acid translocases (CD36 and FAT) and following cytosolic esterification (i.e. conversion to long fatty acyl-CoA by the ATP-dependent acyl-CoA ligase) are directed into the mitochondria through carnitine palmitotransferase isomers (CPT1 and CPT2). These long chain fatty acids are then catabolized by beta oxidation, a multistep process leading to the production of acetyl-CoA, which enters the Kreb's cycle. This Kreb's generates FADH2 and NADH, which are utilized by the electron transport chain coupled to oxidative phosphorylation in the inner membrane of the mitochondria. This process is the primary mechanism for generation of large amounts (relative to that from glycolysis) of ATP in cardiac myocytes. In the healthy adult heart, the aforementioned fatty acid metabolic strategy is dominate. Yet carbohydrates are more efficient fuel sources on a per molar oxygen basis compared with fatty acids and, in addition to being the primary fuel source in the fetal heart, carbohydrates are rapidly mobilized in the adult heart during cardiac stresses, such as hypertrophy and failure[7]. Cytosolic glycolysis converts glucose—which can be taken up into cardiac myocytes independent of (GLUT1) or in response to (GLUT4 transporter) insulin, both of which are increased in the failing heart, augmenting the

availability of glucose—into pyruvate, which is in turn imported into mitochondria and converted by pyruvate dehydrogenase to acetyl-CoA, entering the Kreb's cycle. The liver converts fat into ketone bodies, especially during periods of starvation, that navigate to the heart through the circulation and enter cardiac myocytes, presumably via the membrane bound monocarboxylate transporters 1 and 2. The ketone bodies then make their way to the mitochondrial matrix through unknown mechanisms and, after conversion to acetyl-CoA, the rate limiting enzyme for which is succinyl-CoA:3-oxoacid-CoA transferase (helpfully, SCOT), enter the Kreb's cycle. Proteins, notably branched chain amino acids (BCAAs; leucine, isoleucine and valine—essential amino acids which cannot be synthesized by the body), are catabolized through a series of steps regulated principally by the branched chain alpha keto acid dehydrogenase (BCKDH) to ultimately generate acetyl-CoA and succinyl-CoA (converted from propionyl-CoA), both of which then enter the Kreb's cycle. Elevation in BCAAs has been linked to metabolic syndrome, a precursor to heart failure, through multi-organ effects reviewed in detail elsewhere[8]. The reader notes that, regardless of the source, the goal of all these metabolic pathways is: get carbon chains into the Kreb's cycle and on to ETC and oxidative phosphorylation for ATP production.

Metabolic Inflexibility

Although feasible and logical in animal models, separation of hypertension and diabetes as precipitating factors for heart failure does not occur in humans. Lower levels of insulin, greater hemodynamic load, and mitochondrial biogenesis rapidly transforms the anatomy and functionality of the cardiomyocyte after birth. The transcriptional program associated with mitochondrial biogenesis and substrate preference, namely, switching to the preferential metabolism of fatty acids [9], is driven in large part by the nuclear receptor peroxisome proliferator-activated receptor α (PPAR-α) and its coactivator the PPAR- coactivator 1 (PGC-1α). Genomic targets of PGC-1α in cardiac myocytes are unknown, however a recent study from brown adipose tissue demonstrated, unsurprisingly, that genes bound by the transcription factor enrich in

pathways involved in fatty acid metabolism[10]. The case for PPAR[11], which is likely also true for other transcription factors whose activation has been witnessed in the diseased heart, is that the actions of the molecule are highly dependent on the nature of the stimulus, the time after the stimulus and the molecular interactions with whichever other DNA binding proteins are activated in the cell.

Heart failure has been termed a state of metabolic inflexibility, an interpretation that comes principally from studies in which the disease state is experimentally induced by a unitary stimulus [12]: experimentally restricting the availability of fuel sources to the heart (either favoring glucose or fat) leads to disease. It has been proposed that metabolic derangements, which are to be found in all forms of heart failure, trigger gene expression changes (implying they also precede the gene expression changes) and may also sustain them [13]. Evidence in support of this observation is: (1) experimental alterations in diet and/or metabolic substrate can induce changes in gene expression; (2) all forms of human heart failure involve metabolic derangement; (3) the gene expression programs initiated by the stresses of heart failure, principally metabolic syndrome itself, hypertension/elevated cardiac pressures, and ischemia—which themselves are often chronic and, especially in humans, rarely perfectly ameliorated—include changes to the transcript and protein levels of metabolic machinery to favor glucose over fatty acid metabolism (e.g. expression of GLUT1/4, pyruvate dehydrogenase kinase 2 and glycogen synthase are all decreased), thereby extending the time window of metabolic alteration. What is the precise molecular chain of events connecting changes in metabolism with gene expression and vice versa? Metabolic syndrome and hypertension/pressure overload can be experimentally separated, wherein studies have revealed the former to be associated with increased fatty acid, and the latter with glucose, oxidation (decreasing and increasing PPARα expression, respectively) [9].

One study showed that visceral adiposity (but neither subcutaneous nor total adiposity) was independently associated with incident hypertension (i.e. the development of high blood pressure following a previously normotensive measurement) in humans[14]. Hypertension—along with high fasting blood glucose, elevated triglycerides, low HDL or waist circumference—is a diagnostic criteria for metabolic syndrome, which in turn is a clinical precedent to obesity and type 2 diabetes. Although high blood pressure and metabolic syndrome may not always be causally linked in a given person, the cooccurrence of these conditions at some stage of the progression of cardiovascular disease in humans is extremely common[1]. Precisely because of the fact that heart failure in humans is not the result of only hypertension, metabolism, ischemia *or* genetics—but rather, due to an often imperfectly quantified cooccurrence of these factors—we reason that the actual endogenous sensor-regulator of gene expression and metabolic state is chromatin. This process works through shifting regions of accessibility and probably to a lesser degree structure, moving the transcriptome from a more restricted state to a more dynamic one.

Evolution has contrived some aspects of this transition to reverse themselves in response to pathologies to which mammals commonly subject their hearts, although important caveats abound in this characterization. Impairments of glucose uptake and glucose oxidation compounds the diseased myocyte's ability to metabolize fatty acids; mitochondria go haywire, producing reactive oxygen species as a result of poorly coupled oxidative phosphorylation, losing control of calcium balance, leading to calcium overload (due in part to malfunctioning sarcoplasmic reticulum reuptake during diastole, in turn due to ryanodine receptor leakage), calcium toxicity and catastrophic depolarization (known as permeability transition) and spewing of protein and calcium into the cytosol, causing further havoc, including cell death by apoptosis and necrosis. Ischemia brings with it hypoxia, which further exacerbates reactive oxygen species production, cell death signaling and calcium overload; and the subproteome of contractile molecules is beset by post-translational modification, starved of ATP as a result of the aforementioned mitochondrial

impairment. The cardinal observation of a failing heart is a decrease in the high energy reserve compound phosphocreatine, manifest as a decreased phosphocreatine/ATP ratio, resulting from the coincident stresses of increased energy demand (due to higher workload in response to hypertension, e.g.), decreased contractile ability (due to muscle loss or impairment by ischemia, e.g.) and decreased energy supply (due to systemic metabolic crapping out, due to type II diabetes, due to sustained hypercaloric diet, e.g.) and, curiously, both an increase in muscle protein mass and a change in the expression[15,16] of myosin heavy chain isoforms (See Box 1), sometimes accompanied by gross changes in sarcomeric organization, although without a return to the primitive organization of the contractile apparatus observed in fetal myocardium.

Communication Amongst Organelles

The antediluvian pact whereby eukaryotes offload (some) metabolic and cell death decisions to mitochondria in exchange for ceding to the nucleus and cytoplasm substantial control over synthesis of mitochondrial protein machinery, inextricably links chromatin with metabolism. The conceptual framework of the *histone code* (Figure 2A) in which writers, erasers and readers add, remove and interpret, respectively, nucleosome post-translational modifications to influence genomic function can be helpfully expropriated to discuss post-translational modification of—principally mitochondrial—proteins in the setting of metabolic diseases, an area of research too expansive to do any justice in the present essay but which has been adroitly reviewed elsewhere (for cardiac[17]; for noncardiac and technology [18]). Indeed, research in cancer has revealed multiple direct links between metabolism and gene regulation (see Box 2). Hyperacetylation has been observed [19] on pyruvate dehydrogenase, fatty acid oxidation machinery, Kreb's cycle enzymes and the electron transport chain proteins and associated with their dysfunction, and attenuate of hyperacetylation, by restoration of the NAD(+)/NADH ratio, is beneficial at the molecular and whole organ level in heart failure [20]. There are many origins of this hyperacetylation, including what might be termed writer-mediated (i.e. changes in the acetyltransferase levels or activity) or

eraser-mediated (i.e. changes in the deacetylases); if we stretch the analogy, acetylation machinery also has *ink*, in the form of the acetyl-CoAs themselves, that are used to write the various types of acetylation modifications that have been observed in mammals and which are present in higher than normal levels during heart failure [21], or in the form of cofactors like NAD+ and the NAD(+)/NADH ratio, which are necessary for sirtuin-mediated deacetylation [19,20]. Other post-translational modifications, less obviously coupled to metabolism, have been measured in the heart, but a central issue bedevils understanding of their function: stoichiometric and temporal data are sparse, making unknowable the molecular effects of each individual modification. Computational studies have recently been engineered to address this challenge in mass spectrometry experiments[22], but they have yet to be applied in the setting of disease. The metabolic donor pool changes in heart failure, but this is highly dependent on the model and time frame (for example the NAD(+)/NADH ratio has been shown in different studies to increase[23] and decrease [24] after pressure overload). Indeed fatty acid substrates are more depleted in late stage heart failure [25], the time point at which mitochondrial and gross metabolic disturbances are most pronounced [17]. The concept of distinct metabolite pools in different subcompartments of the cell has been established for some time[26]—this hypothesis is receiving renewed interest with the recognition of cross talk between metabolism and various cellular processes, including chromatin accessibility.

PPAR nuclear receptors heterodimerize with retinoid receptors to activate transcription in response to excess intracellular fatty acids and genetic disruption of PPARα leads to decreased fatty acid oxidation and increased metabolism of glucose [27]. The PPARγ receptor coactivator, PCG1α, is downregulated in human failing hearts [28] and its deficiency[29], or that of its cousin PGC1β[30], exacerbates heart failure in the setting of pressure overload. Depending on the experimental model of heart failure, the involvement of PPARα signaling can work in opposite directions[9]: pressure overload, mimicking hypertension, is associated with decreased PPARα

signaling and increased glucose utilization, whereas mice overexpressing PPARα exhibit a metabolic syndrome like phenotype, increasing utilization of fatty acids (diabetic mouse models also exhibit elevated PPARα). Glucose, more abundant in the failing heart and less efficiently oxidized, may itself directly modify transcription factors, disrupting their function[31]. Myocyte enhancer factor 2A (MEF2A), which plays an essential role in myocyte differentiation, regulates PGC-1α and mitochondrial content and function [32], whereas MEF2A is downregulated in diabetic patients with heart failure [33]. Various histone modifying enzymes have been implicated in heart failure through genetic and pharmacologic means (for review[34-36]) with recent studies implicating cardiac-specific writers in the regulation of normal adult metabolism. The striated muscle-specific histone methyltransferase Smyd1, loss of which induces precipitous heart failure[37] and reduced respiratory capacity of mitochondria[38], is required for normal expression of a panel of metabolic transcription factors including PGC-1α, PPARα, and RXRα through direct regulation of histone H3 lysine 4 trimethylation at gene promoters[38]. Hypoxia, a central component of injury and long term stress in cardiovascular disease, can directly modulate chromatin independent of the hypoxia inducible factor (HIF) transcription factor complex: two studies recently showed Hif-independent modification of locus-selective, but genome-wide, H3K4me3 (KDM5A dependent[39]) and H3K27me3 (KDM6A dependent[40]) modifications, mobilizing gene expression programs in response to hypoxia without transcription factor activation (note: these processes were also found to be independent of the oxygen sensors 2-oxoglutarate (OG)-dependent dioxygenases—implicating the histone modifying enzymes themselves as oxygen sensors). It is also apparent that under certain circumstances, metabolic machinery (e.g. Kreb's cycle enzymes) can directly localize to the nucleus and regulate cell fate decisions such as zygotic genome activation [41] and cancer progression [42,43] by coordinating with histone modifications and the binding of other transcriptional regulators, such as histone variants[44]. The frequency of direct genomic actions by

metabolic enzymes, and the relative stoichiometry of these proteins in nuclei versus perinuclear mitochondria, are areas of active investigation.

Chromatin as Memory Substrate

Evolution inserted large portions of non-mRNA-encoding DNA into eukaryotic genomes, corresponding with the ability of these genomes to produce dozens and, in higher organisms, hundreds of cell types and transcriptomes from the same genome, ostensibly by varying the structure of the genome at some scale. At present, global chromatin structure-function models are rapidly evolving (*i.e.* If we wanted to extend the central dogma beyond the codon, what would be the rules?). Mediator complexes, chromatin readers and transcription factors operate within the context of adult myocyte chromatin architecture and a global landscape of accessibility that has been established by writers, erasers, chromatins structural proteins (and perhaps DNA methylation, although this modification seems to follow cues laid down in structure) some of which is cell type and developmental stage specific.

Chromatin conformation capture techniques applied genome-wide (e.g. HiC) initially described topologically associating domains as local regions of higher than average intrachromosomal interactions separated by boundaries, or places at which the interactions abruptly switch from favoring 5' to 3' regions (or vice versa). While tempting to view these TADs as structural operons, wherein genes of similar activity are oriented in a similar manner in 3D (rather than along the linear chromosome, as occurs in bacteria), subsequent studies revealed that TADs and their boundaries are largely conserved across adult mammalian cell types, and indeed are specified early in differentiation, thus implying this scale of organization cannot, alone, specify different transcriptomes. Since TADs and their boundaries are conserved, the chromatin structural proteins, like CTCF and cohesins, that preferentially populate these boundaries are unlikely to drive cell type specification, although they have been shown to regulate disease-associated chromatin remodeling and gene expression. During differentiation along the cardiac

lineage from embryonic stem cells to neonatal cardiomyocytes, substantial reassignment of the genome to different compartments of chromatin is observed, either as record or driver of changes in the transcriptome [45,46]. After birth, cardiomyocyte maturation is associated with changes in histone post-translational modifications but minor changes in compartmentalization [45,46].

The biological relevance of chromatin compartmentalization is not immediately clear however: it may relate to regions within the nucleus of local increased plasticity and accessibility to transcriptional machinery, for example in the center versus the periphery of the nucleus. Chromosomes reproducibly segregate into territories within the interphase nucleus, but within these territories, intra- and inter-chromosomal interaction are dynamic and membraneless suborganelles can form through a process likened to phase separation[47] (Figure 2B). Together, compartmentalization of chromatin (an emergent property of histone isoforms, histone PTMs [and the associated suite of writers, erasers and readers], chromatin structural proteins and remodeling enzymes, themselves regulated by metabolic processes and substrate levels) may combine with chromosome territory cues, subnuclear localization cues (principal among these being tethering of chromatin regions to the nuclear lamina [48]) and phase separation behavior to establish structure-function neighborhoods within the nucleus. Unlike a crystal structure of a nucleosome or the 5-24nm chromatin fibers visible by microscopy, these structural neighborhoods are not perfectly replicated across individual cells, but rather are the lowest energy state organizational feature that segregates active from inactive regions, thereby functionally compartmentalizing the nucleus. Indeed, recent single cell chromatin capture studies indicate a high level of cell-to-cell variability in the *absolute* structure of TADs (i.e. the exact location of their boundaries)[49]: removal of CTCF or cohesins can disrupt TAD boundaries in bulk HiC experiments[50] (indeed, loss of CTCF from cardiac myocytes is sufficient to induce heart failure and chromatin disorganization [51 52]), yet similar interventions do not eliminate TADs in single cell experiments—instead, loss of the CTCF-cohesin complex results in greater variability in the formation of TADs [53] suggesting (a) TADs are

a basic structural feature of DNA and protein, formed by the physical chemical principles of phase separation (or perhaps due to sequence cues, such as transposons and their transcription [54]), independent of the actions of any single given protein; and (b) the actions of the CTCF-cohesin complex are to entrain/stabilize TADs across different cell types. It has been proposed that long noncoding RNAs may serve as scaffolds for phase separation of chromosomes. Unlike other forms of RNA like mRNA and microRNA, no unifying mechanism of action has been revealed for lncRNAs. Could their role be to seed transcription factories, such that the actual sequence matters less than their positioning along the genome? Nucleosome turnover rate and nucleosome density, along with higher order structure, contribute to accessibility and transcription. Regions with high nucleosome density often have high turnover and low positional stability of nucleosomes, but there are exceptions (e.g. insulators, which are higher density, low turnover, but accessible)[55]. Lastly, histone post-translational modifications, in part responding to metabolic signals, may influence the formation of local microenvironments of activation or silencing, thereby contributing to the formation of membraneless suborganelles (e.g. high transcription of rRNA defining the nucleolus).

Timing

The phenomena of fully reversible 'physiological' types of hypertrophy observed in athletes or during pregnancy (neither of which have metabolic syndrome or hypertension, despite increased cardiac mass and chamber volume), which share neither gene expression profiles nor metabolic rearrangements of pathologic hearts [56,57], support the concept that metabolic syndrome or elevated mean arterial pressure are necessary to maintain the gene expression regime in the diseased state. This gives some window into the stimulus type (elevated MAP and/or metabolic syndrome) and duration (sustained).

How does sensing of metabolic changes occur and what is the order of cellular operations that respond to, adjust and remember these metabolic changes? Changes in gene expression

may be unnecessary for short term regulation of metabolism, which can occur through the actions of signaling proteins to modify metabolic enzymes and by the availability of various substrates. However, these processes do not occur in isolation and will simultaneously activate gene expression machinery through the actions of transcription factors and by direct coupling of metabolites to chromatin [39,40,58,59]. Metabolic fluxes (i.e. the time it takes to deplete existing metabolic stores in the absence of input) occur on the timescale of a minute in mammalian cells, whereas protein production takes several minutes. Acute changes in metabolites thus can induce changes in gene and protein expression, but there is a time delay, meaning that some hysteresis will result—at the protein abundance level—if the cell experiences imbalance in metabolite source and utilization. How long does it take to entrain this information in chromatin? ATP-dependent chromatin remodeling complexes regularly physically engage chromatin in nonproductive binding events, waiting for appropriate transcription factor signaling (and perhaps ejection of nucleosomes) to convert this continuous sampling activity into productive remodeling, which can in turn occur on the timescale of seconds to minutes[60,61]. Furthermore, physical forces alone are sufficient to remodel chromatin, again operating in seconds or minutes[62]. While the specific time constants for these processes in adult cardiac myocytes have not been determined, we can safely estimate that both metabolic gene expression and chromatin remodeling are sensitive to similar cardiac stresses (notably mechanical disruption and metabolic flux) and can respond over similar timescales, making the issue of temporal regulation not *a priori* obvious and therefore wanting for experimental determination.

Concluding Remarks and Hypotheses

Here is precisely what we think is going on: the abnormal cellular environment in the failing heart entrains—through physical, post-translational and metabolic signaling—chromatin towards a distinct organizational regime that adapts gene expression to resist pathologic stress, thereby producing both the beneficial and detrimental phenotypes observed in cardiac cells. Chromatin is

organized based on cues across the genome that draw together regions with similar modifications (to histones and DNA, and due in part to other chromatin binding proteins) to create neighborhoods of transcriptional silencing or activation, similar to phase separation principles operative in oil partitioning from water and driven less by specific enzymatic or transcription factor pathways converging on a handful of target genes, and more by a global shift in the deposition of various modifications controlled by said enzymes as well as by the present and past metabolic environment. The epigenome can serve as an integrator of multiple forms of metabolic stress: if the rules can be uncovered for how it responds in general to stress conditions that cause disease, we may learn how evolution came to utilize chromatin as a memory substrate and cellular decision tree. Therapeutic approaches resulting from our evolving understanding of the coupling of epigenome to metabolome in heart failure may take one of several broad approaches: modify the fuel source (changing diet); modify the metabolic pathways directly (e.g. GLUT transporters, PDH; changing the abundance of enzymes that control flux of metabolic intermediates or utilization of one fuel source over another); modify the molecular intermediates (e.g. acetyl-CoA or NADH; changing the availability of intermediate substrates, thereby influencing processes like post-translational modification of proteins); modifying the crosstalk apparatus that integrates epigenomic and metabolic circuits (changing the transcription factor or chromatin modifying enzymes that regulate metabolism); or targeting chromatin accessibility directly. If chromatin is indeed a substrate of cellular memory, strategies that screen chromatin as a functional readout of new therapies may improve durability of treatment.

Text Box 1: Isoform Switching in Heart Failure

A “myosin heavy chain isoform switch”—in which β-MHC (MHC7), which predominates in fetal hearts and is lowly expressed in healthy adults, is upregulated and α-MHC (MHC6), predominating in adult hearts and lowly expressed in the fetus, downregulated—in the hearts of mice with symptoms of hypertrophy or failure has been reported in hundreds of papers, so as to

become itself a tacit phenotype of heart failure. Complicating this interpretation are the observations that: (1) in humans the β-MHC isoform predominates throughout life and is up-regulated in failing hearts (while the lower expressed α-MHC is further down-regulated); and (2) even in rodent hearts, the cells actually hypertrophying in the wake of pathologic stress are not the same cells with altered MHC isoform expression (i.e., β-MHC expressing cells are smaller, as measured either by antibody-based flow cytometry[15] or mRNA FISH and single cell RNA-seq[16]. The molecular role, thus, of this change in isoform expression in the function of a diseased, hypertrophying myocardium, and as a readout of transcriptional remodeling in heart failure, remains obscured.

Text Box 2: Epigenetic-Metabolic Coupling in Cancer

Cancer research provides insights into how coupling of metabolism and the epigenome can go awry, causing disease. Cytosolic isocitrate dehydrogenase 1 (IDH1) and mitochondrial IDH2 convert isocitrate to α-ketoglutarate (α-KG). Mutations of IDH1 or IDH2, observed most commonly in gliomas, further converts α-KG to 2-hydroxyglutarate (2-HG) [63,64], and overproduction of this so-called “oncometabolite” inhibits DNA demethylation by binding to ten eleven translocation (TET) family proteins and histone demethylation by Jumonji C (JMJC) family proteins [65]. Hypermethylation occurs as 2-HG competes with α-KG, a hallmark of aggressive tumors [66]. In human IDH mutant gliomas, CTCF and cohesion binding sites are subject to hypermethylation, disrupting TAD domain insulation and resulting in disruption of gene expression, specifically of a constitutive enhancer interacting with the oncogene PDGFRA [67]. Additionally, loss of function mutations to succinate dehydrogenase or fumarase lead to high levels of succinate or fumarate, respectively, to inhibit TET and JMJC demethylation [68].

Post-translational modification of metabolic enzymes alter their enzymatic activity and localization in cancer progression. In the final step of glycolysis, pyruvate kinase (PKM) catalyzes the conversion of phosphoenolpyruvate and ADP to pyruvate and ATP through phosphorylate

transfer. Pathological stimulation of EGFR and PDGFR [69] induces increased expression of PKM2 (upregulated in numerous cancer types [70]). Phosphorylation of PKM2 by ERK1 or ERK2 recruits PIN1, inducing isomerization and exposing the nuclear localization sequence [71]. Nuclear translocation of PKM2 enables interaction with phosphorylated β-catenin and recruitment to CCND1 and MYC promoter regions, binding to and phosphorylating histone H3, which displaces HDAC3 for H3K9 acetylation [72]. CCND1 promotes cell division through promoting G1/S transition and MYC induces increased glucose uptake. Additionally, PKM2 drives glucose uptake by binding to hydroxylated HIF1α, inducing increased target gene expression [73].

Conflicts: The authors report no conflicts of interest related to this article.

Funding: The Vondriska lab is funded by the National Institutes of Health, the American Heart Association and the David Geffen School of Medicine at UCLA.

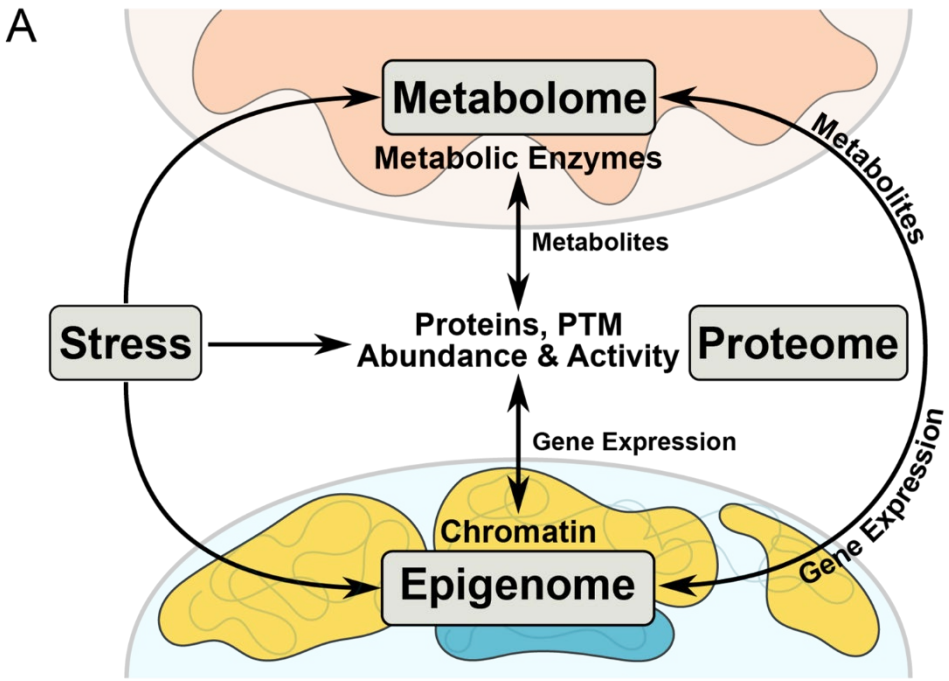

Figure 1-1. Inter-Organelle and Inter-omic Cooperation in Times of Stress. Cardiac stress (e.g. ischemia, diet, genetics, hypertension) affects the metabolome, proteome, and epigenome, forcing a coordinated, time-sensitive response. Stress-induced changes in metabolic substrate utilization causes a shift in metabolic enzymatic activity and metabolite pools. These metabolites act on proteins through post-translational modifications (PTMs), changing protein activity or localization. Protein PTM induced nuclear localization directly or indirectly influences epigenetic processes (e.g. histone modifications or DNA methylation), causing changes in chromatin accessibility and gene expression. Metabolites can be shuttled to the nucleus to be utilized as substrates for epigenetic modifications, thereby changing local chromatin accessibility, influencing gene expression and ultimately protein abundance.

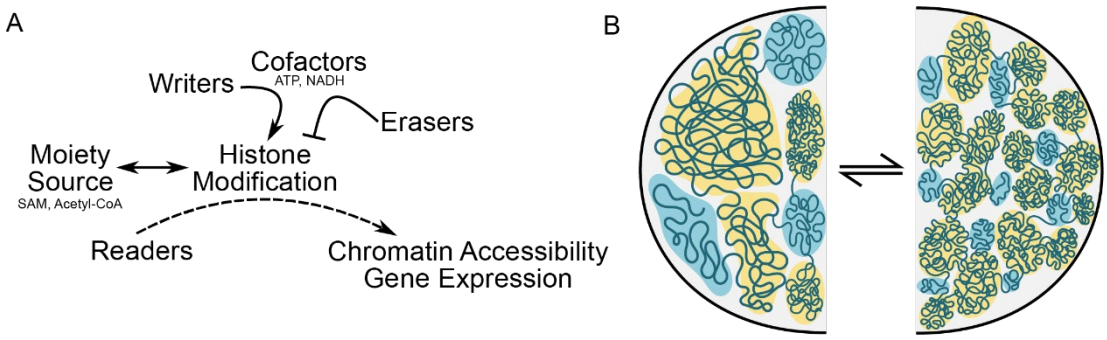

Figure 1-2. Chromatin Compaction and Histone Modifications Affect Gene Expression. **A.** Metabolic cofactors, such as ATP and NADH, work in concert with writers and erasers to orchestrate histone modifications and chromatin condensation. Histone modifications are added by writer, which utilize metabolites as moiety sources (e.g. SAM, Acetyl-CoA and again ATP, and others) to add marks (erasers, accordingly, remove the marks) so that readers, which continuously navigate to and sample histones for proper modifications, can influence gene expression by recruiting transcriptional machinery. **B.** Rather than a rigid invariant architecture between cells, chromatin organization appears to arise similar to a phase separation, with local regions of accessibility and inaccessibility influenced by protein binding and PTM in response to cell specification cues and environmental stimuli. In this representation, open and active (blue) or closed and inactive (yellow) regions shift in terms of their relative abundance, the features of the domains they occupy and their localization within the nucleus. Chromatin compaction can flow between multiple states, shown here as one with larger more continuous regions of activity or silencing (left) versus smaller more segmented regions of differing accessibility and transcriptional behavior (right).

Chapter 1: Bibliography

1 Benjamin, E. J. *et al.* Heart Disease and Stroke Statistics-2019 Update: A Report From the American Heart Association. *Circulation* **139**, e56-e528, doi:10.1161/CIR.0000000000000659 (2019).

2 Neubauer, S. *et al.* Myocardial phosphocreatine-to-ATP ratio is a predictor of mortality in patients with dilated cardiomyopathy. *Circulation* **96**, 2190-2196, doi:10.1161/01.cir.96.7.2190 (1997).

3 Liao, R., Nascimben, L., Friedrich, J., Gwathmey, J. K. & Ingwall, J. S. Decreased energy reserve in an animal model of dilated cardiomyopathy. Relationship to contractile performance. *Circ Res* **78**, 893-902, doi:10.1161/01.res.78.5.893 (1996).

4 Hearse, D. J. Oxygen deprivation and early myocardial contractile failure: a reassessment of the possible role of adenosine triphosphate. *Am J Cardiol* **44**, 1115-1121, doi:10.1016/0002-9149(79)90177-2 (1979).

5 Li, X., Egervari, G., Wang, Y., Berger, S. L. & Lu, Z. Regulation of chromatin and gene expression by metabolic enzymes and metabolites. *Nat Rev Mol Cell Biol* **19**, 563-578, doi:10.1038/s41580-018-0029-7 (2018).

6 Keating, S. T. & El-Osta, A. Epigenetics and metabolism. *Circ Res* **116**, 715-736, doi:10.1161/CIRCRESAHA.116.303936 (2015).

7 Goodwin, G. W., Taylor, C. S. & Taegtmeyer, H. Regulation of energy metabolism of the heart during acute increase in heart work. *J Biol Chem* **273**, 29530-29539, doi:10.1074/jbc.273.45.29530 (1998).

8 Arany, Z. & Neinast, M. Branched Chain Amino Acids in Metabolic Disease. *Curr Diab Rep* **18**, 76, doi:10.1007/s11892-018-1048-7 (2018).

9 Aubert, G., Vega, R. B. & Kelly, D. P. Perturbations in the gene regulatory pathways controlling mitochondrial energy production in the failing heart. *Biochim Biophys Acta* **1833**, 840-847, doi:10.1016/j.bbamcr.2012.08.015 (2013).

10 Chang, J. S., Ghosh, S., Newman, S. & Salbaum, J. M. A map of the PGC-1alpha- and NT-PGC-1alpha-regulated transcriptional network in brown adipose tissue. *Sci Rep* **8**, 7876, doi:10.1038/s41598-018-26244-4 (2018).

11 Warren, J. S., Oka, S. I., Zablocki, D. & Sadoshima, J. Metabolic reprogramming via PPARalpha signaling in cardiac hypertrophy and failure: From metabolomics to epigenetics. *Am J Physiol Heart Circ Physiol* **313**, H584-H596, doi:10.1152/ajpheart.00103.2017 (2017).

12 Karwi, Q. G., Uddin, G. M., Ho, K. L. & Lopaschuk, G. D. Loss of Metabolic Flexibility in the Failing Heart. *Front Cardiovasc Med* **5**, 68, doi:10.3389/fcvm.2018.00068 (2018).

13 Taegtmeyer, H., Sen, S. & Vela, D. Return to the fetal gene program: a suggested metabolic link to gene expression in the heart. *Ann N Y Acad Sci* **1188**, 191-198, doi:10.1111/j.1749-6632.2009.05100.x (2010).

14 Chandra, A. *et al.* The relationship of body mass and fat distribution with incident hypertension: observations from the Dallas Heart Study. *J Am Coll Cardiol* **64**, 997-1002, doi:10.1016/j.jacc.2014.05.057 (2014).

15 Lopez, J. E. *et al.* {beta}-Myosin Heavy Chain Is Induced by Pressure Overload in a Minor Subpopulation of Smaller Mouse Cardiac Myocytes. *Circ Res*, doi:CIRCRESAHA.111.243410 [pii]
10.1161/CIRCRESAHA.111.243410 (2011).

16 Satoh, M. *et al.* High-throughput single-molecule RNA imaging analysis reveals heterogeneous responses of cardiomyocytes to hemodynamic overload. *J Mol Cell Cardiol* **128**, 77-89, doi:10.1016/j.yjmcc.2018.12.018 (2019).

17 Zhou, B. & Tian, R. Mitochondrial dysfunction in pathophysiology of heart failure. *J Clin Invest* **128**, 3716-3726, doi:10.1172/JCI120849 (2018).

18 Carrico, C., Meyer, J. G., He, W., Gibson, B. W. & Verdin, E. The Mitochondrial Acylome Emerges: Proteomics, Regulation by Sirtuins, and Metabolic and Disease Implications. *Cell Metab* **27**, 497-512, doi:10.1016/j.cmet.2018.01.016 (2018).

19 Horton, J. L. *et al.* Mitochondrial protein hyperacetylation in the failing heart. *JCI Insight* **2**, doi:10.1172/jci.insight.84897 (2016).

20 Karamanlidis, G. *et al.* Mitochondrial complex I deficiency increases protein acetylation and accelerates heart failure. *Cell Metab* **18**, 239-250, doi:10.1016/j.cmet.2013.07.002 (2013).

21 Bedi, K. C., Jr. *et al.* Evidence for Intramyocardial Disruption of Lipid Metabolism and Increased Myocardial Ketone Utilization in Advanced Human Heart Failure. *Circulation* **133**, 706-716, doi:10.1161/CIRCULATIONAHA.115.017545 (2016).

22 Bagwan, N. *et al.* Comprehensive Quantification of the Modified Proteome Reveals Oxidative Heart Damage in Mitochondrial Heteroplasmy. *Cell Rep* **23**, 3685-3697 e3684, doi:10.1016/j.celrep.2018.05.080 (2018).

23 Oka, S. *et al.* PPARalpha-Sirt1 complex mediates cardiac hypertrophy and failure through suppression of the ERR transcriptional pathway. *Cell Metab* **14**, 598-611, doi:10.1016/j.cmet.2011.10.001 (2011).

24 Lee, C. F. *et al.* Normalization of NAD+ Redox Balance as a Therapy for Heart Failure. *Circulation* **134**, 883-894, doi:10.1161/CIRCULATIONAHA.116.022495 (2016).

25 Sansbury, B. E. *et al.* Metabolomic analysis of pressure-overloaded and infarcted mouse hearts. *Circ Heart Fail* **7**, 634-642, doi:10.1161/CIRCHEARTFAILURE.114.001151 (2014).

26 Ingwall, J. S. Transgenesis and cardiac energetics: new insights into cardiac metabolism. *J Mol Cell Cardiol* **37**, 613-623, doi:10.1016/j.yjmcc.2004.05.020 (2004).

27 Campbell, F. M. *et al.* A role for peroxisome proliferator-activated receptor alpha (PPARalpha) in the control of cardiac malonyl-CoA levels: reduced fatty acid oxidation rates and increased glucose oxidation rates in the hearts of mice lacking PPARalpha are associated with higher concentrations of malonyl-CoA and reduced expression of malonyl-CoA decarboxylase. *J Biol Chem* **277**, 4098-4103, doi:10.1074/jbc.M106054200 (2002).

28 Sack, M. N. *et al.* Fatty acid oxidation enzyme gene expression is downregulated in the failing heart. *Circulation* **94**, 2837-2842, doi:10.1161/01.cir.94.11.2837 (1996).

29 Arany, Z. *et al.* Transverse aortic constriction leads to accelerated heart failure in mice lacking PPAR-gamma coactivator 1alpha. *Proc Natl Acad Sci U S A* **103**, 10086-10091, doi:10.1073/pnas.0603615103 (2006).

30 Riehle, C. *et al.* PGC-1beta deficiency accelerates the transition to heart failure in pressure overload hypertrophy. *Circ Res* **109**, 783-793, doi:10.1161/CIRCRESAHA.111.243964 (2011).

31 Young, M. E. *et al.* Proposed regulation of gene expression by glucose in rodent heart. *Gene Regul Syst Bio* **1**, 251-262, doi:10.4137/grsb.s222 (2007).

32 Czubryt, M. P., McAnally, J., Fishman, G. I. & Olson, E. N. Regulation of peroxisome proliferator-activated receptor gamma coactivator 1 alpha (PGC-1 alpha) and mitochondrial function by MEF2 and HDAC5. *Proc Natl Acad Sci U S A* **100**, 1711-1716, doi:10.1073/pnas.0337639100 (2003).

33 Razeghi, P., Young, M. E., Cockrill, T. C., Frazier, O. H. & Taegtmeyer, H. Downregulation of myocardial myocyte enhancer factor 2C and myocyte enhancer factor 2C-regulated gene expression in diabetic patients with nonischemic heart failure. *Circulation* **106**, 407-411, doi:10.1161/01.cir.0000026392.80723.dc (2002).

34 McKinsey, T. A. & Olson, E. N. Dual roles of histone deacetylases in the control of cardiac growth. *Novartis Found Symp* **259**, 132-141; discussion 141-135, 163-139 (2004).

35 Rosa-Garrido, M., Chapski, D. J. & Vondriska, T. M. Epigenomes in Cardiovascular Disease. *Circ Res* **122**, 1586-1607, doi:10.1161/CIRCRESAHA.118.311597 (2018).

36 Gillette, T. G. & Hill, J. A. Readers, writers, and erasers: chromatin as the whiteboard of heart disease. *Circ Res* **116**, 1245-1253, doi:10.1161/CIRCRESAHA.116.303630 (2015).

37 Franklin, S. *et al.* The chromatin-binding protein Smyd1 restricts adult mammalian heart growth. *Am J Physiol Heart Circ Physiol* **311**, H1234-H1247, doi:10.1152/ajpheart.00235.2016 (2016).

38 Warren, J. S. *et al.* Histone methyltransferase Smyd1 regulates mitochondrial energetics in the heart. *Proc Natl Acad Sci U S A* **115**, E7871-E7880, doi:10.1073/pnas.1800680115 (2018).

39 Batie, M. *et al.* Hypoxia induces rapid changes to histone methylation and reprograms chromatin. *Science* **363**, 1222-1226, doi:10.1126/science.aau5870 (2019).

40 Chakraborty, A. A. *et al.* Histone demethylase KDM6A directly senses oxygen to control chromatin and cell fate. *Science* **363**, 1217-1222, doi:10.1126/science.aaw1026 (2019).

41 Nagaraj, R. *et al.* Nuclear Localization of Mitochondrial TCA Cycle Enzymes as a Critical Step in Mammalian Zygotic Genome Activation. *Cell* **168**, 210-223 e211, doi:10.1016/j.cell.2016.12.026 (2017).

42 Chen, J. *et al.* Compartmentalized activities of the pyruvate dehydrogenase complex sustain lipogenesis in prostate cancer. *Nat Genet* **50**, 219-228, doi:10.1038/s41588-017-0026-3 (2018).

43 Wang, Y. *et al.* KAT2A coupled with the alpha-KGDH complex acts as a histone H3 succinyltransferase. *Nature* **552**, 273-277, doi:10.1038/nature25003 (2017).

44 Choi, S. *et al.* Oxoglutarate dehydrogenase and acetyl-CoA acyltransferase 2 selectively associate with H2A.Z-occupied promoters and are required for histone modifications. *Biochim Biophys Acta Gene Regul Mech*, 194436, doi:10.1016/j.bbagrm.2019.194436 (2019).

45 Nothjunge, S. *et al.* DNA methylation signatures follow preformed chromatin compartments in cardiac myocytes. *Nat Commun* **8**, 1667, doi:10.1038/s41467-017-01724-9 (2017).

46 Gilsbach, R. *et al.* Distinct epigenetic programs regulate cardiac myocyte development and disease in the human heart in vivo. *Nat Commun* **9**, 391, doi:10.1038/s41467-017-02762-z (2018).

47 Adriaens, C. *et al.* Blank spots on the map: some current questions on nuclear organization and genome architecture. *Histochem Cell Biol* **150**, 579-592, doi:10.1007/s00418-018-1726-1 (2018).

48 Poleshko, A. *et al.* Genome-Nuclear Lamina Interactions Regulate Cardiac Stem Cell Lineage Restriction. *Cell* **171**, 573-587 e514, doi:10.1016/j.cell.2017.09.018 (2017).

49 Stevens, T. J. *et al.* 3D structures of individual mammalian genomes studied by single-cell Hi-C. *Nature* **544**, 59-64, doi:10.1038/nature21429 (2017).

50 Nora, E. P. *et al.* Targeted Degradation of CTCF Decouples Local Insulation of Chromosome Domains from Genomic Compartmentalization. *Cell* **169**, 930-944 e922, doi:10.1016/j.cell.2017.05.004 (2017).

51 Rosa-Garrido, M. *et al.* High-Resolution Mapping of Chromatin Conformation in Cardiac Myocytes Reveals Structural Remodeling of the Epigenome in Heart Failure. *Circulation* **136**, 1613-1625, doi:10.1161/CIRCULATIONAHA.117.029430 (2017).

52 Lee, D. P. *et al.* Robust CTCF-Based Chromatin Architecture Underpins Epigenetic Changes in the Heart Failure Stress-Gene Response. *Circulation* **139**, 1937-1956, doi:10.1161/CIRCULATIONAHA.118.036726 (2019).

53 Bintu, B. *et al.* Super-resolution chromatin tracing reveals domains and cooperative interactions in single cells. *Science* **362**, doi:10.1126/science.aau1783 (2018).

54 Zhang, Y. *et al.* Transcriptionally active HERV-H retrotransposons demarcate topologically associating domains in human pluripotent stem cells. *Nat Genet*, doi:10.1038/s41588-019-0479-7 (2019).

55 Klemm, S. L., Shipony, Z. & Greenleaf, W. J. Chromatin accessibility and the regulatory epigenome. *Nat Rev Genet* **20**, 207-220, doi:10.1038/s41576-018-0089-8 (2019).

56 Abel, E. D. & Doenst, T. Mitochondrial adaptations to physiological vs. pathological cardiac hypertrophy. *Cardiovasc Res* **90**, 234-242, doi:10.1093/cvr/cvr015 (2011).

57 Gibb, A. A. & Hill, B. G. Metabolic Coordination of Physiological and Pathological Cardiac Remodeling. *Circ Res* **123**, 107-128, doi:10.1161/CIRCRESAHA.118.312017 (2018).

58 Carey, B. W., Finley, L. W., Cross, J. R., Allis, C. D. & Thompson, C. B. Intracellular alpha-ketoglutarate maintains the pluripotency of embryonic stem cells. *Nature* **518**, 413-416, doi:10.1038/nature13981 (2015).

59 Lombardi, A. A. *et al.* Mitochondrial calcium exchange links metabolism with the epigenome to control cellular differentiation. *Nat Commun* **10**, 4509, doi:10.1038/s41467-019-12103-x (2019).

60 Erdel, F., Schubert, T., Marth, C., Langst, G. & Rippe, K. Human ISWI chromatin-remodeling complexes sample nucleosomes via transient binding reactions and become immobilized at active sites. *Proc Natl Acad Sci U S A* **107**, 19873-19878, doi:10.1073/pnas.1003438107 (2010).

61 Padinhateeri, R. & Marko, J. F. Nucleosome positioning in a model of active chromatin remodeling enzymes. *Proc Natl Acad Sci U S A* **108**, 7799-7803, doi:10.1073/pnas.1015206108 (2011).

62 Iyer, K. V., Pulford, S., Mogilner, A. & Shivashankar, G. V. Mechanical activation of cells induces chromatin remodeling preceding MKL nuclear transport. *Biophys J* **103**, 1416-1428, doi:10.1016/j.bpj.2012.08.041 (2012).

63 Dang, L. *et al.* Cancer-associated IDH1 mutations produce 2-hydroxyglutarate. *Nature* **462**, 739-744, doi:10.1038/nature08617 (2009).

64 Ward, P. S. *et al.* The common feature of leukemia-associated IDH1 and IDH2 mutations is a neomorphic enzyme activity converting alpha-ketoglutarate to 2-hydroxyglutarate. *Cancer Cell* **17**, 225-234, doi:10.1016/j.ccr.2010.01.020 (2010).

65 Michalak, E. M., Burr, M. L., Bannister, A. J. & Dawson, M. A. The roles of DNA, RNA and histone methylation in ageing and cancer. *Nat Rev Mol Cell Biol* **20**, 573-589, doi:10.1038/s41580-019-0143-1 (2019).

66 Janke, R., Dodson, A. E. & Rine, J. Metabolism and epigenetics. *Annu Rev Cell Dev Biol* **31**, 473-496, doi:10.1146/annurev-cellbio-100814-125544 (2015).

67 Flavahan, W. A. *et al.* Insulator dysfunction and oncogene activation in IDH mutant gliomas. *Nature* **529**, 110-114, doi:10.1038/nature16490 (2016).

68 Letouze, E. *et al.* SDH mutations establish a hypermethylator phenotype in paraganglioma. *Cancer Cell* **23**, 739-752, doi:10.1016/j.ccr.2013.04.018 (2013).

69 Sigismund, S., Avanzato, D. & Lanzetti, L. Emerging functions of the EGFR in cancer. *Mol Oncol* **12**, 3-20, doi:10.1002/1878-0261.12155 (2018).

70 Yang, W. *et al.* EGFR-induced and PKCepsilon monoubiquitylation-dependent NF-kappaB activation upregulates PKM2 expression and promotes tumorigenesis. *Mol Cell* **48**, 771-784, doi:10.1016/j.molcel.2012.09.028 (2012).

71 Yang, W. *et al.* ERK1/2-dependent phosphorylation and nuclear translocation of PKM2 promotes the Warburg effect. *Nat Cell Biol* **14**, 1295-1304, doi:10.1038/ncb2629 (2012).

72 Yang, W. *et al.* PKM2 phosphorylates histone H3 and promotes gene transcription and tumorigenesis. *Cell* **150**, 685-696, doi:10.1016/j.cell.2012.07.018 (2012).

73 Luo, W. *et al.* Pyruvate kinase M2 is a PHD3-stimulated coactivator for hypoxia-inducible factor 1. *Cell* **145**, 732-744, doi:10.1016/j.cell.2011.03.054 (2011).

Chapter 2: Building a Bridge Between Nucleoskeletal Architecture and Chromatin Structure in Cardiac Hypertrophy

[This proposal has been funded by the American Heart Association (20PRE35200059).]

SPECIFIC AIMS

The complex cytoskeletal network provides an often-overlooked link between cell structure and function. In cardiomyocytes, the cytoskeleton provides organization, including structuring sarcomeric proteins to generate force and localizing organelles, including the nucleus, within the cell. Disorganization of these structural proteins can lead to cardiomyopathies[1,2]. Cardiomyocyte hypertrophy, is phenotypically characterized by increased cell size and gene expression changes to compensate for increased workload[3]. However, the extent to which non-sarcomeric cyto- and nucleoskeletal proteins influence gene expression during physical stress remains elusive. The goal of this project is to **determine the role of the cyto- and nucleoskeleton in chromatin remodeling during cardiac hypertrophy.**

While sarcomeric actin and myosin generate contractile force, neither extend to the intercalated discs or costameres, hubs for mechanosensation, signal propagation, and cell-to-cell interactions[4]. Thus, a network of cytoplasmic actin, microtubules, intermediate filaments, and cytoskeletal associated proteins must disperse mechanical forces throughout the cell[5]. In pathologic conditions, gene expression in response to increased workload enables increased production and organization of sarcomeric proteins[6]. **However, the signaling mechanisms linking physical changes in cell phenotype, mechanosensation, and chromatin remodeling are unknown.**

Hypertrophic stress can impact nuclear architecture through physical interactions between intermediate filaments and nuclear envelope[7]. In non-cardiac cells,, increased force applied to the nucleus can affect chromatin tethering at the nuclear lamina[8]. Nuclear lamins dynamically bind to

and influence chromatin structure and gene expression through lamin associated domains (LADs)[9]. Thus, I hypothesize that **physical and mechanical stressors a**ffecting the cytoskeleton may induce changes in nucleoskeletal tension and ***directly*** **influence chromatin accessibility** in cardiac cells.

Our lab has shown the complex and dynamic nature of chromatin architecture in the trans-aortic constriction disease model[10]. By analyzing RNA-seq data, we have identified cyto- and nucleoskeletal proteins with differential regulation and accessibility associated with cardiac disease. The goal of this project is to experimentally manipulate select novel targets to determine the relationship between cytoskeletal proteins, the nuclear membrane and fine-tuned transcriptional responses during pathologic conditions.

Overall Hypothesis. Hypertrophy will increase cardiomyocyte and nuclear rigidity and induce increased nuclear strain, disrupting chromatin architecture through LADs. Knocking down mechanosensitive structural targets will blunt the physical stress changes and prevent chromatin remodeling.

Aim 1. Identify the cytoskeletal and nuclear structural proteins that regulate hypertrophic and physical stress phenotypes of cardiomyocytes. Hypertrophic cardiomyocytes require precise coordination of cyto- and nucleoskeletal proteins to achieve cell size increases while maintaining function. Understanding the proteins regulating hypertrophic stress physical phenotypes will provide insight into fundamental mechanics of hypertrophy and identify possible interventions. Through targeted knockdown and over expression of structural proteins the effects of hypertrophic stimuli on cytoskeletal architecture, cell rigidity, nuclear strain, and gene expression will be investigated.

Aim 2. Determine effects of physical changes to the nuclear cytoskeleton on chromatin organization and spatial gene positioning. Dynamic reorganization of the genome accompanies cardiomyocyte hypertrophy. By investigating LADs during hypertrophy, target

perturbation, and mechanical stress, nuclear architectural proteins and their role in chromatin accessibility and gene expression will be delineated. Furthermore, microscopic identification of heterochromatic changes brought upon by mechanical stress will be assessed.

Significance

Pathological cardiac hypertrophy is a compensatory phenotypic response to increased workload, and, left untreated, will progress to heart failure[11]. Underlying this hypertrophic response, cytoskeletal organization ensures connection of the sarcomere to the cell membrane[12] and is critical for relaying mechanosignals to the nucleus for gene expression[13]. The contractile properties of cardiomyocytes require cytoskeletal interactions to transmit physical forces through the cell and decrease tension on the nuclear membrane[14], ensuring minimal nuclear strain. An essential component of nuclear architecture is chromatin structure itself, including gene suppression by lamina associated domains (LADs)[15]. We will investigate crosstalk between the cyto- and nucleoskeletal network and chromatin in the setting of cardiac hypertrophy (Fig. 1).

Innovation

We plan to expand the lab's existing cardiovascular epigenetics expertise in collaboration with Dr. Amy Rowat to understand the role of cardiomyocyte physical properties in hypertrophy and elucidate how physical forces drive gene regulation. The Rowat lab's expertise in cell physical phenotypes will be fundamental to our study, enabling us to investigate how physical forces are sensed by and regulate chromatin, gene expression and thereby hypertrophic phenotype.

Background

Cardiac Hypertrophy. The heart muscle enlarges with prolonged increased workload, for example in response to hypertension or aortic valve stenosis[11]. Cardiomyocyte structural size increase must be regulated as to not impede cellular function. The cytoskeleton drives cell growth and links diverse cellular mechanisms, from stabilizing intercalated discs (ICDs)[16] to the distribution of tensile force[17], to minimize workload stress on heart function.

Cardiomyocyte Cytoskeletal Organization. Non-contractile cytoskeletal proteins act as a scaffold, connecting sarcolemmal membrane structures to sarcomeric actin and myosin, and ensuring electrical conductance and force transmission remains in sync[18,19]. Contractile function, tensile force dispersion and signal transduction must be managed by the cytoskeletal network[20]. The mechanical stability of the cytoskeletal network also protects the nucleus, where increased strain can affect chromatin interactions and gene expression[21].

Cyto-Nucleoskeletal Interactions and Chromatin Architecture. Chromatin structure is critical for gene expression and is modulated by nuclear morphology[22]. The interaction between cytoplasmic actin and linker of nucleoskeletal and cytoskeletal (LINC) complexes mediates force transduction across the nuclear envelope and provide additional structural support[14]. The LINC complex also connects to the nuclear lamina, which mediates chromatin structure though LADs—heterochromatic regions tethered to the nuclear periphery, thereby repressing gene expression[23]. We will investigate the link between changes in force, LINC complex reorganization, and chromatin architecture during cardiac hypertrophy.

Aim 1. Identify the cytoskeletal and nuclear structural proteins that regulate hypertrophic and physical stress phenotypes of cardiomyocytes. *Hypothesis: Cardiomyocyte hypertrophy will increase cellular and nuclear rigidity, causing increased nuclear strain. Knockdown of cyto- and nucleoskeletal targets will blunt the associated physical changes.*

Aim 1.1: Determine the effects of perturbations of cytoskeletal and nucleoskeletal transcripts on hypertrophic phenotype.

Background, Rationale, and Preliminary Data

Our preliminary RNA-seq experiments from a pressure overload cardiac hypertrophy mouse model revealed differential expression of cyto- and nucleoskeletal gene targets. This approach identified upregulation of vasodilator stimulated phosphoprotein (VASP), an actin nucleation and elongation promoting protein[24] with unknown involvement in heart failure. We will

experimentally manipulate levels of VASP, in addition to inhibiting actin nucleation, to determine their roles in cardiac hypertrophy.

Experimental Design

Hypertrophic Model: Neonatal rat ventricular myocytes (NRVMs) will be treated with β-adrenergic agonist isoproterenol (ISO, 1nM at 0, 24, and 48 hr) to induce hypertrophy[25]. Phenotypic response will be measured by staining F-actin with Phalloidin and nuclei with DAPI (Fig. 2A). Cellular and nuclear size and morphology will be quantified with ImageJ and MATLAB (Fig. 2B). To quantify hypertrophic gene expression (SERCA, αMHC, βMHC, and NPPA), we will perform qRT-PCR (Fig. 2B)[3]. Expression of hypertrophic genes will be determined as a fold difference between control and ISO treated samples (normalized to GAPDH).

Target Knockdown and Overexpression and Mechanism Inhibition: Identified cytoskeletal, nucleoskeletal, and cytoskeletal associated targets will be knocked down via siRNA (scrambled siRNA control) and overexpressed by adenoviral transfection (GFP vector control) to determine the effects on NRVM cellular and nuclear size, survivability, and hypertrophic gene expression. Validation of knockdown and overexpression will be performed by qRT-PCR and Western blot. NRVMs will be treated with ISO in the presence of target perturbation. Our initial target will be VASP based on the preliminary observations (Figure 3A). However, ongoing studies have revealed several other novel cytoskeletal and nucleoskeletal proteins, including LINC complex proteins Sun1 and Nesprin1 (Fig. 3B), and mechanosensitive mechanisms to be explored in a similar manner. We will incorporate drug inhibition of cytoskeletal mechanisms, such as actin nucleation, with cytochalasin B, and severing the LINC complex by KASH 2 overexpression[26].The PI and Vondriska lab have extensive experience with siRNA-mediated knockdown in NRVMs[27-29].

Expected Results, Potential Problems and Alternative Approaches

Knockdown and inhibition of selected targets will blunt hypertrophic cardiomyocyte size increase due to disruption of cytoskeletal organization, while overexpression will exacerbate the phenotype. There is the possibility that knockdown or overexpression will have no effect on hypertrophic phenotype, as alternative cytoskeletal proteins may compensate for the perturbation. By incorporating drug inhibition of cytoskeletal mechanisms, we will identify specific pathways contribution to the hypertrophic phenotype. Identifying these mechanisms will provide insight into regulation of cardiomyocyte physical phenotypes and hypertrophic response.

Aim 1.2: Determine the influence of hypertrophic stimuli and effects of cyto- and nucleoskeletal target perturbation on cardiomyocyte rigidity and nuclear strain.

Background, Rationale, and Preliminary Data

Cardiomyocyte hypertrophy must be accompanied by cellular biophysical changes enabling proper myocardial contraction and force dispersal. Our lab demonstrated that hypertrophy shifts the chromatin towards a euchromatic phenotype, as determined by histone post-translational modifications[30]. We hypothesize increased cardiomyocyte rigidity contributes to this shift, decreasing the flexibility of the cell so that nuclear membrane strain increases and disrupts chromatin interactions. To determine cyto- and nucleoskeletal changes impacting cardiomyocyte rigidity and nuclear physical phenotypes, we will use the biophysical assays parallel microfiltration (PMF)[31] (Fig. 4), which has identified molecular mediators of cellular and nuclear deformability[31-33], but never been employed to investigate cardiomyocyte rigidity, and cell stretch assay to reveal the effects of cyclic stretching on nuclear strain[34]. Probing for identified targets will further delineate the cyto- and nucleoskeletal contribution to rigidity and nuclear strain.

Experimental Design

Cell and Nuclei Rigidity: ISO treated and control NRVM cell and nuclei rigidity will be investigated by PMF. In PMF, a suspension of cells is driven to deform through micron-sized

pores; stiffer cells occlude the pores (Fig. 4A), resulting in an increased volume of cell suspension, a measure of cellular deformability (Fig. 4B). We will set the pore size to ½ median cell size and optimize applied pressure for cardiomyocytes, as described for other cells by Dr. Rowat[35]. To assess nuclear rigidity, we will decrease pore size so the nucleus rate-limits cell transit through the pores (Fig. 4C)[36]. Identified targets and mechanisms from Aim 1.1 will be used to observe selected perturbations effect whole cell or nuclear rigidity.

Cell Stretch Assay: Mechanical stress will be applied to NRVMs, with and without ISO and target perturbation, using a custom-built cell stretching apparatus[26] on a prepared flexible PDMS membrane[35]. To quantify nuclei strain, cells will be stained with Hoechst and subjected to stretching by 5% of the length of the cardiomyocyte membrane for 2 hours at 0.5 Hz (analysis with ImageJ). To determine the effects of repetitive stretch on cell viability and nuclei strain, cells will be subjected to 24 h of stretching (viability quantified by trypan blue and propidium iodide).

Expected Results, Potential Problems and Alternative Approaches

We reason that larger myofibrillar size will come at the expense of cell flexibility, leading to a more rigid cells and higher nuclear strain. Although rigidity can be assessed at the cardiomyocyte level, the lack of fibroblasts and extracellular contributions to whole heart mechano-properties cannot be assessed through this assay. By utilizing the cell stretch assay, we will have a better assessment of the impact of non-myocyte stressors. Nuclear deformability by PMF will provide nuclear deformability data, but it is not independent from cytoskeletal involvement. Isolating cardiomyocyte nuclei and performing the PMF assay will highlight nuclear structure physical phenotypes. We anticipate some challenges using the rigidity assay on cardiac cells, which are not in suspension, but are confident we can overcome them working closely with Dr. Rowat. We will also examine isolated cardiac nuclei to directly measure changes in nuclear rigidity.

Aim 2. Determine how the physical stress phenotypes of the nucleus influence chromatin structure and spatial gene positioning. *Hypothesis: Downstream effects of cytoskeletal perturbations and hypertrophic stimuli will alter chromatin structure through regulation of nuclear rigidity and differential accessibility of Lamin associated domains.*

Background, Rationale, and Preliminary Data

Spatial organization of chromatin requires precise interactions between nucleosomes, chromatin architectural proteins, and the nuclear lamina. A combination of LADs and the histone mark H3K9me2 localize heterochromatic regions to the nuclear periphery (Fig 4A)[15], conferring a repressive state. Our lab has measured spatial reorganization of pathological genes *in vivo* during cardiac disease (Fig 4B)[37]. The LINC complex mediates cyto-to-nucleoskeletal interactions, providing indirect connections between the cytoskeleton and nuclear lamina[38]. Upon mechanical stress, epidermal skin cells alter LINC complex proteins inducing changes in LAD and heterochromatic architecture[13]—whether this is a cell type specific phenomenon is unknown. In Aim 2, we will identify changes in LADs, histone marks, and spatial gene organization in response to hypertrophic and mechanical stress.

Experimental Design

LAD Identification. NRVMs will be treated with ISO and exposed to 24 hr of cyclical mechanical strain on the stretching apparatus. LADs will be identified by lamin A chromatin immunoprecipitation followed by sequencing (ChIP-seq)[28,29]. Lamin A-ChIP library will be sequenced on an Illumin HiSeq 2000 instrument with the guidance of Dr. Matteo Pelligrini. ChIP-seq bioinformatics for identification of differential LADs will be performed with guidance from Dr. Chapski in the Vondriska lab[10,39]. LINC complex disruption via KASH2 OE will delineate cell and nuclear structure dynamics on chromatin architecture. We will compare our LAD domains with those from other cell types, stem cell derived myocytes in particular[15].

Chromatin Architecture Microscopy. Visualization of the nuclear lamina, LADs and nearby genes will enable quantification of hypertrophic stimuli and mechanical stress-induced chromatin restructuring at specific genes. NRVMs will be treated as described and the nuclei stained with lamin A and the LAD specific histone mark H3K9me2[3]. Additionally, the identification of dynamic LAD genes through ChIP-seq allows subsequent evaluation of spatial reorganization via fluorescent *in situ* hybridization (FISH) as described by our lab[40,41]. Imaging will be done by confocal microscopy and analyzed for distance of FISH probe to the nuclear lamina using Imaris software.

Expected Results, Potential Pitfalls, and Alternative Approaches

Cardiomyocyte hypertrophy and mechanical strain will drive dynamic changes in LADs that will be linked to differential gene regulation based on chromatin architectural rearrangement. Additionally, through FISH of selected LAD genes, the spatial reorganization of hypertrophic genes will be observed, from shifts to the nucleoplasm or periphery based on differential expression and LADs. Viewing LADs as on or off switches greatly oversimplifies the complexity of chromatin architecture—thus expression of select differential LAD genes may not be tied to spatial rearrangement. Additionally, a shift from the LAD (away from the nuclear periphery) may not confer a euchromatic state. Staining for additional euchromatic and heterochromatic histone marks in addition to FISH may have resolution limitations, but ChIP-qPCR for select differential LAD genes using antibodies against heterochromatic marks would identify if genes that moved away from the periphery indeed shift to a euchromatic state.

Ethical Aspects of the Proposed Research

This project relies on *in vitro* models and therefore it will be necessary to use rodents in a portion of this project. Specifically, we will use neonatal rats to generate primary cell cardiomyocyte cultures for initial target screening and follow up cell biophysical assays, molecular tests, and microscopy. For more details, please see Vertebrate Animals section.

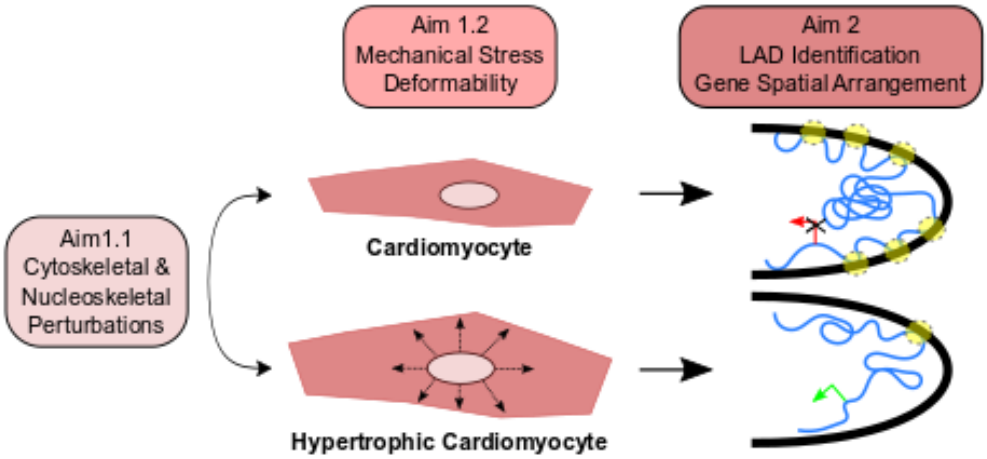

Figure 2-1. Linking the Cyto- and Nucleoskeleton to Hypertrophic Biophysics and Chromatin Architecture. Identify cyto- and nuceloskeletal involvement in hypertrophic phenotype (Aim 1.1). We hypothesize hypertrophy will induce increased cardiomyocyte rigidity, affecting tension and nuclear strain, denoted by dashed arrows (Aim 1.2). Increase in nuclear strain is hypothesized to disrupt LAD chromatin organization (yellow dashed circles) and gene expression (Aim 2). (TK unpublished hypothesis)

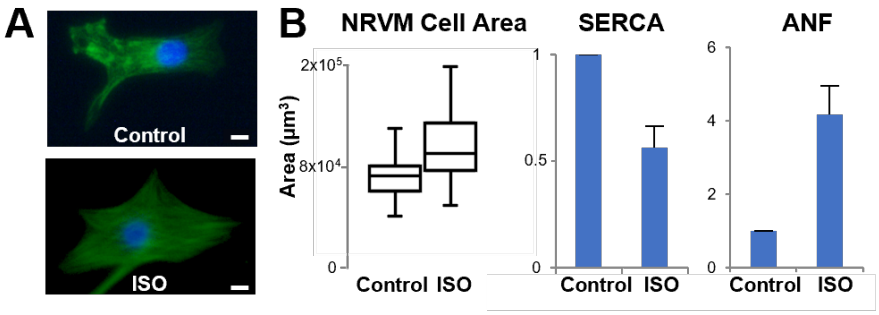

Figure 2-2. Hypertrophic Phenotype End Points. A. NRVM: Top: Control, bottom ISO treated (1 µM, 48hr, bar = 50 µm) **B.** Hypertrophic end ponts: cellarea from control and ISO treated NRVMs. (n=3, >50 cells, * = $p<0.05$). qRT-PCR SERCA and ANF (n=2, $\pm$SD). (TK, ongoing studies)

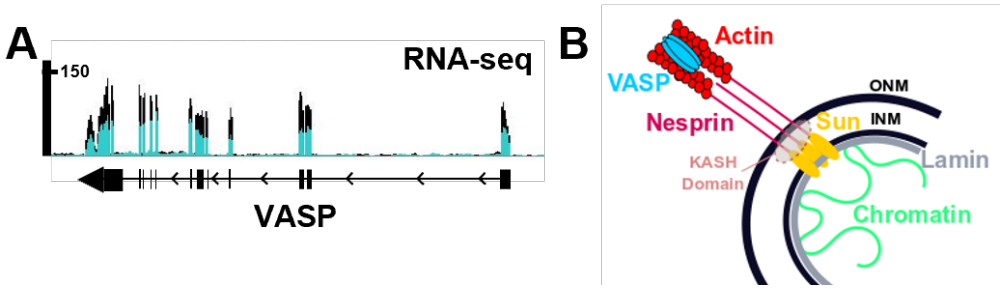

Figure 2-3. Cytoskeletal and Nucleoskeletal Target Identification. A. VASP RNA-seq, upregulation in TAC (black) compared to control (blue). **B.** Schematic of possible LINC complex targets. KASH2 overexpression disrupts the complex, identifying nucleoskeletal involvement in hypertrophic phenotype (dashed circle). (TK and TV, ongoing studies)

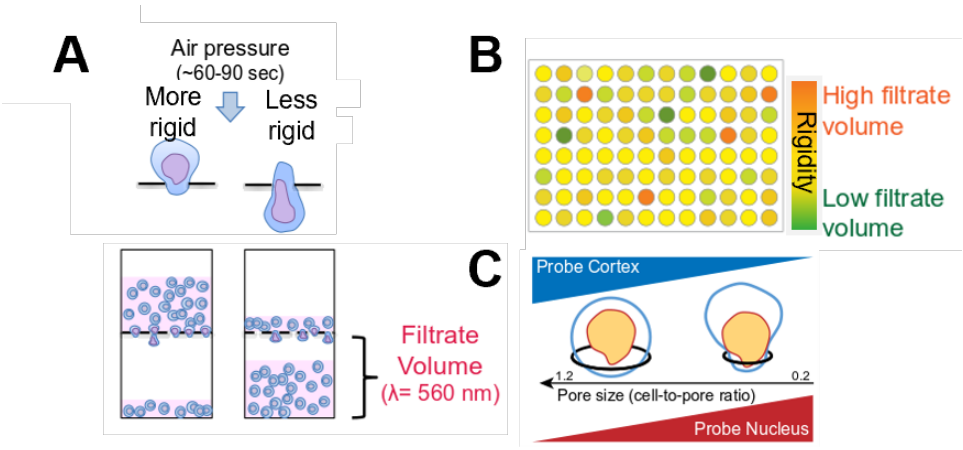

Figure 2-4. Parallel Microfiltration Rigidity Assay. A. Cell rigidity measured by cell migration through pores. **B.** Absorbance as a quantification of cardiomyocyte rigidity. **C.** Nuclear rigidity measured by decreasing pore size. (Images provided by collaborator Dr. Amy Rowat)

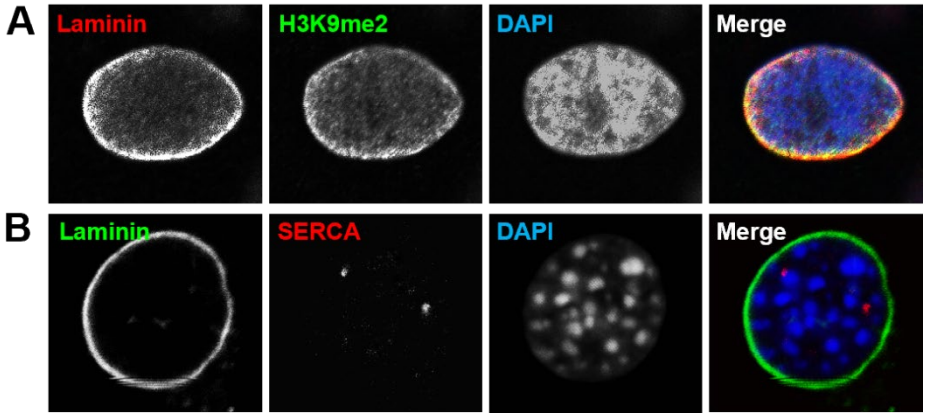

Figure 2-5. Chromatin Architecture Microscopy. A. NRVM IHC, nuclear laminin and H3K9me2 localized to the nuclear periphery. **B.** 3T3 cell IHC with SERCA FISH. Laminin signal on nuclear periphery and SERCA in the nucleoplasm, indicative of active transcription. (Vondriska lab, unpublished)

Chapter 2: Bibliography

1 Sato, H. *et al.* Microtubule stabilization in pressure overload cardiac hypertrophy. *J Cell Biol* **139**, 963-973, doi:10.1083/jcb.139.4.963 (1997).

2 Lyon, R. C., Zanella, F., Omens, J. H. & Sheikh, F. Mechanotransduction in cardiac hypertrophy and failure. *Circ Res* **116**, 1462-1476, doi:10.1161/CIRCRESAHA.116.304937 (2015).

3 Rajabi, M., Kassiotis, C., Razeghi, P. & Taegtmeyer, H. Return to the fetal gene program protects the stressed heart: a strong hypothesis. *Heart Fail Rev* **12**, 331-343, doi:10.1007/s10741-007-9034-1 (2007).

4 Rybakova, I. N., Patel, J. R. & Ervasti, J. M. The dystrophin complex forms a mechanically strong link between the sarcolemma and costameric actin. *J Cell Biol* **150**, 1209-1214, doi:10.1083/jcb.150.5.1209 (2000).

5 Tsikitis, M., Galata, Z., Mavroidis, M., Psarras, S. & Capetanaki, Y. Intermediate filaments in cardiomyopathy. *Biophys Rev* **10**, 1007-1031, doi:10.1007/s12551-018-0443-2 (2018).

6 Kooij, V. *et al.* Profilin modulates sarcomeric organization and mediates cardiomyocyte hypertrophy. *Cardiovasc Res* **110**, 238-248, doi:10.1093/cvr/cvw050 (2016).

7 Belaadi, N., Aureille, J. & Guilluy, C. Under Pressure: Mechanical Stress Management in the Nucleus. *Cells* **5**, doi:10.3390/cells5020027 (2016).

8 Miroshnikova, Y. A., Nava, M. M. & Wickstrom, S. A. Emerging roles of mechanical forces in chromatin regulation. *J Cell Sci* **130**, 2243-2250, doi:10.1242/jcs.202192 (2017).

9 van Steensel, B. & Belmont, A. S. Lamina-Associated Domains: Links with Chromosome Architecture, Heterochromatin, and Gene Repression. *Cell* **169**, 780-791, doi:10.1016/j.cell.2017.04.022 (2017).

10 Rosa-Garrido, M. *et al.* High-Resolution Mapping of Chromatin Conformation in Cardiac Myocytes Reveals Structural Remodeling of the Epigenome in Heart Failure. *Circulation* **136**, 1613-1625, doi:10.1161/CIRCULATIONAHA.117.029430 (2017).

11 Shimizu, I. & Minamino, T. Physiological and pathological cardiac hypertrophy. *J Mol Cell Cardiol* **97**, 245-262, doi:10.1016/j.yjmcc.2016.06.001 (2016).

12 Craig, S. W. & Pardo, J. V. Gamma actin, spectrin, and intermediate filament proteins colocalize with vinculin at costameres, myofibril-to-sarcolemma attachment sites. *Cell Motil* **3**, 449-462 (1983).

13 Le, H. Q. *et al.* Mechanical regulation of transcription controls Polycomb-mediated gene silencing during lineage commitment. *Nat Cell Biol* **18**, 864-875, doi:10.1038/ncb3387 (2016).

14 Kim, J. K. *et al.* Nuclear lamin A/C harnesses the perinuclear apical actin cables to protect nuclear morphology. *Nat Commun* **8**, 2123, doi:10.1038/s41467-017-02217-5 (2017).

15 Poleshko, A. *et al.* Genome-Nuclear Lamina Interactions Regulate Cardiac Stem Cell Lineage Restriction. *Cell* **171**, 573-587 e514, doi:10.1016/j.cell.2017.09.018 (2017).

16 Bennett, P. M. Riding the waves of the intercalated disc of the heart. *Biophys Rev* **10**, 955-959, doi:10.1007/s12551-018-0438-z (2018).

17 Kim, D. H. & Wirtz, D. Cytoskeletal tension induces the polarized architecture of the nucleus. *Biomaterials* **48**, 161-172, doi:10.1016/j.biomaterials.2015.01.023 (2015).

18 Benz, P. M. *et al.* Mena/VASP and alphaII-Spectrin complexes regulate cytoplasmic actin networks in cardiomyocytes and protect from conduction abnormalities and dilated cardiomyopathy. *Cell Commun Signal* **11**, 56, doi:10.1186/1478-811X-11-56 (2013).

19 Israeli-Rosenberg, S., Manso, A. M., Okada, H. & Ross, R. S. Integrins and integrin-associated proteins in the cardiac myocyte. *Circ Res* **114**, 572-586, doi:10.1161/CIRCRESAHA.114.301275 (2014).

20 Kim, D. H., Chambliss, A. B. & Wirtz, D. The multi-faceted role of the actin cap in cellular mechanosensation and mechanotransduction. *Soft Matter* **9**, 5516-5523, doi:10.1039/C3SM50798J (2013).

21 Guilluy, C. *et al.* Isolated nuclei adapt to force and reveal a mechanotransduction pathway in the nucleus. *Nat Cell Biol* **16**, 376-381, doi:10.1038/ncb2927 (2014).

22 Bronshtein, I. *et al.* Loss of lamin A function increases chromatin dynamics in the nuclear interior. *Nat Commun* **6**, 8044, doi:10.1038/ncomms9044 (2015).

23 Finlan, L. E. *et al.* Recruitment to the nuclear periphery can alter expression of genes in human cells. *PLoS Genet* **4**, e1000039, doi:10.1371/journal.pgen.1000039 (2008).

24 Chesarone, M. A. & Goode, B. L. Actin nucleation and elongation factors: mechanisms and interplay. *Curr Opin Cell Biol* **21**, 28-37, doi:10.1016/j.ceb.2008.12.001 (2009).

25 Zou, Y. *et al.* Isoproterenol activates extracellular signal-regulated protein kinases in cardiomyocytes through calcineurin. *Circulation* **104**, 102-108, doi:10.1161/hc2601.090987 (2001).

26 Kim, P. H. *et al.* Disrupting the LINC complex in smooth muscle cells reduces aortic disease in a mouse model of Hutchinson-Gilford progeria syndrome. *Sci Transl Med* **10**, doi:10.1126/scitranslmed.aat7163 (2018).

27 Monte, E. *et al.* Systems proteomics of cardiac chromatin identifies nucleolin as a regulator of growth and cellular plasticity in cardiomyocytes. *Am J Physiol Heart Circ Physiol* **305**, H1624-1638, doi:10.1152/ajpheart.00529.2013 (2013).

28 Monte, E. *et al.* Reciprocal Regulation of the Cardiac Epigenome by Chromatin Structural Proteins Hmgb and Ctcf: IMPLICATIONS FOR TRANSCRIPTIONAL REGULATION. *J Biol Chem* **291**, 15428-15446, doi:10.1074/jbc.M116.719633 (2016).

29 Franklin, S. *et al.* The chromatin-binding protein Smyd1 restricts adult mammalian heart growth. *Am J Physiol Heart Circ Physiol* **311**, H1234-H1247, doi:10.1152/ajpheart.00235.2016 (2016).

30 Franklin, S. *et al.* Quantitative analysis of the chromatin proteome in disease reveals remodeling principles and identifies high mobility group protein B2 as a regulator of hypertrophic growth. *Mol Cell Proteomics* **11**, M111 014258, doi:10.1074/mcp.M111.014258 (2012).

31 Qi, D. *et al.* Screening cell mechanotype by parallel microfiltration. *Sci Rep* **5**, 17595, doi:10.1038/srep17595 (2015).

32 Kim, T. H. *et al.* Stress hormone signaling through beta-adrenergic receptors regulates macrophage mechanotype and function. *FASEB J* **33**, 3997-4006, doi:10.1096/fj.201801429RR (2019).

33 Gill, N. K. *et al.* DYT1 Dystonia Patient-Derived Fibroblasts Have Increased Deformability and Susceptibility to Damage by Mechanical Forces. *Front Cell Dev Biol* **7**, 103, doi:10.3389/fcell.2019.00103 (2019).

34 Verstraeten, V. L., Ji, J. Y., Cummings, K. S., Lee, R. T. & Lammerding, J. Increased mechanosensitivity and nuclear stiffness in Hutchinson-Gilford progeria cells: effects of farnesyltransferase inhibitors. *Aging Cell* **7**, 383-393, doi:10.1111/j.1474-9726.2008.00382.x (2008).

35 Gill, N. K. *et al.* A scalable filtration method for high throughput screening based on cell deformability. *Lab on a Chip* **19**, 343-357, doi:10.1039/c8lc00922h (2019).

36 Rowat, A. C. *et al.* Nuclear envelope composition determines the ability of neutrophil-type cells to passage through micron-scale constrictions. *J Biol Chem* **288**, 8610-8618, doi:10.1074/jbc.M112.441535 (2013).

37 Karbassi, E. *et al.* Relationship of disease-associated gene expression to cardiac phenotype is buffered by genetic diversity and chromatin regulation. *Physiol Genomics* **48**, 601-615, doi:10.1152/physiolgenomics.00035.2016 (2016).

38 Crisp, M. *et al.* Coupling of the nucleus and cytoplasm: role of the LINC complex. *J Cell Biol* **172**, 41-53, doi:10.1083/jcb.200509124 (2006).

39 Chapski, D. J., Rosa-Garrido, M., Hua, N., Alber, F. & Vondriska, T. M. Spatial Principles of Chromatin Architecture Associated With Organ-Specific Gene Regulation. *Front Cardiovasc Med* **5**, 186, doi:10.3389/fcvm.2018.00186 (2018).

40 Karbassi, E. *et al.* Direct visualization of cardiac transcription factories reveals regulatory principles of nuclear architecture during pathological remodeling. *J Mol Cell Cardiol* **128**, 198-211, doi:10.1016/j.yjmcc.2019.02.003 (2019).

41 Bienko, M. *et al.* A versatile genome-scale PCR-based pipeline for high-definition DNA FISH. *Nat Methods* **10**, 122-124, doi:10.1038/nmeth.2306 (2013).

Chapter 3: Concentric Hypertrophy Induces Nucleoskeletal Ultrastructural Reorganization Through Lamin A/C

Introduction

Cardiac hypertrophy is a tissue and cellular response to elevated workload on the heart. Cardiac stressors, such as hypertension induced pressure overload, force an adaptive remodeling of the myocardium to alleviate stress on the left ventricular wall.[1] At the cellular level, hypertrophy causes an increase in cardiomyocyte size without proliferation, and in the pressure overload model, concentric remodeling, with myocytes adding sarcomeric units in parallel, increasing cellular width. During left ventricular (LV) concentric remodeling, the cardiac tissue demonstrates increased LV wall thickness, with a decrease or no change in chamber size and increased interstitial fibrosis.[2] While these mechanisms serve to decrease LV wall stress during hypertrophy, a byproduct is a stiffening of the myocardial tissue.[3]

While all cells of the body are responsive to their environment, the constant work cycle of contraction-relaxion by cardiomyocytes against the stiffness of the heart tissue makes their sensitivity to changes in biophysical parameters vital for cardiac function. Cardiomyocyte hubs for mechanosensitive proteins, including the sarcomeric z-disk, sarcolemma, and intercalated disks, respond to these cues and translate these signals into various molecular processes, some of which result in changes in gene regulation.[4] Early in cardiac stress, compensatory pathological gene programs and chromatin architecture are reactive prior to pathological phenotypes.[5] There remains the question of the direct physical mechanisms by which cardiomyocytes sense stress to the myocardium

and how these signals are relayed to the nucleus to change gene expression in a coordinated, specific manner.

Intermediate filaments connect the sarcomeric z-disk to the nuclear membrane via the linker of nucleoskeleton and cytoskeleton (LINC) complex.[6] The LINC complex connects the sarcomeric and cytoskeletal architecture to the nucleus and the nucleoskeletal scaffold lamin proteins (Lamin A/C and LaminB1).[7] The lamins have dual roles within the nucleus, one to structurally support the nucleoskeleton from compressive forces, and two, to bind to heterochromatic chromatin regions at the nuclear periphery, termed lamin-associated domains (LADs).[8] While the gene regulatory function and the effect of the rearrangement of LADs on chromatin architecture during disease,[9] the ultrastructural changes to nuclear lamins during increased stress and cardiac workload have not been defined. We hypothesized pressure overload-induced concentric hypertrophy induces increased Lamin A/C transcription, via a process that involves reorganized local chromatin structure. This change in Lamin A/C transcription leads to thicker nuclear Lamin A/C deposits, which may play a role to protect the nucleus against increased forces associated with cardiac hypertrophy.

Materials and Methods

Neonatal Rat Ventricular Myocyte Isolation, Hypertrophic Stimulus, and Imaging

Neonatal rat ventricular myocytes (NRVMs) were isolated via enzymatic dissociation from 1-day-old litters and placed in DMEM supplemented with 1% penicillin, 1% streptomyocin, 1% ITS, and 10% FBS for the first 24h, after which the cells were cultured in serum- and antibiotic-free media. To induce NRVM hypertrophy, isoproterenol (1μM) or phenylephrine (10 uM) were added to the cell media and incubated for 48h. For fluorescent imaging, NRVMs were fixed with 3.7% formaldehyde in PBS for 10min, washed with PBS, permeabilized in 0.1% Triton X-100 for 5min, and blocked in 1% BSA for 30min. NRVMs were incubated with Alexa Fluor 488 Phalloidin (Thermo: A12379, 1:1000 dilution) and DAPI for 20min, rinsed and imaged with Zeiss Axio Vert.A1. Images were analyzed using ImageJ.

RNA Isolation and RT-qPCR

Total RNA was isolated from NRVMs by Trizol extraction and quantified and normalized by NanoDrop and process for cDNA according to manufacturer instruction (Bio-Rad: 1708891) real-time PCR was performed in a CFX96 Real-Time PCR Detection System (Bio-Rad) using SsoFast EvaGreen Supermix (Bio-Rad: 1725201). Relative expression was obtained by $\Delta\Delta$Ct methodology.[10]

Parallel Microfiltration Assay

NRVM stiffness was measured using parallel microfiltration (PMF).[11,12] NRVMs were treated with hypertrophic agonists and detached from the plates using trypsin

without spinning down a pellet, trypsin and pelleting the cells, and scraping the cells. Cells were counted and size distributions were obtained by a cell counter (TC20, Bio-Rad) and resuspended to a concentration of $5x10^5$/ml. Cells were loaded into a the PMF wells overlayed on a 10 μm pore polycarbonate membrane (Millipore), and air pressure (2.0 kPa for 30s) was applied to force cells through the membrane pores. The magnitude of cell filtrations was determined by measuring the absorbance of the retained volume at λ560 using a plate reader (SpectraMax M2, Molecular Devices).[12] Cells with increased stiffness would occlude the pores and exhibit a higher retention volume, with PMF Retention % quantified by volume retained/volume loaded.

Adult Murine Cardiomyocyte and Culture

For culturing and immunohistoflourescence experiments, prior to isolation, coverslip or plastic culture dishes were coated with 5 μg/ml laminin for at least 1 hour prior to plating.

Adult mice were treated with heparin (100 USP units) for 20 minutes to prevent blood coagulation followed by anesthetization with sodium pentobarbital (100 μl of 50 mg/ml dilution, intra-peritoneal). Upon loss of rear foot reflex, the heart was removed and instantaneously arrested in ice-cold phosphate buffered saline (PBS). The aorta was canulated with a blunt ended 22-gauge needle and mounted on a modified Langendorff apparatus for perfusion with Tyrode's solution, digestion buffer, and Krebs buffer (KB).

To optimize cardiomyocyte culture, multiple versions of Perfusion Buffer were used, ultimately finding Tyrode's solution (130mM NaCl, 5.4mM KCl, 1mM $MgCl_2$, 0.6mM Na_2HPO_4, 10mM glucose, and 10mM HEPES, pH 7.37, oxygenated with 95% (v/v) O_2-

5% (v/v) CO_2) supplemented with 10 mM BDM[13] achieved optimal rod-shaped cardiomyocytes. The addition of EGTA to chelate calcium[14] did not improve viability. Digestion buffer (50 ml Tyrode's buffer with 70mg collagenase type-II and 5mg protease type-XIV) was perfused through the heart for 10-20 minutes. For culturing conditions, following 4 minutes of perfusion with digestion buffer, 12.5mM of $CaCl_2$ was added to the digestion buffer to introduce calcium back into the cardiac tissue. The heart was washed for 5min with Krebs buffer (KB) (25mM KCl, 10mM KH_2PO_4, 2mM $MgSO_4$, 20mM glucose, 20mM taurine, 5mM creatine, 100mM potassium glutamate, 10mM aspartic acid, 0.5mM EGTA, 10 mM BDM, 5mM HEPES, pH 7.18) oxygenated with 95% O_2-5% (v/v) CO_2. Cardiomyocytes were dissociated in KB solution, filtered (100µm strainer), adding 25 µM blebbistatin to and centrifuged 2 min at 200g for further usage.

Cardiomyocytes must become calcium tolerant in order to remain viable in culture media. Calcium reintroduction gradually introduces higher concentrations of calcium before resuspension in culture media. Two versions were attempted, one by using step wise $CaCl_2$ addition, 100 µM, 400 µM, 900µM concentrations before adding culture buffer.[13] Another method was a dilution of culture media in KB (25:75, 50:50, and 75:25).[14] The culture media with the best results was Gibco MEM, Hanks' Balanced Salt (11575-032), MEM 11095 was also used to limited success, and calcium free media (21068028) was attempted to no success. If the culture conditions yielded rod shaped myocytes post culture media introduction, LIVE/DEAD Viability Cytotoxicity Kit (Thermo: L3224) was performed at time 0h, 24h, 48h, and 72h per manufacturer instructions.

TAC Surgery and Echocardiography

All animal surgery, echocardiography and euthanasia procedures were approved by the UCLA Animal Research Committee in compliance with the National Institutes of Health Guide for the Care and Use of Laboratory Animals. Transverse aortic constriction was performed as described.[15,16] Briefly, C57BL/6J (8 weeks) animals were anesthetized, intubated, and ventilated with 2% isoflurane in 98% O_2, 2% CO_2 during surgery. After shaving hair, the chest was entered from the left side via the third intercostal space, the aorta identified at the T8 region and a venous vascular clamp (Fine Science Tools), which is outfitted with a band of silastic tubing at its distal edge, was placed around the vessel. The internal diameter of the resulting modified clamp was that of a 27-gauge needle. The chest was then closed using 6-0 prolene sutures, and negative pressure in the thorax was returned via removal of air by a PE 50 chest tube attached to a syringe. Mouse chest was then closed, and the animals extubated. Post-operatively, animals were administered analgesics (buprenorphine, subcutaneously, 0.05–0.1 mg/kg) if they exhibit signs of distress (vocalizing, failure to groom, immobility) until the animal improves or is euthanized. After the TAC procedure, mice were monitored by echocardiography (Vevo 3100, Visualsonics) under anesthesia (2% isoflurane in 98% O_2, 2% CO_2 using an anesthesia chamber for initial sedation and a nosecone to maintain delivery of anesthetic throughout the course of the procedure) every 7 days and considered to be in compensatory hypertrophy when the LV wall thickness was increased significantly above the mean of the SHAM group (3 weeks). After diagnosis, the mice were sacrificed by a lethal dose of sodium pentobarbital (80–100 mg/kg) administered intraperitoneally, a method approved by the UCLA Animal Research Committee.

Isolated Cardiomyocyte Fluorescent and Confocal Imaging

For florescent imaging experiments, isolated cardiomyocytes were fixed with 3.7% formaldehyde in PBS for 10min, washed with PBS, permeabilized in 0.1% Triton X-100 for 5min, and blocked in 1% BSA for 30min. Cardiomyocytes were incubated with Alexa Fluor 488 Phalloidin (Thermo: A12379, 1:1000 dilution) and DAPI for 20min, rinsed and imaged with Zeiss Axio Vert.A1. Images were analyzed using ImageJ.

For confocal imaging, isolated cardiomyocytes, as described[17] were fixed with chilled methanol for 10min at -20°C. Myocytes were washed and blocked for 1h in Sea Block blocking buffer (Thermo: 37527). Cells were incubated for 24-48h in primary antibodies at 4°C at dilution of 1:100 in blocking buffer (Lamin A/C: abcam: ab8984, LaminB1: abcam: ab16048, Sarcomeric Actin: abcam: ab137346). Cells were washed and incubated with secondary antibodies (Thermo: Alexa Phalloidin-488, Alexa Fluor-568 and Alexa Fluor-647 species specific to primary antibody) for 1h at room temperature. Cells were washed and stained with DAPI for 10min before a final wash and mounting with ProLong Gold Antifade Reagent (Thermo: P10144). Confocal images were taken using a Nikon A1R, using 60x objective for whole cell imaging and 100x for nuclear ultrastructural imaging. Image analysis done with ImageJ.

MELTRON Hi-C Analysis

Hi-C data set was analyzed for a previous publication.[16] The MELTRON algorithm code and analysis were performed as previously described[18] with a 300 Mbp bin size around the Lmna locus.

Results

α_1 and β-Adrenergic Stimulation of NRVMs Induced Hypertrophy and Effects on Cellular Stiffness

Neonatal rat ventricular myocytes (NRVMs) were used to investigate the connection between cellular physical dynamics in cardiac hypertrophy and chromatin architecture. NRVMs were treated with PBS (Control), isoproterenol (ISO, 1 μM), or phenylephrine (PHE, 10 μM), known hypertrophic inducing β-adrenergic[19] and α_1-adrenergic agonist,[20] respectively, for 48 hours to induce and assess hypertrophic phenotype. NRVMs were stained for F-actin and imaged with a fluorescent microscope to quantify agonist effect on cell size (**Figure 1A**). PHE treatment led to a significantly larger NRVM size, compared to ISO and Control, with ISO inducing a modest effect on NRVM size (**Figure 1B**, left). The 'fetal gene program[21]' becomes activated during cardiac hypertrophy, including beta-myosin heavy chain (bMHC), atrial natriuretic factor (ANF), and natriuretic peptide B (BNP), and qPCR analysis in the groups showed similar results, PHE induced greater relative expression of the expected gene expression profile than ISO (**Figure 1B**, right). Cardiomyocyte hypertrophy induces a stiffer cardiac muscle,[3] and while the extracellular matrix plays a large role, to relieve stress on the left ventricular wall,[22] it was unknown how much the cardiomyocyte population contributed to this stiffening. To assess whether larger NRVM size was associated with a stiffer cellular phenotype, we attempted to use the Parallel Microfiltration Assay (PMF), a cell population stiffness readout, which uses pressure to force cells through 10 μM pores, the stiffer the cell, the less would be filtered through the pore.[11] The results were inconclusive (**Figure**

1C), showing high variability between how the cells were detached from the plate. While the PMF assay has been utilized for cardiac fibroblasts,[23] cardiomyocyte stiffness is a result of sarcomeric structure, with the z-disk spanning titin protein contributing the most to passive stiffness,[24] and NRVMs, even in a hypertrophic state, due to their immaturity, have low levels of striated, sarcomeric organization and tended to ball up upon detachment.

Adult Cardiomyocyte Isolation and Culture

Adult cardiomyocytes were isolated and cultured for cellular characterization and identification of novel cardiomyocyte specific mechanosensitive mechanisms contributing to hypertrophy in a mature, functional cardiomyocyte. Isolation conditions have been well documented in the lab,[16] but culturing conditions for murine cardiomyocytes had not been elucidated. While many labs have shown success in the culturing of murine cardiomyocytes, each has its own set of parameters and culturing conditions specific to the protocol, and compared to other rodent or immature cardiomyocyte models has therefore been extremely challenging. Cardiomyocytes need specific calcium conditions in the media to survive with their rod-shaped form: however, if the conditions of isolation buffers or culture prep are not ideal, isolated cardiomyocytes hypercontract and are no longer viable. We first set to use the isolation conditions from O'Connell et al.[25] This protocol uses 2,3-butanedione monoxime (BDM) to inhibit actin-myosin crossbridge formation and a calcium reintroduction protocol that uses increased concentrations of calcium to induce calcium tolerance in surviving myocytes. This led to variable results, however, to increase cell viability, the addition of blebbistatin (25 μM), another actin-myosin crossbridge inhibitor, led to a higher success rate.[26] Cardiomyocyte viability assay

was performed at time 0, immediately after cell attachment and 72 hours, which showed cells remaining attached positive for calcien AM, a live cell dye, with minimal ethidium homodimer-1 stained cells (dead), while the percentage of live cells remained consistent, the number of cells counted diminished over time, likely due to cell death and detachment (**Figure 2A and B**). Another observation was the loss of identifiable sarcomeric organization under brightfield, with many myocytes having a bubbly look, which could indicate the start of cell death, or dedifferentiation, which happens the longer myocytes are removed from the tissue environment and inhibited from contracting. However, the success rate of viable culturing methods remained problematic, estimated at 10%. Another culturing protocol[14] proposed a different calcium reintroduction method, by a dilution of the culture media. This, again, led to minimal success. Isolate methods demonstrated rod-shaped and viable cardiomyocytes (**Figure 2C,** left), but the calcium reintroduction and the addition of culture media consistently resulted in hypercontraction (**Figure 2C**, right). Attempts to improve these sections included pH balancing the media, which would become more acidic with time and changing the media to differing levels of $CaCl_2$, including one with no calcium, however these made no significant difference to the success rate. The end result of these trials did lead to a reproducible cardiomyocyte isolation method and cell attachment for cardiomyocyte immunohistofluorescence analysis (**Figure 2D**). By keeping the cardiomyocytes in Kreb's buffer supplemented with blebbistatin and BDM, the attached to laminin coated coverslips in 1 hour and can be immediately fixed and stained for microscopic analysis (Buffer and attachment conditions, **Table 1-1**).

Pressure Overload Induced Concentric Hypertrophy

Transverse aortic constriction (TAC), a pressure overload model of heart disease,[27] was used to induce hypertrophy *in vivo* to characterize the phenotype 3 weeks after TAC surgery and identify mechanosensitive pathways connecting cell physical dynamics with chromatin gene position and regulation. The TAC model exhibits increased fibrosis[28] and an initial phase of concentric hypertrophy until the heart eventually succumbs to heart failure.[15] The hypertrophic phase represents a compensatory middle ground, with increased cardiomyocyte and tissue size, without significant detriment to tissue function. The 3-week time point was chosen as the end point, as 5-6 weeks leads to failure. At 3 weeks, M-mode images (**Figure 3A**) show the left ventricular wall thickening with less apparent systolic and diastolic distinction. The TAC group displayed reduced ejection fraction at 3 weeks and increased LV wall thickness (**Figure 3B**). TAC group also had a modestly significant increase in heart weight to body weight ratio. These results indicate that the myocardium is being remodeled, with increased wall thickness, which affects cardiac contraction cycles, reducing ejection fraction.

Cardiomyocyte Concentric Hypertrophy

Concentric hypertrophy of cardiomyocytes occurs with sarcomeric units being placed in parallel, or stacked, which increases cell width, whereas eccentric hypertrophy has sarcomeres placed in tandem, elongating the cell.[1] To characterize the hypertrophic phenotype of our 3 week TAC model, cardiomyocytes were isolated and stained for F-actin for cell size and dimensional analysis (**Figure 4A**). The TAC group exhibited significantly increased cellular area, increased cell width, and decreased length to width

ratio, but not cell length. These cellular parameters indicate that 3 weeks after TAC surgery, the cardiomyocytes exhibit concentric hypertrophy.

Lamin A/C Expression, Chromatin Environment, and Nucleoskeletal Reorganization in Concentric Hypertrophy

To investigate mechanosensitive mechanisms in hypertrophy, I examined our lab's previously acquired RNA-seq data from the 3 week time point after TAC. With a focus on nuclear and linker of the nucleoskeleton and cytoskeleton (LINC) complex proteins for a direct connection between cytoskeletal and sarcomeric organization and chromatin architecture, Lamin A/C was identified as an upregulated gene of interest (**Figure 5A**). The nuclear lamins (Lamin A/C and LaminB1) form part of the nucleoskeletal structure, lining the inside of the inner nuclear membrane and binding to chromatin at lamin associated domains, thereby tethering heterochromatin to the nuclear periphery.[8] Interestingly, Lamin A/C protein expression scales with tissue stiffness, as stiffer tissues, such as the heart have more Lamin A/C expression than softer tissues, such as the brain[29] and chromatin itself responds to changes in environmental stiffness, as shown in fibroblast *in vitro* experiments plating fibroblasts on different substrate stiffnesses.[30] Thus, I examined the chromatin environment around the Lmna locus and Lamin A/C protein localization to explore their connection to hypertrophic cardiac stiffening. To explore the regulation of this gene, I examined chromatin conformation capture data from our lab. At the gene level, the Lmna locus experiences changes in DNA-DNA contacts as determined by Hi-C interactions (**Figure 5B**, top), and chromatin decondensation, scored by the Hi-C condensation algorithm MELTRON,[18] demonstrated by the diminished yellow

color in the Insulation Score heat map (right, TAC), which leads to higher transcription (RNA-seq track below).

To determine ultrastructural changes to the nucleoskeletal Lamin A/C, cardiomyocytes were isolated, stained, and imaged by confocal microscopy (**Figure 5C**). The total area of Lamin A/C occupancy was significantly increased in the TAC model, while LaminB1 showed no change (**Figure 5D**), which agrees with previous findings that indicate Lamin A/C responds to changes in cellular environment and tunes to reinforce the nuclear stability.[29] Interestingly, there was also a preferential increase in Lamin A/C at the nuclear poles, but not along the nuclear edges (running parallel to cardiomyocyte length) (**Figure 5E**), which indicated a restructuring of the nucleus to reinforce the areas where cardiomyocyte shortening would induce the greater force.

Discussion

NRVMs are suitable, well studied models of cardiac hypertrophy, as adrenergic stimulation of these cells results in hallmarks of the hypertrophic phenotype seen *in vivo*. Cell size increases and the 'fetal gene program' becomes activated. While NRVMs can be paced to beat, which requires actin-myosin cross-bridging, they remain an immature physical phenotype, lacking the rod-shaped characteristics of adult cardiomyocytes. When examining the effects of hypertrophy on mechanosensation and gene expression cellular environment is of key importance. Studies plating NRVMs on varying levels of substrate stiffness has resulted in a more mature phenotype, yet disease mimicking stiffnesses resulted in unaligned sarcomeres and stress fibers.[31] Plating NRVMs on nanopatterned plates induces cell alignment and more cell-to-cell contacts[17] and alignment with stretch induces mechanotransductive nuclear translocation of focal adhesion kinases from the mechanosensitive hub of the focal adhesion.[32] Our goal was to determine if NRVM hypertrophy induced changes to cellular stiffness and then assess chromatin organization and transcriptional readouts contributing or reacting to NRVM stiffness. However, in their immature state, NRVMs, without sarcomeric organization, even in hypertrophy, were not able to maintain their morphology to properly assess a stiffness phenotype via microfiltration. It remains to be seen if a more direct approach, such as atomic force microscopy, on hypertrophic NRVMs would reveal a cell size-cell stiffness correlation. It is interesting NRMVs transduced to have a Lmna mutation had increased Young Modulus score and force required for deformation,[33] highlighting the nuclear biophysics to cellular stiffness connection, while our methods were examining the opposite.

Through isolation and culturing of adult mouse cardiomyocytes we hoped to achieve a method to knockout or overexpress genes in a controlled environment and observe effects on cellular and nuclear structure. However, culturing mouse cardiomyocytes remains the holy grail. Numerous studies, each with a new twist to an old paradigm, have given hope to young researchers. Whether adding BDM and introducing calcium chloride,[25] including EGTA to chelate calcium before adding calcium to the buffers,[13] or performing the isolation Langendorff-free and introducing calcium from the culture media,[14] the end results were all too variable. Our isolation methods were sound, insofar as we consistently observed rod-shaped myocytes tissue dissociation. However, we were unsuccessful in discovering the secret cocktail of buffer and calcium to achieve calcium tolerant cells that would survive in culture for extended periods of time. Another issue in adult cardiomyocyte culture is that over time the cells will begin to dedifferentiate.[34] We have found a reliable, consistent method to isolate and plate rod-shaped mouse cardiomyocytes, which can be used for immunofluorescence or gene expression studies.

The gene expression and ultrastructural changes to Lamin A/C in response to pressure overload is noteworthy. The nuclear lamins line the inner nuclear membrane to provide the nucleus with structural support and to bind to peripheral heterochromatin.[7] We show that gene expression is partially due to the changes in the chromatin topology around the Lmna gene, with decreased DNA-DNA contacts, which decondense the region, allowing for transcriptional machinery to increase expression. We hypothesize that the increase in nuclear Lamin A/C area is a structural response to increased cardiac stiffness, as Lamin A/C scales with different tissue stiffnesses.[29] We initially believed that

due to increased compensatory gene regulation[5] during later stages of disease, portions of the genome would switch from less accessible heterochromatin to more accessible euchromatin. As LADs bind large portions of heterochromatin at the nuclear periphery,[35] this was a locale ripe for such conversion. However, these regions are gene poor or are largely intergenic regions of chromatin,[36] which makes large scale changes in gene expression due to nuclear lamin expression highly unlikely. This idea was supported by a recent study in induced pluripotent stem cell-derived cardiomyocytes (iPSC-CMs) carrying a haploinsufficient Lmna mutation, which exhibited minimal chromatin architectural reorganization and modest gene expression changes, decreasing the support for a “chromatin hypothesis” of Lmna mutations, in which dysregulation of chromatin leads to aberrant gene expression.[9] Alternatively, introduction of a different Lmna mutation introduced in iPSC-CMs, hepatocytes and adipocytes, induced aberrant gene expression and decreased LaminB1 genomic contacts in the cardiomyocyte cell line only.[37] However, chromatin of iPSC-CMs, due to their immaturity, still remain plastic, with heterochromatic histone marks found only at the nuclear periphery.[8] In contrast, in adult cardiomyocytes, heterochromatin marks are found throughout the nucleus,[38] thus alterations of chromatin dynamics would be more observable. While local changes in chromatin condensations drive increased Lmna expression in the compensatory hypertrophy and drives ultrastructural changes to the nucleoplasm through Lamin A/C, it is unlikely that LADs are disrupted. While experiments in iPSC-CMs have shown changes in LADs when certain mutations have been introduced, in order to assess if pathological stimuli alone affects Lamin A/C-chromatin contacts and cause aberrant gene expression, Lamin A/C ChIP-seq experiments would have to be performed to confirm this assertion.

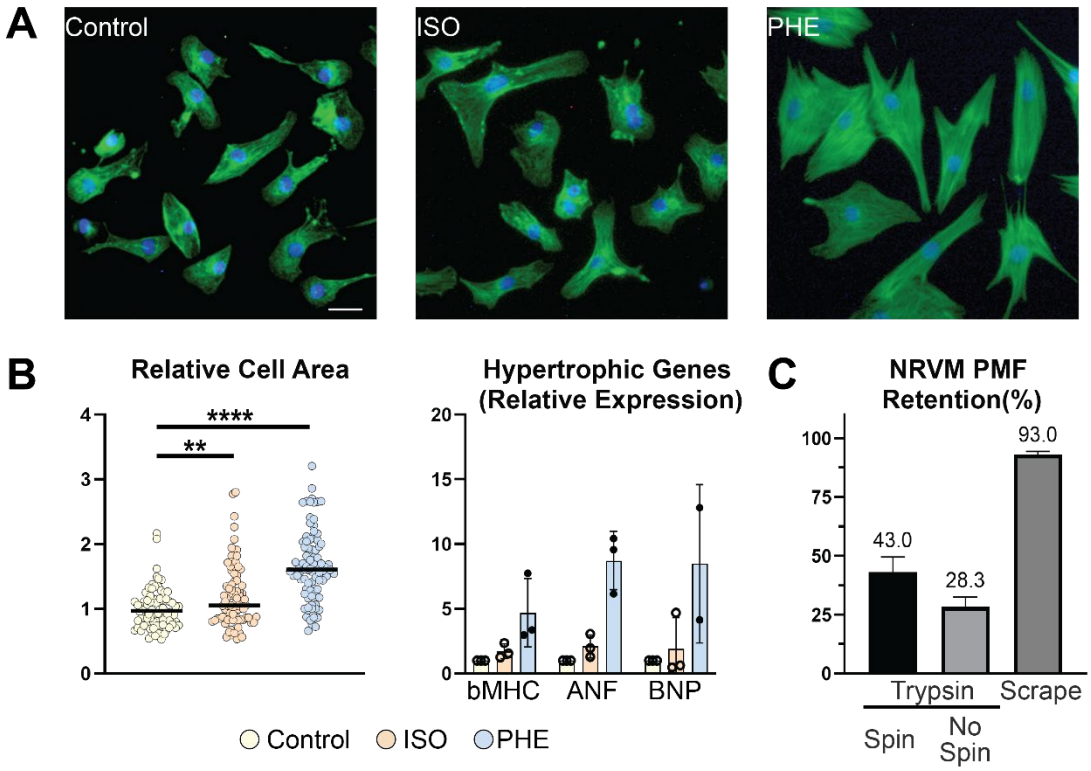

Figure 3-1. NRVM Hypertrophic Agonist Cellular and Transcriptional Response. A. Representative fluorescent microscope images of NRVMs treated with PBS (Control), ISO, or PHE (F-actin – green, DAPI – blue, scale bar = 100 μm). **B.** Relative NRVM area measurements of ISO treated (orange) and PHE treated (blue) cells compared to control (yellow), showing PHE induces greater NRVM hypertrophy *in vitro* (n=80 cells/group, **p<0.01, ****p<0.001, One-Way Anova, cell size analysis done with ImageJ). **B.** Hypertrophic gene expression relative to control. bMHC, ANF, and BNP are upregulated by ISO and PHE (bars SD) **C.** Parallel Microfiltration Assay on different NRVM detachment methods. Data shows NRVMs are highly variable by this assay based on detachment method due to loss of cytoskeletal and possible sarcomeric organization, highly influencing assay results (Median Retention % above each group, bars SD).

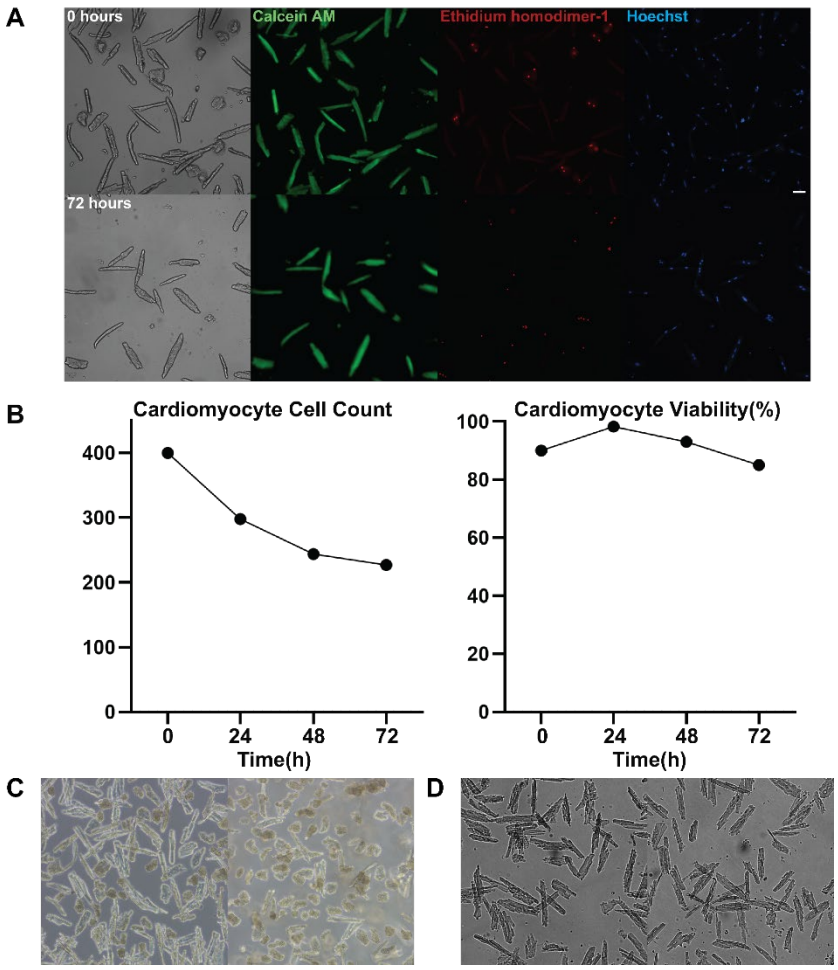

Figure 3-2. Adult Murine Cardiomyocyte Isolation, Culture and Viability. A. Fluorescent microscopy images of plated isolated adult mouse cardiomyocytes (top row) showing rod shaped morphology with minimal hypercontraction (brightfield, left). Calcein AM staining (green) staining of viable cells and ethidium homodimer-1 (red) staining of non-viable cells, nuclei (blue) stained with Hoechst. 72h post plating (bottom row) demonstrating decrease in cell density, but cells remaining attached remain viable by calcein AM fluorescence. **B.** Quantification of adult mouse cardiomyocyte per well of a 6 well plate over 72 hrs. Cell count decreases with time (left) while viability remains consistent (right). **C.** Brightfield imaging of cardiomyocytes post plating in culture media.

Images represent poor culturing results, defined by hypercontracted myocytes, demonstrating high variability in culture methodology, cardiomyocytes remained rod shaped until cell culture media was added **D.** Brightfield images of current isolation and plating method for immunohistochemistry, showing rod shaped morphology and minimal hypercontracted myocytes.

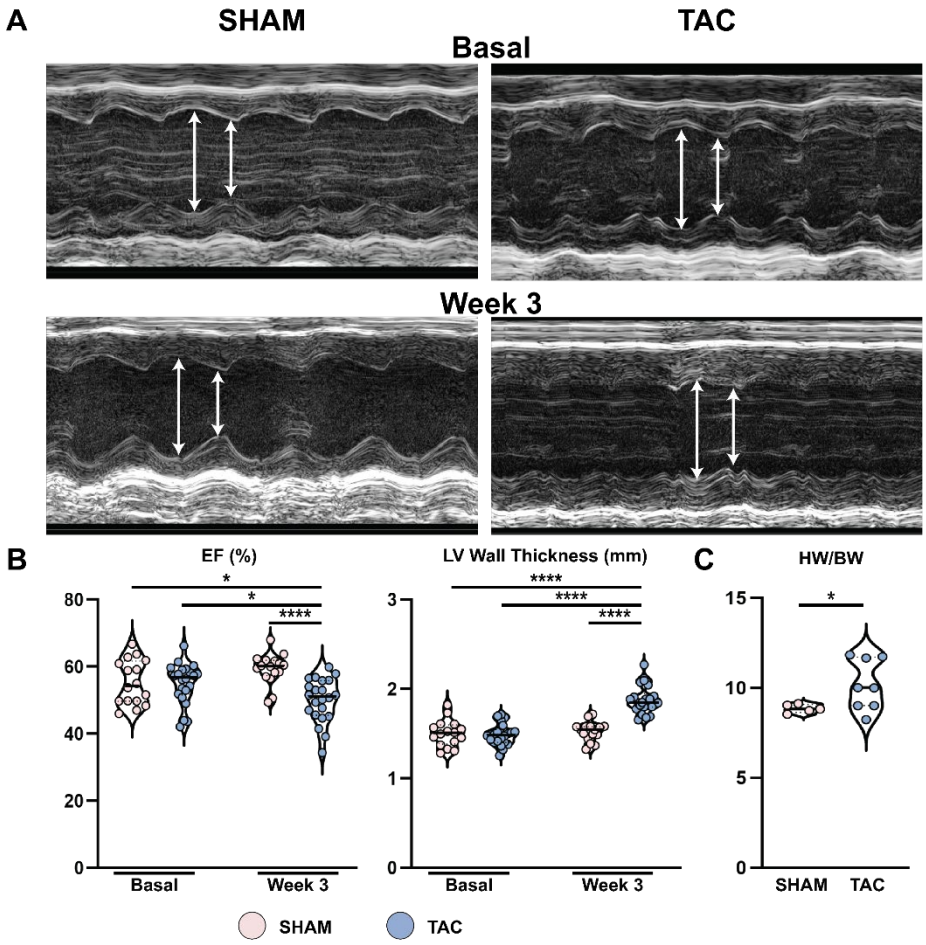

Figure 3-3. Pressure Overload Induces Cardiac Hypertrophy. A. M-mode echocardiography of left ventricle of SHAM (left) and TAC (right) hearts at Basal (top) and Week 3 (bottom) timepoints. White arrows denote left ventricular (LV) internal diameter in diastole (left arrow) and systole (right arrow). **B.** Physiological measurements of LV systolic function, Ejection fraction (EF) and LV wall thickness in SHAM (pink) and TAC (blue) hearts at basal and 3 week time points, showing hypertrophic phenotypical significantly decreased EF and increased LV wall thickness. (n=16 SHAM, 22 TAC, *p<0.01, ****p<0.001, One-Way Anova). **C.** Heart weight:Body weight ratio (HW/BW)

demonstrating increased cardiac tissue in the TAC group (n=5 SHAM, 8 TAC, *p=0.03, Welch's t-test).

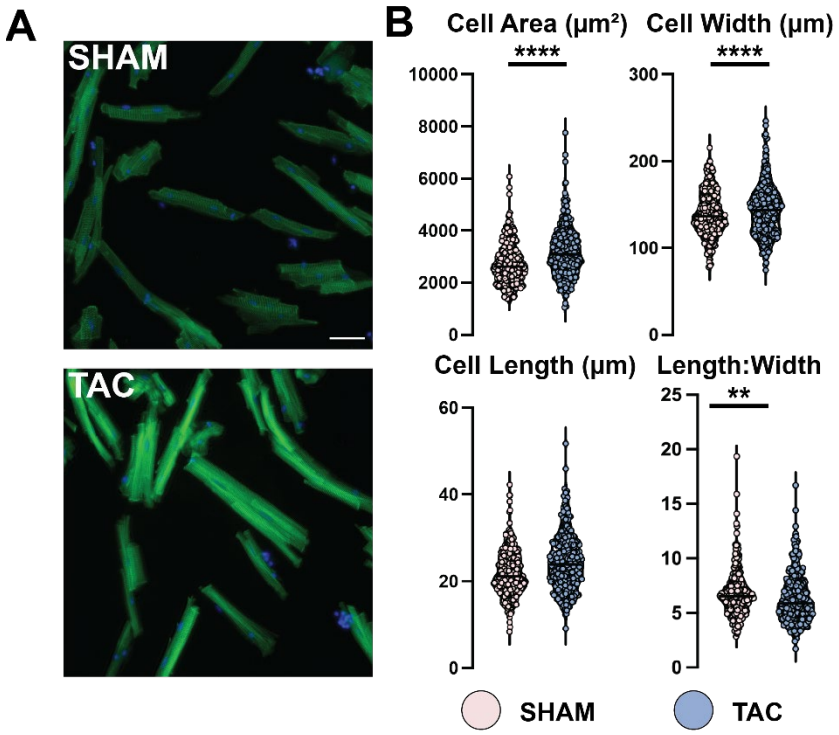

Figure 3-4. TAC Induced Hypertrophic Cardiomyocyte Structural Changes. A. Fluorescent imaging of isolated cardiomyocytes for cell geometric analysis to compare SHAM (top) and TAC (bottom) structural changes. Cardiomyocytes were isolated, attached to coverslip and stained for F-actin (green) and DAPI (blue) (Scale bar = 50 μm). **B.** Quantification of isolated cardiomyocyte geometric parameters. TAC (blue) myocytes demonstrated significantly increased cell area (top left), cell width (top right), and length to width ratio (bottom right), while no significant change to cell length (bottom left). These cardiomyocyte changes are indicative of concentric hypertrophy, with sarcomeres stacked in tandem (hence increased cell width) (n = 3 mice/group, 350 cells analyzed, **p=0.01**,****p<0.001, Welch's t test, cardiomyocyte structural parameters analyzed with ImageJ).

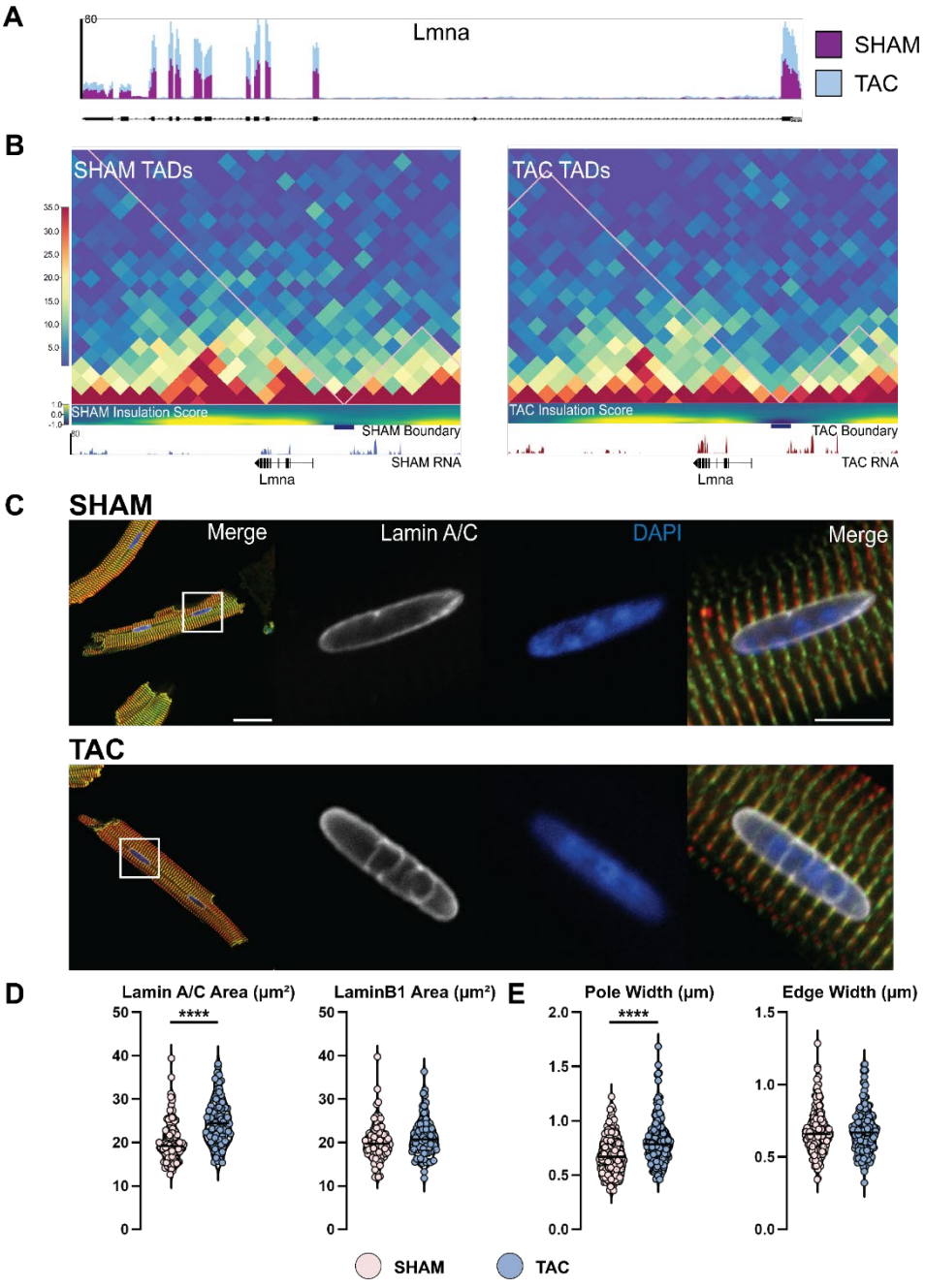
A
Lmna
SHAM
TAC
B
SHAM TADs
TAC TADs
SHAM Insulation Score
TAC Insulation Score
SHAM Boundary
TAC Boundary
SHAM RNA
TAC RNA
Lmna
Lmna
C
SHAM
Merge
Lamin A/C
DAPI
Merge
TAC
D
Lamin A/C Area (μm²)
LaminB1 Area (μm²)
****
E
Pole Width (μm)
Edge Width (μm)
****
SHAM
TAC

Figure 3-5. Chromatin Rearrangement, Gene Transcription, and Structural Reorganization of Lamin A/C. A. RNA-seq track of published TAC 3 Week isolated cardiomyocyte transcriptomics showing significant upregulation of Lmna via TAC (blue) in comparison to SHAM (purple). **B.** MELTRON analysis of published Hi-C data at 300 Mbp resolution centered on the Lmna locus of SHAM (left) and TAC (right) cardiomyocytes. While the TAD boundaries around the locus (where the triangles meet and the blue Boundary boxes are located) are unaffected, during the hypertrophic TAC stimuli, the insulation score decreases (shown my decreased yellow color in the TAC) and the region around the TAD boundary have decreased contact scores (denoted by less intense red color). This indicates that the DNA-DNA contacts around the Lmna locus are diminished, decondensing the region for increased transcription. **C.** Representative confocal microscopy images of isolated cardiomyocyte immunohistofluorescence (IHF) for quantification of Lamin A/C structural differences between SHAM (top) and TAC (bottom). Individual cardiomyocyte morphology was assessed at 60x (far left) and zoomed into the nucleus at 100x for ultrastructural analysis (enlargement of white box). Cells were stained with F-actin (green), sarcomeric actinin (red), Lamin A/C (white), and DAPI (blue). **D.** Quantification of Lamin A/C and LaminB1 area in SHAM (pink) and TAC (blue) isolated cardiomyocytes, showing significant increases in Lamin A/C area, but not LaminB1, corroborating the role of Lamin A/C being the more stress responsive of the nuclear lamins. (n=2 mice/group, 90 nuclei analyzed/group, ****$p<0.0001$, Welch's t test). **E.** Ultrastructural quantification of Lamin A/C, assessing pole width (curves of the cardiomyocyte nuclei) and the edge width (straight edge running parallel to cardiomyocyte width). TAC nuclei had increased pole width, but not edge width (n=2 mice/group, 90

nuclei analyzed/group, ****p<0.0001, Welch's t test), suggesting during hypertrophic increases in sarcomeric density and contraction-relaxation, the Lamin A/C increased area and pole localization protect the nucleus from increased forces. (All analysis done with ImageJ)

Tyrode's Ca^{2+}- free solution (10x)		
Chemical	**Concentration (mM)**	**Per 500 ml (g)**
NaCl	130	37.99
KCl	5.4	2.01
$NaH_2PH_4 – H_2O$	0.6	0.36
$MgCl_2 – 6H_2O$	1	1.02
HEPES	10	11.92
BDM	10	0.50
Glucose	10	0.90
Digestion Buffer		
Chemical	**Concentration (mM)**	**Per 500 ml (g)**
1X Tyrode's Ca^{2+}- free solution	130	37.99
Collagenase Type II		0.07
Protease Type XIV		0.003
Kreb's Buffer (KB)		
Chemical	**Concentration (mM)**	**Per 500 ml (g)**
KCl	25	0.93
KH_2PO_4	10	0.68
$MgSO_4$	2	0.12
HEPES	5	0.60
Taurine	20	1.25
Creatine	5	0.33
K-Glutamate	100	10.16
Aspartic Acid	10	0.67
EGTA	0.5	0.10
BDM	10	0.50
Glucose	20	1.80

Table 3-1. Cardiomyocyte Isolation Buffers

Chapter 3: Bibliography

1 Nakamura, M. & Sadoshima, J. Mechanisms of physiological and pathological cardiac hypertrophy. *Nat Rev Cardiol* **15**, 387-407, doi:10.1038/s41569-018-0007-y (2018).

2 Kehat, I. & Molkentin, J. D. Molecular pathways underlying cardiac remodeling during pathophysiological stimulation. *Circulation* **122**, 2727-2735, doi:10.1161/CIRCULATIONAHA.110.942268 (2010).

3 Hieda, M. *et al.* Increased Myocardial Stiffness in Patients With High-Risk Left Ventricular Hypertrophy: The Hallmark of Stage-B Heart Failure With Preserved Ejection Fraction. *Circulation* **141**, 115-123, doi:10.1161/CIRCULATIONAHA.119.040332 (2020).

4 Lyon, R. C., Zanella, F., Omens, J. H. & Sheikh, F. Mechanotransduction in cardiac hypertrophy and failure. *Circ Res* **116**, 1462-1476, doi:10.1161/CIRCRESAHA.116.304937 (2015).

5 Chapski, D. J. *et al.* Early adaptive chromatin remodeling events precede pathologic phenotypes and are reinforced in the failing heart. *J Mol Cell Cardiol* **160**, 73-86, doi:10.1016/j.yjmcc.2021.07.002 (2021).

6 Stroud, M. J., Banerjee, I., Veevers, J. & Chen, J. Linker of nucleoskeleton and cytoskeleton complex proteins in cardiac structure, function, and disease. *Circ Res* **114**, 538-548, doi:10.1161/CIRCRESAHA.114.301236 (2014).

7 Carmosino, M. *et al.* Role of nuclear Lamin A/C in cardiomyocyte functions. *Biol Cell* **106**, 346-358, doi:10.1111/boc.201400033 (2014).

8 Poleshko, A. *et al.* Genome-Nuclear Lamina Interactions Regulate Cardiac Stem Cell Lineage Restriction. *Cell* **171**, 573-587 e514, doi:10.1016/j.cell.2017.09.018 (2017).

9 Bertero, A. *et al.* Chromatin compartment dynamics in a haploinsufficient model of cardiac laminopathy. *J Cell Biol* **218**, 2919-2944, doi:10.1083/jcb.201902117 (2019).

10 Livak, K. J. & Schmittgen, T. D. Analysis of relative gene expression data using real-time quantitative PCR and the 2(-Delta Delta C(T)) Method. *Methods* **25**, 402-408, doi:10.1006/meth.2001.1262 (2001).

11 Qi, D. *et al.* Screening cell mechanotype by parallel microfiltration. *Sci Rep* **5**, 17595, doi:10.1038/srep17595 (2015).

12 Gill, N. K. *et al.* A scalable filtration method for high throughput screening based on cell deformability. *Lab Chip* **19**, 343-357, doi:10.1039/c8lc00922h (2019).

13 Judd, J., Lovas, J. & Huang, G. N. Isolation, Culture and Transduction of Adult Mouse Cardiomyocytes. *J Vis Exp*, doi:10.3791/54012 (2016).

14 Ackers-Johnson, M. *et al.* A Simplified, Langendorff-Free Method for Concomitant Isolation of Viable Cardiac Myocytes and Nonmyocytes From the Adult Mouse Heart. *Circ Res* **119**, 909-920, doi:10.1161/CIRCRESAHA.116.309202 (2016).

15 Franklin, S. *et al.* Quantitative analysis of the chromatin proteome in disease reveals remodeling principles and identifies high mobility group protein B2 as a regulator of hypertrophic growth. *Mol Cell Proteomics* **11**, M111 014258, doi:10.1074/mcp.M111.014258 (2012).

16 Rosa-Garrido, M. *et al.* High-Resolution Mapping of Chromatin Conformation in Cardiac Myocytes Reveals Structural Remodeling of the Epigenome in Heart Failure. *Circulation* **136**, 1613-1625, doi:10.1161/CIRCULATIONAHA.117.029430 (2017).

17 Heffler, J. *et al.* A Balance Between Intermediate Filaments and Microtubules Maintains Nuclear Architecture in the Cardiomyocyte. *Circ Res* **126**, e10-e26, doi:10.1161/CIRCRESAHA.119.315582 (2020).

18 Winick-Ng, W. *et al.* Cell-type specialization is encoded by specific chromatin topologies. *Nature* **599**, 684-691, doi:10.1038/s41586-021-04081-2 (2021).

19 Zou, Y. *et al.* Isoproterenol activates extracellular signal-regulated protein kinases in cardiomyocytes through calcineurin. *Circulation* **104**, 102-108, doi:10.1161/hc2601.090987 (2001).

20 Eble, D. M. *et al.* Contractile activity is required for sarcomeric assembly in phenylephrine-induced cardiac myocyte hypertrophy. *Am J Physiol* **274**, C1226-1237, doi:10.1152/ajpcell.1998.274.5.C1226 (1998).

21 Rajabi, M., Kassiotis, C., Razeghi, P. & Taegtmeyer, H. Return to the fetal gene program protects the stressed heart: a strong hypothesis. *Heart Fail Rev* **12**, 331-343, doi:10.1007/s10741-007-9034-1 (2007).

22 Yamamoto, K. *et al.* Myocardial stiffness is determined by ventricular fibrosis, but not by compensatory or excessive hypertrophy in hypertensive heart. *Cardiovasc Res* **55**, 76-82, doi:10.1016/s0008-6363(02)00341-3 (2002).

23 Yokota, T. *et al.* Type V Collagen in Scar Tissue Regulates the Size of Scar after Heart Injury. *Cell* **182**, 545-562 e523, doi:10.1016/j.cell.2020.06.030 (2020).

24 Linke, W. A. & Hamdani, N. Gigantic business: titin properties and function through thick and thin. *Circ Res* **114**, 1052-1068, doi:10.1161/CIRCRESAHA.114.301286 (2014).

25 O'Connell, T. D., Rodrigo, M. C. & Simpson, P. C. Isolation and culture of adult mouse cardiac myocytes. *Methods Mol Biol* **357**, 271-296, doi:10.1385/1-59745-214-9:271 (2007).

26 Callaghan, N. I. *et al.* Functional culture and in vitro genetic and small-molecule manipulation of adult mouse cardiomyocytes. *Commun Biol* **3**, 229, doi:10.1038/s42003-020-0946-9 (2020).

27 Rockman, H. A. *et al.* Segregation of atrial-specific and inducible expression of an atrial natriuretic factor transgene in an in vivo murine model of cardiac hypertrophy. *Proc Natl Acad Sci U S A* **88**, 8277-8281, doi:10.1073/pnas.88.18.8277 (1991).

28 Moore-Morris, T. *et al.* Resident fibroblast lineages mediate pressure overload-induced cardiac fibrosis. *J Clin Invest* **124**, 2921-2934, doi:10.1172/JCI74783 (2014).

29 Swift, J. *et al.* Nuclear lamin-A scales with tissue stiffness and enhances matrix-directed differentiation. *Science* **341**, 1240104, doi:10.1126/science.1240104 (2013).

30 Walker, C. J. *et al.* Author Correction: Nuclear mechanosensing drives chromatin remodelling in persistently activated fibroblasts. *Nat Biomed Eng* **5**, 1517-1518, doi:10.1038/s41551-021-00748-3 (2021).

31 Jacot, J. G., McCulloch, A. D. & Omens, J. H. Substrate stiffness affects the functional maturation of neonatal rat ventricular myocytes. *Biophys J* **95**, 3479-3487, doi:10.1529/biophysj.107.124545 (2008).

32 Senyo, S. E., Koshman, Y. E. & Russell, B. Stimulus interval, rate and direction differentially regulate phosphorylation for mechanotransduction in neonatal cardiac myocytes. *FEBS Lett* **581**, 4241-4247, doi:10.1016/j.febslet.2007.07.070 (2007).

33 Lanzicher, T. *et al.* AFM single-cell force spectroscopy links altered nuclear and cytoskeletal mechanics to defective cell adhesion in cardiac myocytes with a nuclear lamin mutation. *Nucleus* **6**, 394-407, doi:10.1080/19491034.2015.1084453 (2015).

34 Zhang, Y. *et al.* Dedifferentiation and proliferation of mammalian cardiomyocytes. *PLoS One* **5**, e12559, doi:10.1371/journal.pone.0012559 (2010).

35 van Steensel, B. & Belmont, A. S. Lamina-Associated Domains: Links with Chromosome Architecture, Heterochromatin, and Gene Repression. *Cell* **169**, 780-791, doi:10.1016/j.cell.2017.04.022 (2017).

36 Guelen, L. *et al.* Domain organization of human chromosomes revealed by mapping of nuclear lamina interactions. *Nature* **453**, 948-951, doi:10.1038/nature06947 (2008).

Chapter 4: Acute Mechanosensitive Adaptation to Phenylephrine Induced Cardiac Hypertrophy in Cardiomyocytes and Fibroblasts

Introduction

Pathological cardiac hypertrophy is a compensatory remodeling response to increased workload, as the left ventricle wall thickens, decreasing the chamber size. Underlying this tissue remodeling are cell-type specific mechanisms, as contractile cardiomyocytes enlarge and fibroblasts exit their quiescent state to reorganize the extracellular matrix to alleviate left ventricular wall stress.[1] The pathologically induced phenotypic changes to cardiomyocytes and fibroblasts alters their crosstalk to perpetuate cardiac remodeling and contributes to ventricular stiffness (**Figure 1**).[2] I have previously shown TAC induced ventricular remodeling induces cardiomyocyte nuclear Lamin A/C restructuring to support the nucleoskeleton from increased hypertrophic force generation. However, gene expression responses to TAC happen sooner than phenotypic changes, so I turned to an acute adrenergic signaling model[3] to induce a more consistent phenotype and investigate early gene activation happening alongside cardiac hypertrophy. The hypothesis is cardiac mechanosensitive mechanisms drive initial changes in gene expression, which induce cellular adaptation.

The compensatory concentric hypertrophic response activates pathological gene programs prior to the emergence of pathological phenotypes.[4] Thus, signaling mechanisms must become activated during stress that differentially induce cell specific remodeling cardiac tissue.[5] Fibrotic deposition and cardiomyocyte growth during concentric hypertrophy have the adverse effect of stiffening the myocardial wall,[6] which cells respond to by mechanosensitive mechanisms. Stiffness induced changes to

fibroblasts include proliferation and increased ECM protein production and remodeling,[7] while cardiomyocyte hypertrophy results from their increased workload to contract a stiffened tissue. Thus, identifying heretofore unknown mechanosensation mechanisms during cardiac hypertrophy will highlight novel approaches to mitigate pathological phenotypes.

While ECM composition contributes most of the myocardial tissue stiffness,[8] cardiomyocyte passive stiffness is a result of the sarcomeric structural protein titin.[9] The sarcomeric I-band region contains the titin spring region, the passive tension generator, and the ratio of titin N2B:N2BA isoforms dictates passive stiffness, with the shorter N2B region being the stiffer of the two.[10] Mechanosensitive proteins bind to the N2BA regions and upon cardiac stress are transduced to activate various molecular signaling pathways.[11] Of these titin bound mechanosensitive proteins, Ankrd1 is upregulated by pathogenic stressors, including pressure overload and myocardial infarction,[12] and translocates to the nucleus to regulate gene expression.[13] However, the acute response of Ankrd1 and other mechanosensitive proteins as part of immediate compensation to stress in adult cardiomyocytes has not been resolved.

Here we characterize an acute α_1-adrenergic stress induced cardiac hypertrophic model and concomitant tissue remodeling, characterizing cell type-specific mechanotransductive pathways. We demonstrate phenylephrine (PHE) induced cardiomyocyte hypertrophy drives differential gene expression of Ankrd1, which translocates to the nucleus. The fibroblast population rapidly proliferates, producing excessive ECM proteins, leading to fibrotic deposition. The proliferative state of the fibroblast population has increased mechanosensitive properties, responding to the PHE

hypertrophic stimulus in a manner distinct from the activation of these cells during prolonged forms of heart failure.

Materials and Methods

Phenylephrine Administration and Echocardiography

All animal surgery, echocardiography and euthanasia procedures were approved by the UCLA Animal Research Committee in compliance with the National Institutes of Health Guide for the Care and Use of Laboratory Animals. Phenylephrine administration was performed as previously described,[3] with modifications. Briefly, echocardiography for systolic and diastolic measurements were obtained at day 0 for basal time points. Phenylephrine (PHE, 20 mg/kg) was administered on day 1 and every other day until day 7 by subcutaneous injection. On day 7 (Week 1), echocardiography was performed for systolic and diastolic measurements for analysis, and animals were sacrificed on day 8. For echocardiography (Vevo 3100, VisualSonics) left ventricular (LV) systolic measurements included long and short axis B-mode imaging and short axis M-mode for ejection fraction, LV wall thickness and chamber diameter. Diastolic measurements for the LV were taken from the 4-chamber apical view, with E/A ratio from the pulse wave doppler and E/e' from tissue doppler.

Tissue Section Histology

Cardiac tissue samples were fixed in 10% formalin buffered solution (Sigma: HT501128) overnight, dehydrated in 70% ethanol and sent to the UCLA Translational Pathology Core to generate paraffin blocks. Samples were cut into 4μm thick slices, put on slides, and stained with hematoxylin and eosin, Masson's trichrome stain (Sigma: HT15-1KT), and Picro Sirius (abcam: ab150681) to detect fibrosis. Fibrotic area for each

slide was quantified and expressed as the percentage of the area occupied by the whole heart on a given slide using FibroSoft.[14]

For cardiomyocyte cross-sectional area, cell size was determined using Zeiss Axio Vert.A1 on heart slices labeled with wheat germ agglutinin (WGA) (Thermo: W11262). Images were taken with the 20x objective, taking 5 image fields from each tissue area (LV septum, LV wall, and apex (4-chamber view only)) and cell size was traced using ImageJ. To further characterize cardiomyocyte size in relation to fibrotic area, each image was scored as fibrotic or non-fibrotic based on WGA morphology. Tracings were separated and plotted using GraphPad.

Cardiomyocyte Isolation

Using an established protocol,[15] adult mice were treated with heparin (100 USP units) for 20 minutes to prevent blood coagulation, and then anesthetized with sodium pentobarbital (100µl of 50mg/ml dilution, intra-peritoneal). Upon loss of rear foot reflex, the heart was removed and instantaneously arrested in ice-cold phosphate buffered saline (PBS) and mounted on a modified Langendorff apparatus. After 5 min of perfusion with Tyrode's solution (130mM NaCl, 5.4mM KCl, 1mM MgCl2, 0.6mM Na2HPO4, 10mM glucose, and 10mM HEPES, pH 7.37, oxygenated with 95% (v/v) O2-5% (v/v) CO2) at 37°C, the heart was perfused for 15-30 min with 30 ml Tyrode's containing 20mg collagenase type-II and 3mg protease type-XIV and then washed for an additional 10 min with Krebs buffer (KB) (25mM KCl, 10mM KH2PO4, 2mM MgSO4, 20mM glucose, 20mM taurine, 5mM creatine, 100mM potassium glutamate, 10mM aspartic acid, 0.5mM EGTA, 5mM HEPES, 10 mM BDM, pH 7.18) oxygenated with 95% O2-5% (v/v) CO2.

Cardiomyocytes were dissociated in KB solution, filtered (100μm strainer, 25 μM blebbistatin added if used for imaging purposes) and centrifuged 2 min at 200xg for further usage. This method obtained cells that were ≥95% cardiomyocytes by visual inspection of rod-shaped cell morphology.

RNA-seq

Left ventricular cardiomyocytes were isolated and flash frozen from PBS and PHE treated animals for RNA-sequencing. The Technology Center for Genomics and Bioinformatics Core (UCLA) isolated RNA from the cardiomyocytes Ribosomal RNA was then removed using an Illumina Ribo-Zero rRNA Removal Kit and the RNA-seq libraries prepared by the Technology Center for Genomics & Bioinformatics Core (UCLA) following standard protocols. Libraries were sequenced in an Illumina NovaSeq 6000 sequencer using as many lanes as are needed to ensure 40 million reads per sample.

Data analysis with three PBS and 5 PHE samples were performed in our lab using custom pipelines. Paired-end 150 bp reads were demultiplexed into sample-specific *_R1.fastq and *_R2.fastq files using custom scripts and then pseudoaligned to the mm10 genome using the ultra-fast pseudoalignment tool, Salmon.[16] Briefly, we ran *salmon index* to generate a mm10 (mouse) transcriptome index using the appropriate "known cDNA" FASTA file from Ensembl release 81[17]. Corresponding read pairs were pseudoaligned to the appropriate transcriptome using *salmon quant* with mm10-specific index, *_R1.fastq and *_R2.fastq files as inputs. This ultra-fast process results in a transcript count for each known gene in the genome and facilitates downstream calculation of count-based statistics. Salmon transcript quantifications (*.sf files) for all

samples were loaded into a single R object using the tximport package,[18] and then differential expression analysis was performed using DESeq2[19]: First, any genes with no transcript counts in any sample were excluded from the analysis because they registered 0 measurements in the entire RNA-seq experiment. Then, we converted loaded Salmon quantifications into a DESeqDataSet and filtered to keep genes that have at least 10 observed reads amongst the samples. Differential expression analysis was performed on the filtered DESeqDataSet using the DESeq() function with default parameters, providing *p*-values and adjusted *p*-values (adjusted using the Benjamini-Hochberg method) for each gene. Significantly differentially expressed genes were those with adjusted *p*-value <0.05. Heatmaps were generated using the heatmap.2() function within the gplots package in R (https://CRAN.R-project.org/package=gplots), with unbiased hierarchical clustering on the rows. Principal component analysis was performed using the DESeq2 package. Gene ontology analysis was performed using g:Profiler[20] with the default g:SCS multiple testing correction method.

Fibroblast Isolation

Primary cardiac fibroblasts were isolated from PBS and PHE treated mice using enzymatic digestion (7 mg/ml collagenase type II: Worthington Biochemical Corporation: LS004177) followed by centrifugation (2000 rpm for 8 minutes at 4°C) and cell plating in DMEM/F12 media supplemented with 10% fetal bovine serum (FBS), 1% antibiotics (penicillin and streptomycin), and 0.1% insulin-transferrin-selenium (ITS; Corning: 354350). After 2 hours,cells were maintained in DMEM/F12 media supplemented with 10% fetal bovine serum (FBS), 1% antibiotics (penicillin and streptomycin), human basic

fibroblast growth factor (hbFGF, 1:10000 concentration from 200X stock; Millipore Sigma: 11123149001) and 0.1% insulin-transferrin-selenium (ITS; Corning: 354350). Cells were fixed 18h later for confocal imaging.

Immunofluorescence and Confocal Imaging

For cardiomyocyte confocal imaging, prior to cardiomyocyte isolation, coverslips were coated with 5 μg/ml of laminin (Sigma: L2020) for at least 1h prior to plating. Post tissue dissociation and cell filtering, blebbistatin was added to the KB buffer at a final concentration of 25 μM and cell suspension was plated at 37°C for at 1-2h. KB buffer and unattached cardiomyocytes were gently washed and fixed with chilled -20° C methanol for 10min. Cells were washed and blocked with SEA BLOCK blocking buffer (Thermo: 37527) for 1h. Cells were incubated for 24-48h in primary antibodies at 4°C at dilution of 1:100 in blocking buffer (Lamin A/C: abcam: ab8984, Ankrd1: abcam: ab272894, Sarcomeric Actin: Millipore: A7811, αTubulin: Cell Signaling: 3873, detyrosinated tubulin: abcam: ab48389, H3K9me2: abcam: abcam: ab1220 H3K9me3: abcam: ab8898). Cells were washed and incubated with secondary antibodies (Thermo: Alexa Phalloidin-488, Alexa Fluor-568 and Alexa Fluor-647 species specific to primary antibody) for 1h at room temperature. Cells were washed and stained with DAPI for 10min before a final wash and mounting with ProLong Gold Antifade Reagent (Thermo: P10144). Confocal images were taken using a Nikon A1R, using 60x objective for whole cell imaging and 100x for nuclear imaging.

For fibroblasts confocal imaging, tissue sections were deparaffinized and antigen retrieval by vegetable steamer for 50min in sodium citrate buffer. Slides were blocked in 5% BSA in PBST for 1 hr and incubated with primary antibodies (Vimentin: abcam: ab45939, αSmooth Muscle

Actin: abcam: ab7817 for 24h at 4°C). Slides were washed and incubated with secondary antibodies (Thermo: Alexa Phalloidin-488, Alexa Fluor-568 and Alexa Fluor-647 species specific to primary antibody) for 1h at room temperature. Cells were washed and stained with DAPI for 10min before a final wash and mounting with ProLong Gold Antifade Reagent (Thermo: P10144). Confocal imaging captured with 40x objective.

For isolated fibroblasts, cells were fixed at room temperature for 20 min using 1.6% PFA. Fixed cells were permeabilized and blocked for 1 hour using blocking buffer (5% BSA, 0.1% Triton X-100) and incubated overnight at 4°C with primary antibody (αSMA, Vimentin, and Mrtfa (1:50, Santa Cruz: sc-398675). Appropriate concentration of secondary antibodies (including Alexa Fluor-488 phalloidin) was incubated at room temperature for 1h. Imaging was performed at a confocal microscope (Nikon A1R, 60x). Nuclei were stained using 4',6-diamidino-2-phenylindole (DAPI).

To analyze histone mark localization, a Matlab algorithm was performed as previously described[21].

Immunoblotting and antibodies

Protein was extracted from whole heart and isolated cardiomyocytes using homemade lysis buffer (50mM Tris pH 7.4, 10mM EDTA, 1% sodium dodecyl sulfate (SDS), 10mM sodium butyrate, 1.2mM phenylmethanesulfonyl fluoride, 1mM sodium fluoride, 1mM sodium orthovanadate) containing protease inhibitors (Roche: 04693159001) and phosphatase inhibitors (Roche: 04906837001). Cell and tissue fractionation was performed as previously described.[22] Protein concentration was measured using a Pierce BCA Protein Assay (Thermo: 23225). An equal amount of

protein was loaded into an SDS-containing polyacrylamide gel. After electrophoresis, proteins were transferred to a nitrocellulose membrane (Bio-Rad: 1620115). Membranes were blocked with 5% BSA for one hour, incubated with appropriate primary (Ankrd1: ProteinTech: 11427-1-AP, H3: Cell Signaling: 9715, GapDH: Cell Signaling 2118, H3K9ac: abcam: ab32129, H3K9me2: abcam: ab1220, H3K9me3: abcam: ab8898) and fluorescent secondary antibodies and developed using a ChemiDoc MP Imaging System (Bio-Rad).

MELTRON Hi-C Analysis

Hi-C data set was analyzed for a previous publication.[23] The MELTRON algorithm code and analysis were performed as previously described[24] with a 300 Mbp bin size around the Ankrd1 locus.

Quantification and Statistical Analysis

Data presented as the mean ±SD, unless otherwise indicated in the figure legends. Statistical analyses were performed using Prism software v9.0 (GraphPad Software) using Welch's t-test between two groups and one-way ANOVA with Tukey's multiple comparison analysis between three or more groups. A p-value less than 0.05 was considered statistically significant.

Results

Acute α_1-Adrenergic Stimulation via Phenylephrine Induces Cardiac Hypertrophy

Adrenergic stimulation causes cardiac hypertrophy, as adrenergic receptor activation induces increases in protein synthesis and cardiomyocyte cell growth.[25] While *in vivo* studies of cardiac hypertrophy have mostly relied on either *chronic* β-adrenergic stimulation via osmotic pump, recently reports of *acute* α_1-adrenergic stimulation produces increased heart weight to body weight and fetal gene expression.[3] We set to establish and phenotypically characterize an *acute* α_1-adrenergic stress mouse model of cardiac hypertrophy. Phenylephrine (PHE) was subcutaneously administered (20 mg/kg) every other day for one week, with basal and day 7 echocardiography analysis (**Figure 2A**). Initial reports administered 10 mg/kg every other day, but this was insufficient to produce a difference in echocardiographic parameters at 7 days in our hands. Increasing the dose to 20 mg/kg, however, revealed a striking phenotype. At the 7-day time point, long axis B-mode and short axis M-mode images showed significant wall thickening and concomitant decrease in chamber size (**Figure 2B**, left and middle panels). Systolic function was measured and PHE treated mice showed significant increase in ejection fraction (EF) and left ventricular wall thickness, (LV Wall) and a decrease in left ventricular chamber diameter (LVID). PHE mice also showed dysfunctional diastolic measurements, with a reduced E/A ratio and E/e' ratio (E/A - blood flow during diastolic filling (E) and atrial contraction (A), E/e' - mitral inflow velocity (E) to diastolic mitral annulus velocity (e') **(Figure 2B**, right panel white traces and yellow traces respectively and **Figure 2D**).[26] PHE group also displayed higher heart weight to body weight ratios, confirming increased heart size (**Figure 2E**).

PHE Induced Fibrotic Deposition and Cardiomyocyte Hypertrophy

To elucidate tissue level remodeling, hearts were excised and paraffin embedded for histological and immunofluorescent analysis. Whole heart section imaging in both the coronal and transverse planes, revealed PHE treated mice had increased left ventricular wall thickness at the interventricular septum, left ventricular wall, and apex. Picro Sirius red staining for fibrosis revealed elevated interstitial fibrotic areas in the PHE group (**Figure 3A**, quantified **Figure 3C**). To assess cardiomyocyte hypertrophy, PHE cardiomyocytes had a significantly increased cross sectional area by cell tracing of wheat germ agglutinin stained (**Figure 3B**, quantified in **Figure 3D**) tissue sections. While PHE treated mice had overall increased fibrotic area, not all fields analyzed showed fibrotic deposition. Further characterization of PHE heart sections revealed larger cross sectional area in fibrotic areas of the myocardium than in non-fibrotic area, with non-fibrotic areas having cardiomyocyte areas similar to PBS mice (**Figure 3E**). This quantifiable observation suggests specific cross talk between extracellular matrix deposition by fibroblasts and the hypertrophic cardiomyocyte response, and the hypothesis that there the tissue response to adrenergic stimulus is heterogenous, leading to areas of highly mechanoresponsive cells within the myocardial tissue.

RNA-seq Uncovers Transcriptional Basis for PHE-Induced Extracellular Matrix Rearrangement

To uncover cardiomyocyte specific gene transcriptional changes of PHE induced cardiac hypertrophy, cardiomyocytes from PHE and PBS treated mice were isolated for

RNA-sequencing. The PHE treated group showed a distinct transcriptional profile separate from the PBS controls (**Figure 4A**). A total of 990 genes were significantly upregulated ($p_{adj}<0.05$, $\log_2$ fold change ≥ 0.6), and were subject to Gene Ontology. The top 10 molecular function terms are listed in **Figure 5B**. There is a strong upregulation of extracellular matrix (ECM) genes, supporting the fibrotic phenotype seen by histology, and suggesting cardiomyocytes themselves directly contribute to ECM remodeling as they hypertrophy, while at the same time potentially activating such signaling in nearby fibroblasts to induce *fibroblast-dependent* ECM deposition. The cardiomyocytes display a fetal gene program gene expression profile (**Figure 4C**) as predicted based on previous investigations. To determine early compensatory mechanisms shared between different models of cardiac stress, transcriptome changes following PHE were compared to those in the acute phases (3 days) after pressure overload (TAC).[4] The shared genes (**Figure 4D**) were then subject to Gene Ontology, and a similar expression profile to PHE only genes showed early phase cardiac stress response share a remodeling of the ECM (**Figure 4E**). These observations lead to the conclusion that the early phase of cardiac stress response includes activating a fibrotic phenotype, to bolster the left ventricle and resist the increased physical stress.

Cardiomyocyte Microtubule Network Density in PHE

Cardiomyocyte passive stiffness is largely due to the sarcomeric spanning protein titin[27,28] and its post-translation modifications.[29] While the spring section of titin is a basis of molecular mechanosensing, the microtubule cytoskeleton plays a role in providing tension to the sarcomeric contraction-relaxation cycle[30] and post-translationally modified

microtubules are more stable and resistant to contraction and relaxation in isolated cardiomyocytes from heart failure patients.[31] To confirm PHE induces microtubule stabilization seen in other PHE stress studies,[3] cardiomyocytes from PHE and PBS treated animals were isolated and stained for αTubulin and detyrosinated tubulin, a post-translationally modified tubulin that binds to the sarcomeric z-disk and is a more stable microtubule that is upregulated in congenital hypertrophic cardiomyopathy and resists compression and relaxation.[3] Confocal imaging was performed, merging 4 μm regions around the nuclear plane to assess microtubule density compared to total cell area (**Figure 5A**). Both αtubulin and detyrosinated tubulin were modestly dense for the whole cell (**Figure 5B and C**, left graphs). However, localized measurements around the nuclear area revealed the density of αtubulin and detyrosinated tubulin to be significantly denser in these regions (**Figure 5B and C**, right graphs), suggesting a network of microtubules around the nucleus creates a nuclear environment that is differentially stiff in different regions.

Ankrd1 Is Upregulated in Cardiac Hypertrophy and Localizes to the Nucleus

The sarcomeric protein titin spans the z-disk and sets the passive tension of the cardiomyocyte. During cardiac disease, the ratio of titin isoforms N2BA:N2B dictates cell stiffness, with N2BA isoform being the longer, more compliant version and N2B, a shorter stiffer isoform, with the ratio becoming smaller as disease progresses.[32] While both isoforms contain the spring like region containing a PEVK domain and an N2B region in the I-zone of the sarcomere, the stiffer N2B isoform lacks the N2A region found in the more compliant N2BA isoform.[10] This titin spring like region, located in the I-zone of the

sarcomere, is a mechanosensitive hub for signal transduction, with mechanosenitive proteins binding to and influenced by changes in cardiomyocyte stiffness dictated by titin and its isoforms.[11]

Examining RNA-seq data from the PHE mice and TAC 3d experiments, four and a half LIM Domain protein 1 (Fhl1) and Ankyrin Repeat Domain 1 (Ankrd1 or Cardiac ankyrin repeat protein CARP), both titin binding proteins, were upregulated following cardiac stress.[33,34] We focused our attention on Ankrd1 due to its reported role as a transcriptional regulator[35,36] and its consistent upregulation in cardiac disease.[12] Mechanistically, Ankrd1 binds to titin at the N2A region and in fetal rat cardiomyocytes, translocates to the nucleus upon static stretch.[37] In NRVMs, Ankrd1 binds to Gata4 and Erk1/2 at the sarcomere and translocates to the nucleus upon PHE treatment.[13] However, studies in adult mouse models have been confounding, where Ankrd1 overexpression has been shown to alleviate TAC induced hypertrophy[38] or induce dilated hypertrophy[39] while Ankrd1 knockout models had no basal phenotype and demonstrated no effect to cardiac physiology post-TAC surgery (i.e, Ankrd1 KO with TAC had the same phenotype as Ankrd1 WT TAC animals).[40] The adult mouse models all lack a definitive conclusion on whether Ankrd1 translocates to the nucleus upon cardiac stress to regulate gene expression.

Since Ankrd1 is highly upregulated in both the PHE and TAC models of cardiac hypertrophy, we examined a Hi-C data set of a TAC heart failure timepoint[23] to determine if the chromatin region around the Ankrd1 locus was locally changed upon cardiac stress (**Figure 6A**). Strikingly, by using the MELTRON Hi-C algorithm[24] the Ankrd1 locus loses DNA-DNA contacts and topologically associated domain strength (as shown by the

diminished red in the top heat map) in TAC group and has a diminished insulation score (less yellow color in the insulation score heat map), suggesting a localized decompaction event, allowing for increased Ankrd1 transcription. Another interesting observation is the loss of a TAD boundary in the Ankrd1 locus, suggesting this region may change its association with other local genomic regions.

To determine if Ankrd1 translocates to the nucleus, isolated cardiomyocytes from PBS and PHE treated mice were isolated and fractionated into cytoplasmic and nuclear fractions (**Figure 6B**). Western blot analysis showed increased Ankrd1 protein quantities in the whole cardiomyocyte fraction (**Figure 6B**, top) and increased Ankrd1 in the nuclear and sarcomeric fraction (**Figure 6B**, bottom). We reasoned it to be a pure nuclei fraction, as evidenced by an absence of GapDH, however the nuclei fraction did have an enrichment of the z-disk binding intermediate filament protein desmin (data not shown). Since Ankrd1 binds to the titin protein in the sarcomere, it is possible that presence of desmin in the nuclear fraction could indicate that the nuclear fraction is contaminated with sarcomeric proteins. To try another approach, whole hearts from PBS and PHE treated mice were subject to a cellular fractionation protocol (**Figure 6C**), and we observe Ankrd1 enriched in the nuclear fraction (top) and in the cytoplasm (bottom). The nuclear fraction contained no GapDH, however it has not been probed for other sarcomeric proteins to assess their separation from the nuclear fraction (**Figure 7)**. To visualize localization, IHF of isolated cardiomyocytes was performed to assess and quantify nuclear localization (**Figure 6D**). Ankrd1 staining was localized to the I-band of the sarcomere throughout the cardiomyocyte and both PBS and PHE treated cardiomyocytes showed nuclear staining. Using Lamin A/C as a marker for nuclear perimeter (this excluded perinuclear sarcomeric

Ankrd1), a threshold of Ankrd1 was determined and the area of nuclear occupancy was determined. Ankrd1 nuclear occupancy was significantly increased in PHE treated mice (**Figure 6D**, right graph). This suggests with cardiac stress, Ankrd1 increases nuclear occupancy and acts as a transcriptional regulator. However, which transcription factors Ankrd1 binds to in the PHE model and what genes it may regulate remain to be determined.

PHE Induced Fibrotic Deposition Without Fibroblast Activation

The striking increase in fibrotic area and ECM remodeling gene expression profile by acute PHE treatment led us to investigate the fibroblast population responsible for localized fibrotic deposition. While cardiomyocyte isolation yields a large population of cardiomyocytes, staining for fibroblast marker vimentin on the cardiomyocyte plating and imaging protocol revealed the presence of cardiac fibroblasts (**Figure 8A**). When staining cardiomyocytes, plating for 1 hour before methanol fixation inhibits the ability of fibroblasts to spread out and increase F-actin staining via phalloidin. Thus positive staining for Lamin A/C or other markers were determined to be cellular debris from the isolation protocol. This observation led to a re-examination of the RNA-seq data, with a realization that certain gene programs may be due to the inclusion of fibroblasts, even though Tgfb signaling may still come from the cardiomyocytes themselves (**Figure 8B**). Tissue sections were stained with vimentin and myofibroblast marker α-smooth muscle actin (αSMA) to determine if the increased fibrotic deposition was due to fibroblast activation (**Figure 8C**). While αSMA staining around the vasculature was positive (staining smooth muscle cells), within the myocardium, PHE treated mice showed no colocalization of

vimentin and αSMA: thus, fibrotic deposition was conclusively not due to activated fibroblasts. We did observe a higher density of fibroblasts in the PHE treated mice, as PHE treatment induces fibroblast proliferation[41] and is used as a secondary interstitial fibrotic stimulator in MI models[42]. Cardiac fibroblasts were isolated for further characterization, and after 18h post-isolation and plating, PHE treated groups showed no αSMA staining (**Figure 8D**). However, F-actin staining showed fibroblasts from PHE treated mice having an increased occurrence of actin stress fibers (**Figure 8D**, white arrows), which indicated these cells had enhanced mechanosensitivity, primed to respond to changes in environmental cues. To explore one mechanosensitive pathway, we focused on myocardin related transcription factor a (Mrtfa), a mechanosensitive transcriptional regulator that binds to G-actin and in times on cardiac stress, as G-actin becomes polymerized as F-actin, is released and moves to the nucleus for gene regulation with serum response factor[43]. In isolated cardiac fibroblasts, only cells from PHE treated mice showed nuclear localization of Mrtfa (**Figure 8E**), adding evidence to PHE treatment influencing cardiac fibroblast mechanosensitivity.

Due to the proliferative effect on PHE treatment, we believe the upregulation of ECM genes seen in the RNA-seq data set may result from the amount of fibroblasts that may have infiltrated the cardiomyocyte isolation. We mined the RNA-seq data for known mechanosensitive genes (**Figure 9, Table 4-1**) and observed a trend of significant upregulation of these genes. Whether this is due to cardiomyocyte upregulation or from the fibroblast inclusion is unknown, but PHE treatment sets a gene expression profile to not only induce ECM remodeling, but also a mechanosensitive phenotype that responds to these changes.

Cardiomyocyte Chromatin as a Mechanosensitive Organelle

With a focus on mechanotransductive pathways in which the end goal of the cell is gene regulation, we examined if cardiomyocyte chromatin architecture itself was altered in response to the PHE induced changes in the myocardium. Our hypothesis was certain regions of the heterochromatin would be unwound (red oval) and become more euchromatic (green oval) affecting gene (**Figure 10A**). This prediction was based on the observation that increased strain on epithelial cells induced loss of heterochromatin upon stretching, which then re-established itself after the cell adjusted to stretch.[44] Isolated cardiomyocytes proteins lysates were probed for euchromatic marker H3K9ac and heterochromatic markers H3K9me2 and H3K9me3, which found no difference between PHE and PBS groups (**Figure 10B**). Our next hypothesis was that while global histone marks may not change, their localization may change upon PHE treatment (**Figure 10C**), which was seen in iPSC-derived cardiomyocytes and tissue sections.[21] However, analysis of DAPI intensity, H3K9me3 and H3K9me2 in isolated cardiomyocytes showed no differential localization of histone marks between the nuclear center and periphery (**Figure 10D**).

Discussion

Adrenergic stimulation has been used to induce models of cardiac disease,[45] mainly through osmotic pumps. Recently, acute PHE administration was implemented to observe hypertrophic protein translation,[3] however while gene expression of select fetal gene program targets and increased heart weight to tibia length were reported, examining the whole tissue phenotype was lacking. We made modifications to their protocol, instead of 10 mg/kg every other day, we increased it to 20 mg/kg every other day, this was to no observable difference by echocardiography in the one-week time point with 10 mg/kg. This increased dosage has led to a decrease in survival, but we have modified the protocol to include a first dose of 10 mg/kg before the four injections of 20 mg/kg and still have similar biological readouts.

While the goal of this project was to identify cardiomyocyte signaling mechanisms, the fibrotic phenotype was striking. A study examining fibroblast heterogenous phenotypes in myocardial infarctions used PHE and angiotensin II to induce fibroblast proliferation away from the infarct zone,[42] and in isolated fibroblasts, PHE increased proliferation.[41] An interesting observation about our population of fibroblasts is their lack of activation marker αSMA, but in the RNA-seq data, periostin, another marker of activated fibroblasts, was significantly increased. In a recent preprint, a mutation in cardiac troponin C, a cardiomyocyte sarcomeric protein responsible for calcium binding allowing actin-myosin cross-bridging, caused a similar fibroblast response: that is, proliferation in the absence of markers of myofibroblast activation.[54] These investigators proposed these cells may have an elevated mechanosenstive phenotype. The RNA-seq data presented here adds credence to mechanosensitive, proliferative fibroblast

population, with a host of genes shown to be mechanosensitive being significantly upregulated. While more experiments are to be done to show their mechanosensitive nature, starting with myocardin related transcription factor, a well-studied mechanosensitive transcription regulator, we believe these fibroblasts represent an as-yet uncharacterized cardiac fibroblast population, more reactive to stress induced changes to the cardiac tissue.

The increase and nuclear localization of Ankrd1 offers some insight into this enigmatic protein. There is no doubt that Ankrd1 is stress responsive[46] and upregulated in many etiologies of heart disease.[47,48] Ankrd1 binds to titin as well as localizes to the nucleus[37] in adult mouse tissue sections when stained for electron microscopy. Here we show Ankrd1 increased expression in TAC and PHE models, and in the PHE, has increased localization in the nucleus. Further experiments will be done to confirm this result, as well as determine which transcription factors it binds to and what genes it regulates. Our HOMER analysis indicated Smad motifs are enriched in our upregulated gene sets, and with Tgfb pathway proteins Tgfb2, Tgfb3, Tgfbr1, and Tgfbr2 being upregulated. Smads are therefore strong candidates, as Ankrd1 has been shown to bind to Smad3[36]. Other studies have shown Ankrd1 has the ability to bind to transcription factors Erk1/2 and Gata4, both of which are required for agonist-induced cardiomyocyte hypertrophy.[49] Interestingly, Ankrd1 also impacts dermal fibroblast wound healing, as it binds to nucleolin to inhibit extracellular matrix maintenance protein Mmp-13 gene expression[50], however its role in cardiac fibroblasts is unknown. In order to determine mechanisms driving Ankrd1 increased nuclear translocation, we also must identify if titin isoforms play a role in the PHE hypertrophic phenotype. Titin sets the cardiomyocyte

passive stiffness,[28] and it is the shorter N2B isoform that is elevated in cardiac disease.[51] The N2B isoform lacks the N2A region of titin, which is where Ankrd1 binds, thus a decrease in N2BA:N2B ratio would dictate that Ankrd1 has less non-nuclear binding partners and may translocate to the nucleus during cardiac disease. However, Ankrd1 has a PEST region, a target for protein degradation machinery, so this could be a case of increased protein translation followed by quick degradation. This scenario may be true in early phases of cardiac disease, such as PHE, but later in the progression to heart failure, protein degradation is altered,[52] and Ankrd1 may progress the disease phenotype.

An interesting observation of this study is the interplay of cardiomyocyte hypertrophy and fibrotic deposition, as we demonstrated greater cross-sectional area in high fibrotic regions. The fibrotic phenotype was further confirmed in the RNA-seq data. However, due to fibroblast inclusion in the isolation protocol, it is unclear whether the increased extracellular matrix transcripts are from cardiomyocytes or fibroblasts. Examination of single cell RNA-seq data sets would provide a foundation for the contribution of each cell type to ECM protein production and maintenance.[53] However, to fully understand the PHE model, mouse models that inhibit fibroblast proliferation (through p53 knockdown) would allow for elucidation of the cardiomyocyte response to PHE, and identify if fibrosis still occurs. Furthermore, proteomic analysis of the ECM via decellularization assays on PHE treated p53 knockdown mice would provide qualitative analysis of cardiomyocyte contribution to ECM organization.

The PHE model of acute hypertrophy developed in this study is robust. The left ventricular remodeling is highly reproducible and the gene expression profile of increased ECM deposition coincides with tissue analysis. We believe these resources will be of

great use to the field in understanding acute adaption to cardiac stress. We have only begun to understand the mechanosenstive mechanisms at play in cardiomyocytes with Ankrd1, and Fhl1, another titin binding protein, being initial targets we have pursued. The fibroblast population is one that needs further characterization, but with collaborating labs showing a similar phenotype in different heart disease models, and identifying this population's mechanome, novel signaling mechanisms and possible therapeutics are likely to follow.

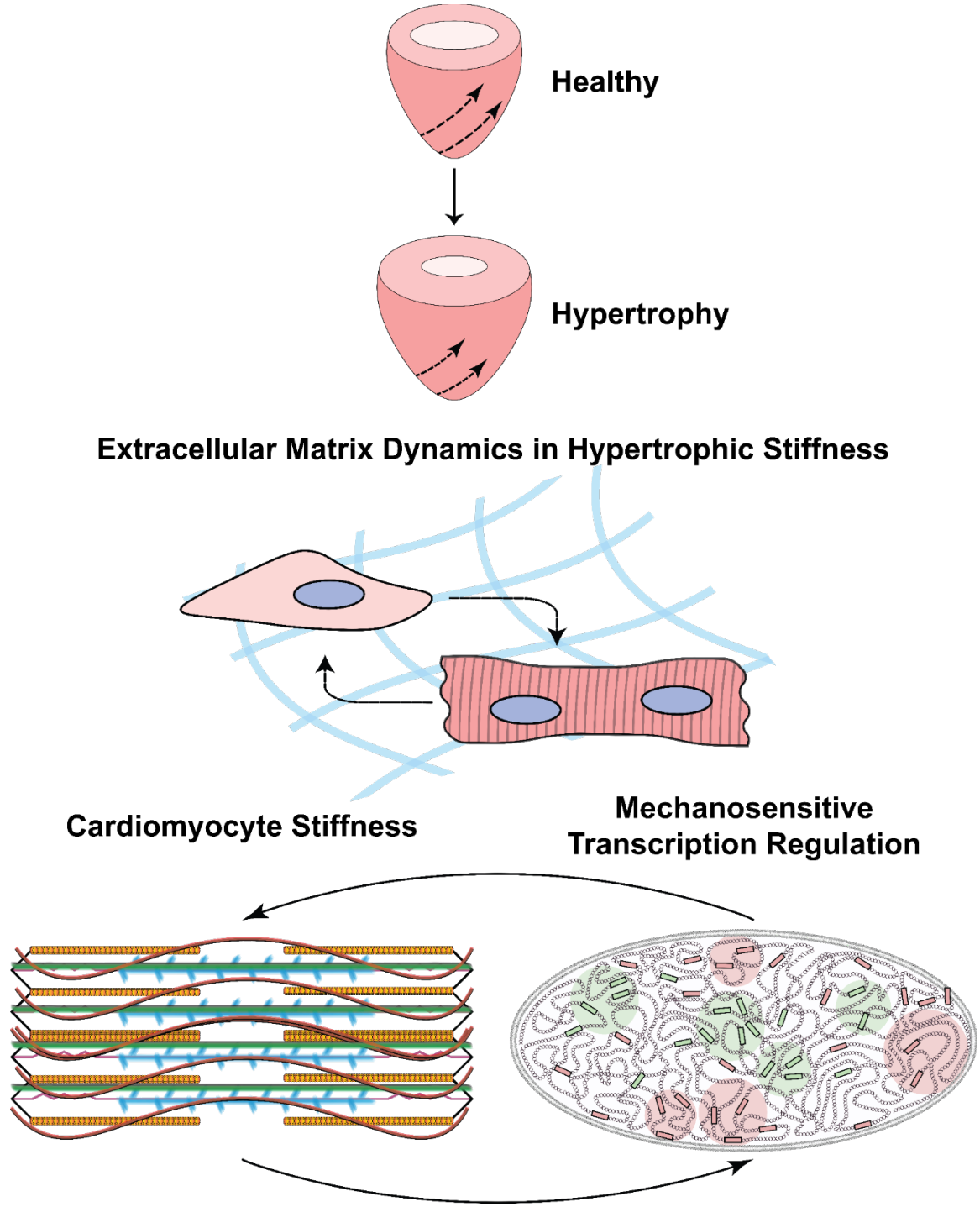
Healthy
Hypertrophy
Extracellular Matrix Dynamics in Hypertrophic Stiffness
Cardiomyocyte Stiffness
Mechanosensitive
Transcription Regulation

Figure 4-1. Cardiac Hypertrophic Stiffening, Cellular Mediators of Tissue Remodeling, and the Cardiomyocyte Mechanosensing Transcriptional Response. Cardiac hypertrophy is characterized by the thickening of the left ventricular wall and decreased chamber size. This remodeling event stiffens the cardiac tissue (denoted by the strain arrows), extracellular matrix deposition by fibroblasts stiffens the left ventricular wall, adding increased forces for cardiomyocytes to work against with each contraction-relaxation cycle, which induces cardiomyocyte hypertrophy via increased sarcomeric production, increasing of cardiomyocyte passive stiffness. Signaling molecules from the mechanosensitive regions of the sarcomeric unit sense changes in cell biophysics, inducing mechanotransduction proteins into the nucleus to mediate mechanosensitive transcriptional responses.

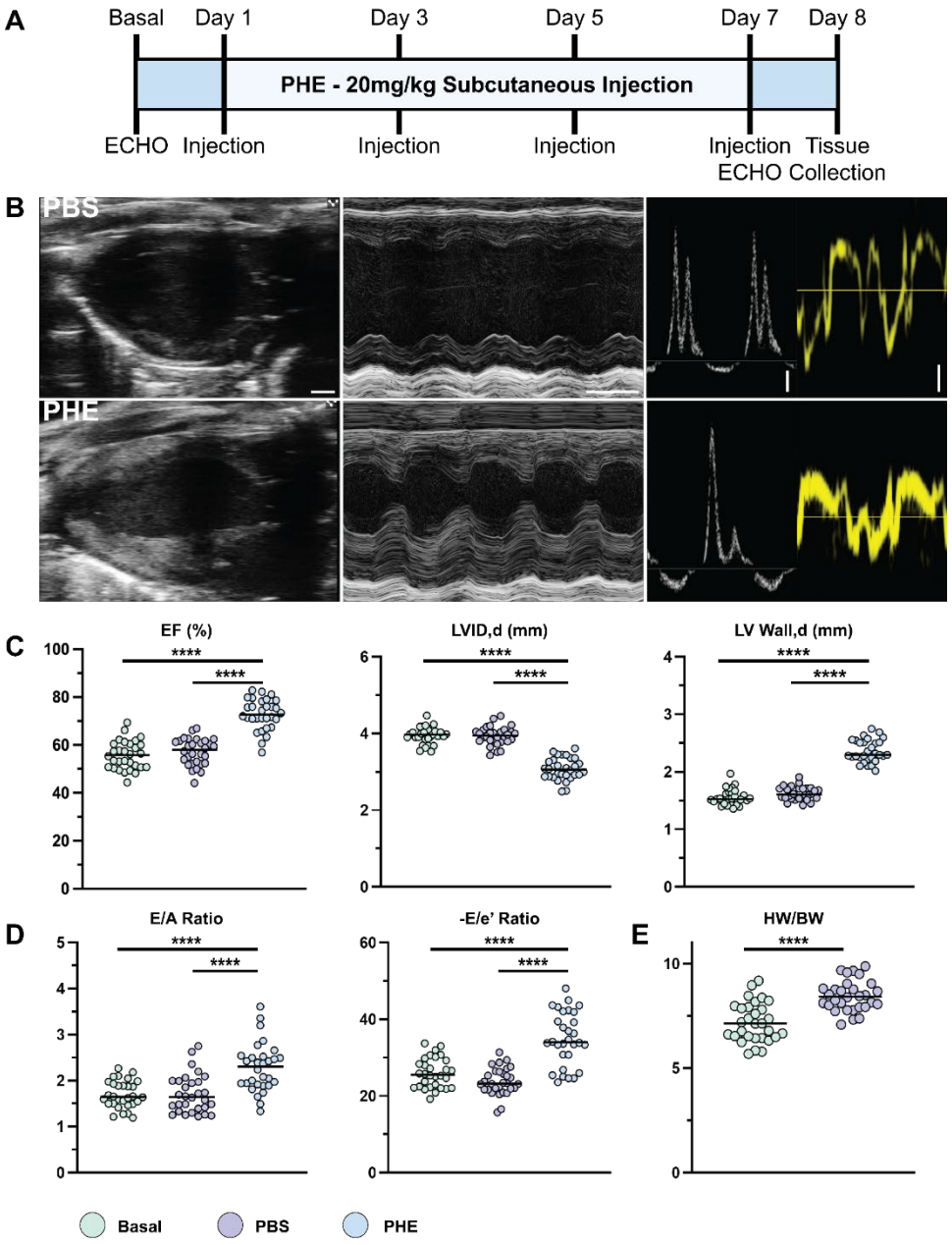

Figure 4-2. Acute Cardiac Hypertrophy Induction Via α_1-Adrenergic Stimulation. A. Timeline of acute phenylephrine (PHE) administration, PHE (20 mg/kg) or Vehicle (PBS) was subcutaneously injected every other day for 7 days, with echocardiographic (ECHO) parameters were measured on Day 0 (basal) and Day 7, tissue was harvested on Day 8. **B.** Representative ECHO images of PBS and PHE treated mice on Day 7 to observe

systolic and diastolic phenotypes. PHE mice show a demonstrative hypertrophic phenotype as seen in the Long Axis B-Mode (far left, scale bar = 1 mm) and Short Axis M-Mode (middle, scale = 100 msec) increase in wall thickness and decrease in chamber size. Diastolic images (far right) of Pulse Wave Doppler blood flow velocity for E/A ratio (white tracks, scale = 100 mm/s) and Tissue Doppler velocity for E/e' measurements (yellow track, scale = -10 mnm/s) indicate diastolic dysfunction. **C.** Quantitative analysis of systolic function at Basal (green), PBS (violet), and PHE (blue), PHE treated animals had significant increases in Ejection Fraction (EF), left ventricular wall thickness (LV Wall,d), with decreases in left ventricular chamber diameter (LVID). **D.** Diastolic phenotype quantification PHE group had significantly increased E/A and -E/e' ratios, indicative of diastolic dysfunction) (n= 30 mice/group, ****$p<0.0001$, One Way ANOVA for systolic and diastolic measurements) **E.** PHE treated group had a significantly increased heart weight/body weight ratio (HW/BW) (n= 30 mice/group, ****$p<0.0001$, Welch's t test).

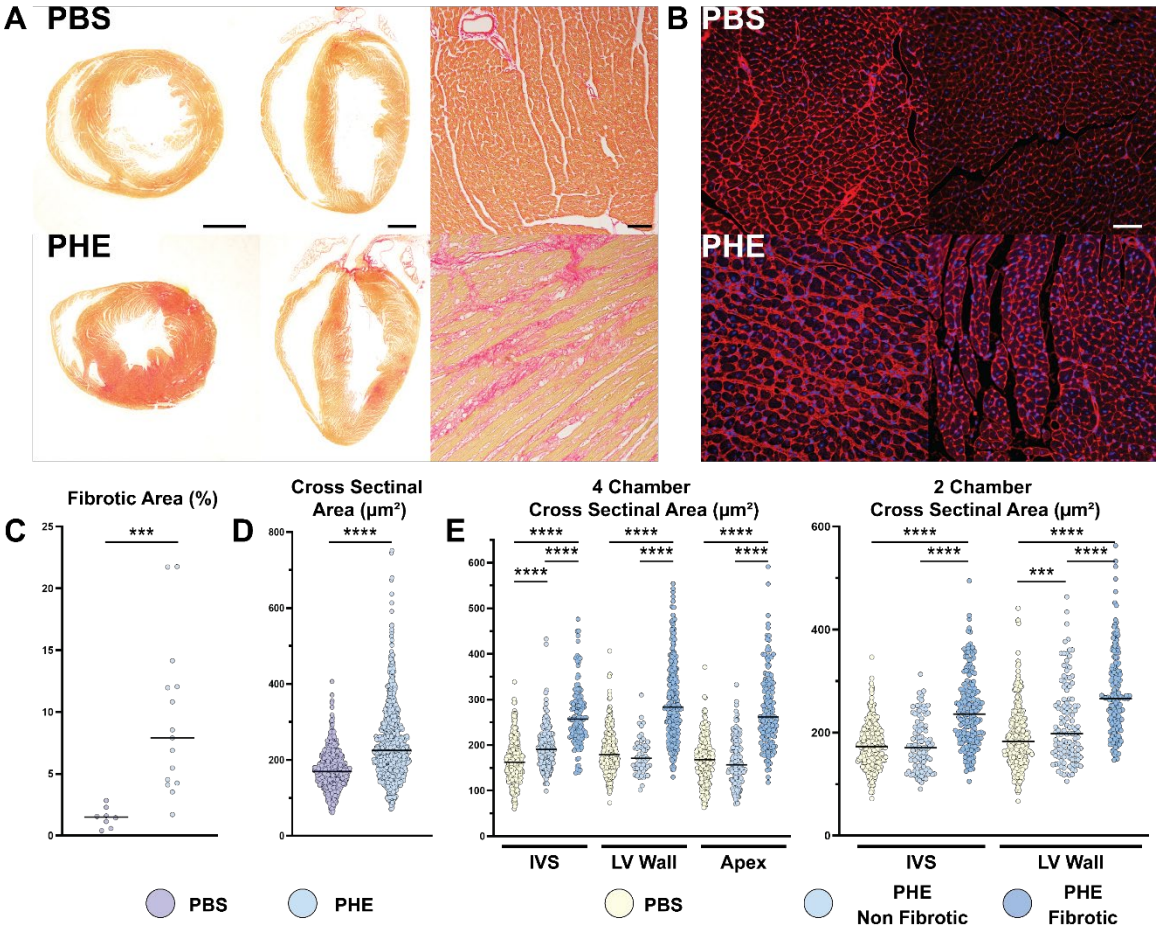

Figure 4-3. PHE Induced Cardiac Tissue and Cellular Remodeling. A. Picro Sirius staining of PBS and PHE cardiac tissue sections. Transverse (far left, scale = 1mm)) and coronal (middle, scale = 1mm) sections of PHE show thickened interventricular septum, LV wall, and apex (coronal only). PHE show increased localized fibrotic deposition (right, scale = 50 µm) (n= 4 PBS, 7 PHE). **B.** Representative fluorescent microscope imaging of wheat germ agglutin (WGA) stained cardiac tissue. PHE show localized increased WGA density (scale = 50 µm). **C.** Whole tissue fibrotic area quantification (analysis with FibroSoft), PHE (blue) demonstrating significantly increased fibrotic area compared to PBS (violet) (n=8 PBS, 15 PHE, ***p=0.0002, Welch's t test). **D.** Cardiomyocyte cross-sectional area measured via WGA staining. PHE induced significantly increased

cardiomyocyte area (n=5 visual fields per animal(4 PBS, 7 PHE), total of 900 cardiomyocytes measured/group, ****p<0.001, Welch's t test). **E.** Cardiomyocytes analyzed in D were further characterized by fibrotic environment (PBS, PHE non fibrotic, and PHE fibrotic) and location of the visual field (4 chamber coronal section: Interventricular septum (IVS), Left Ventricular Wall (LV Wall), and Apex, 2 chamber transverse section: IVS and LV wall). Cardiomyocytes in fibrotic areas were significantly larger than PBS and PHE non fibrotic areas regardless of cardiac landmark (n=4 PBS, 7 PHE , ***p<0.001, ****p<0.001, analysis done with ImageJ).

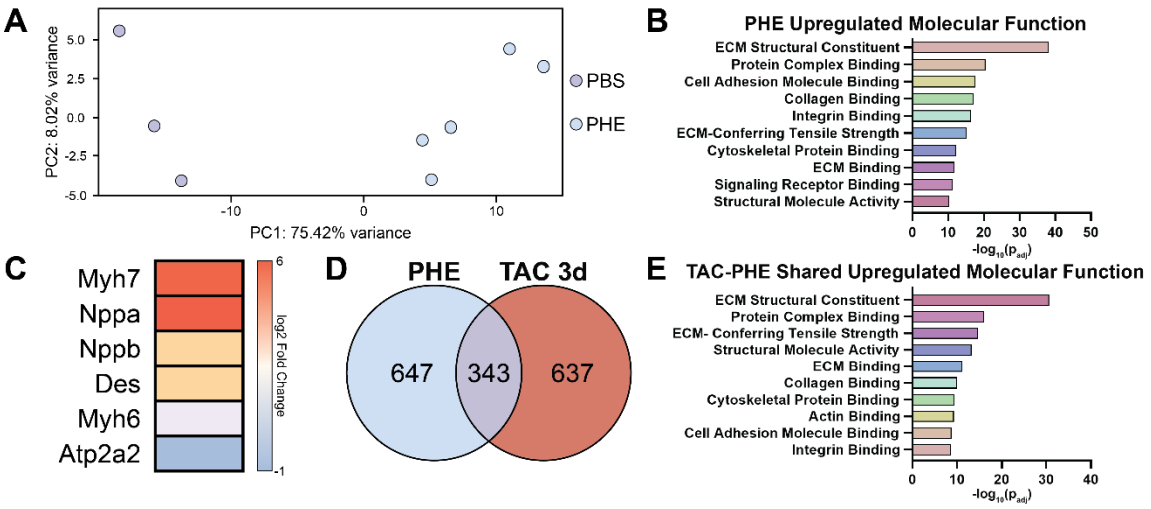

Figure 4-4. PHE RNA-seq Transcriptomics of Isolated Cardiomyocytes. A. PCA plot of PBS (violet) and PHE (blue) samples. Each dot represents an individual sample of isolated cardiomyocytes, showing clear separation. **B.** g profiler Molecular Function analysis of PHE group significantly upregulated genes (log_2 fold change > 0.6), showing a transcriptomic profile of genes mediating and reacting to fibrotic and stiffness induced changes in cellular environment. **C.** Hypertrophic fetal gene program gene heat map, demonstrating well characterized hypertrophic gene response via acute PHE. **D.** Acute PHE transcriptomic venn diagram with early compensatory mechanisms underlying the early transcriptomic response of cardiomyocytes to TAC surgery (3day time point, upregulated genes, log_2 fold change > 0.6). **D.** g Profiler Molecular Function of shared upregulate genes between TAC 3d and PHE show similar enrichment in early fibrotic response.

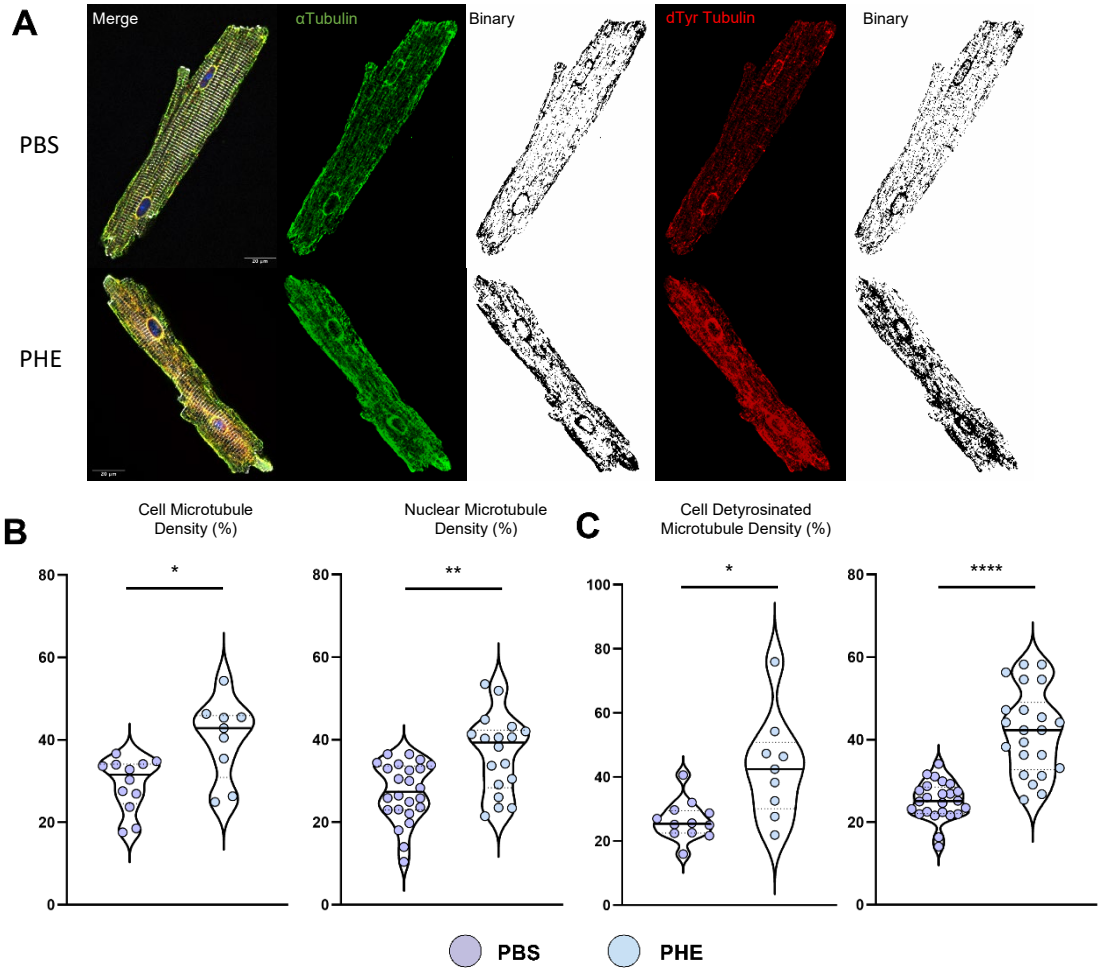

Figure 4-5. Hypertrophic Cardiomyocyte Microtubule Network Reinforcement. A. Confocal z-stack (4 μm merge around the nuclear planes) imaging of the microtubule network in PBS (top) and PHE (bottom) isolated cardiomyocytes. Images were processed for standardized thresholds and binary images were analyzed for microtubule density **B.** αTubulin density compared to total cell area, PHE (blue) showed moderate increase in whole cell αTubulin density compared to PBS (violet), with a more significant increase in nuclear localized αTubulin density **C.** Detyrosinated tubulin, a stiffer, post-translationally modified αTubulin quantification showed similar results, increased total cellular density

with a larger increase in nuclear density (n =2/group, 12 cells analyzed for PBS, 9 for PHE, *p=0.01, **p=0.001, Welch's t test).

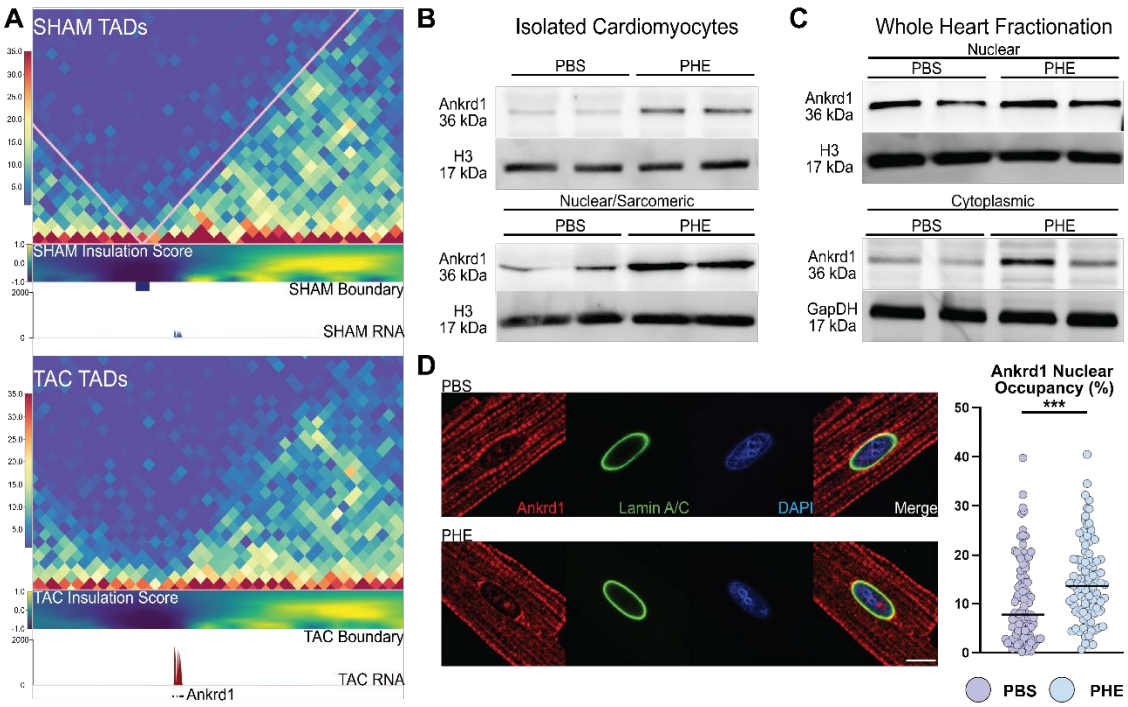

Figure 4-6. Ankrd1 Nuclear Localization in Hypertrophic Cardiomyocytes. A. MELTRON analysis of published Hi-C data at 300 Mbp resolution centered on the Ankrd1 locus of SHAM (top) and TAC (bottom) cardiomyocytes. The local chromatin environment is substantially altered upon TAC, with a loss of the TAD boundary seen in SHAM (where the triangles meet and the blue Boundary boxes are located) and the insulation score decreases (shown my decreased yellow color in the TAC) and the region around the Ankrd1 locus have decreased contact scores (denoted by less intense red color). This indicates that the DNA-DNA contacts around the Ankrd1 locus are diminished, decondensing the region for increased transcription upon hypertrophic stimuli. **B.** Western blots of isolated cardiomyocytes (top) and sub-cellular fractionated (bottom). Whole cell cardiomyocyte fractions show modest increases in Ankrd1 protein levels and that is localized to the nuclear/sarcomeric region (myofibril sarcomeric contamination in nuclear fraction). **C.** Whole heart fractionation of nuclear (top) and cytoplasmic (bottom) protein

quantity. Ankrd1, in whole heart protein fractionation lysates, are enriched in the nuclear fraction. **D.** Confocal microscopy of Ankrd1 in PBS (top) and PHE (bottom) isolated cardiomyocytes. Nuclear occupancy was determined by using Lamin A/C staining as the nuclear area and thresholding Ankrd1 to determine percentage of nuclear occupancy, quantified on the right graph, PHE (blue) had significantly more Ankrd1 nuclear occupancy than PBS (violet) (n=3/group, 50 cells (100 nuclei) analyzed per group, ***p=0.007, Welch's t test).

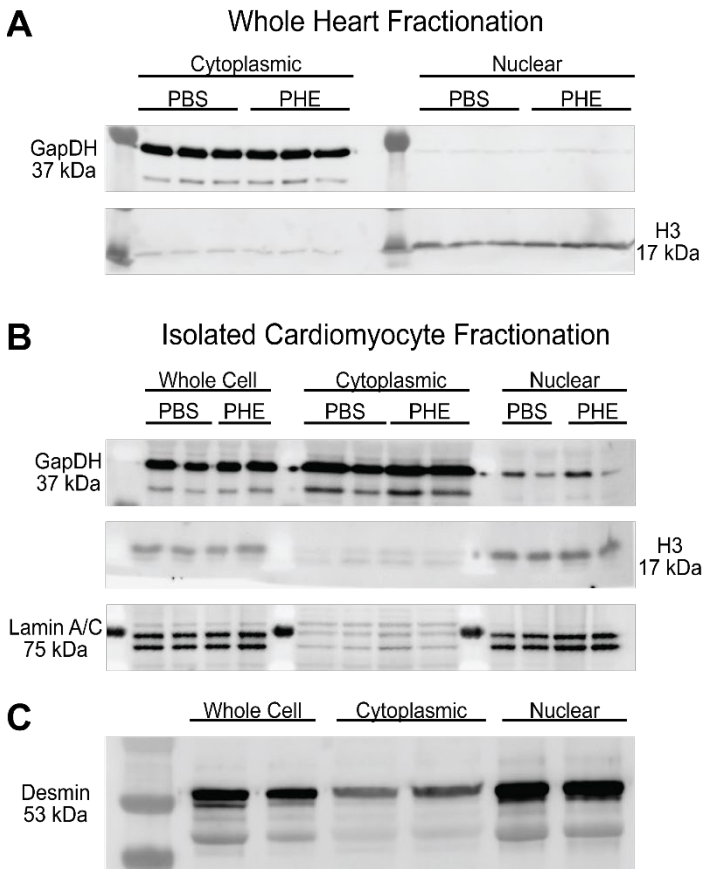

Figure 4-7. Whole Heart and Isolated Cardiomyocyte Protein Fractionation. A. Whole heart tissue fractionation, cytoplasmic (left) and nuclear fractions (right) were probed for fraction specific proteins, GapDH and H3, respectively. GapDH was primarily in the cytoplasmic fraction and H3 was primarily observed in the nuclear fraction. **B.** Fractionation of isolated cardiomyocytes, separated into whole cell, cytoplasmic and nuclear fractions. Membranes were probed for cytoplasmic GapDH and nuclear H3 and Lamin A/C. Fractionation shows GapDH in the whole cell and cytoplasmic fractions and H3 and Lamin A/C in the nuclear fractions. **C.** Whole cell, cytoplasmic, and nuclear fractions were probed for sarcomeric intermediate filament protein desmin to confirm nuclear and sarcomeric separation. However, desmin was observably enriched in the nuclear fraction, signifying nuclear fraction contained sarcomeric proteins.

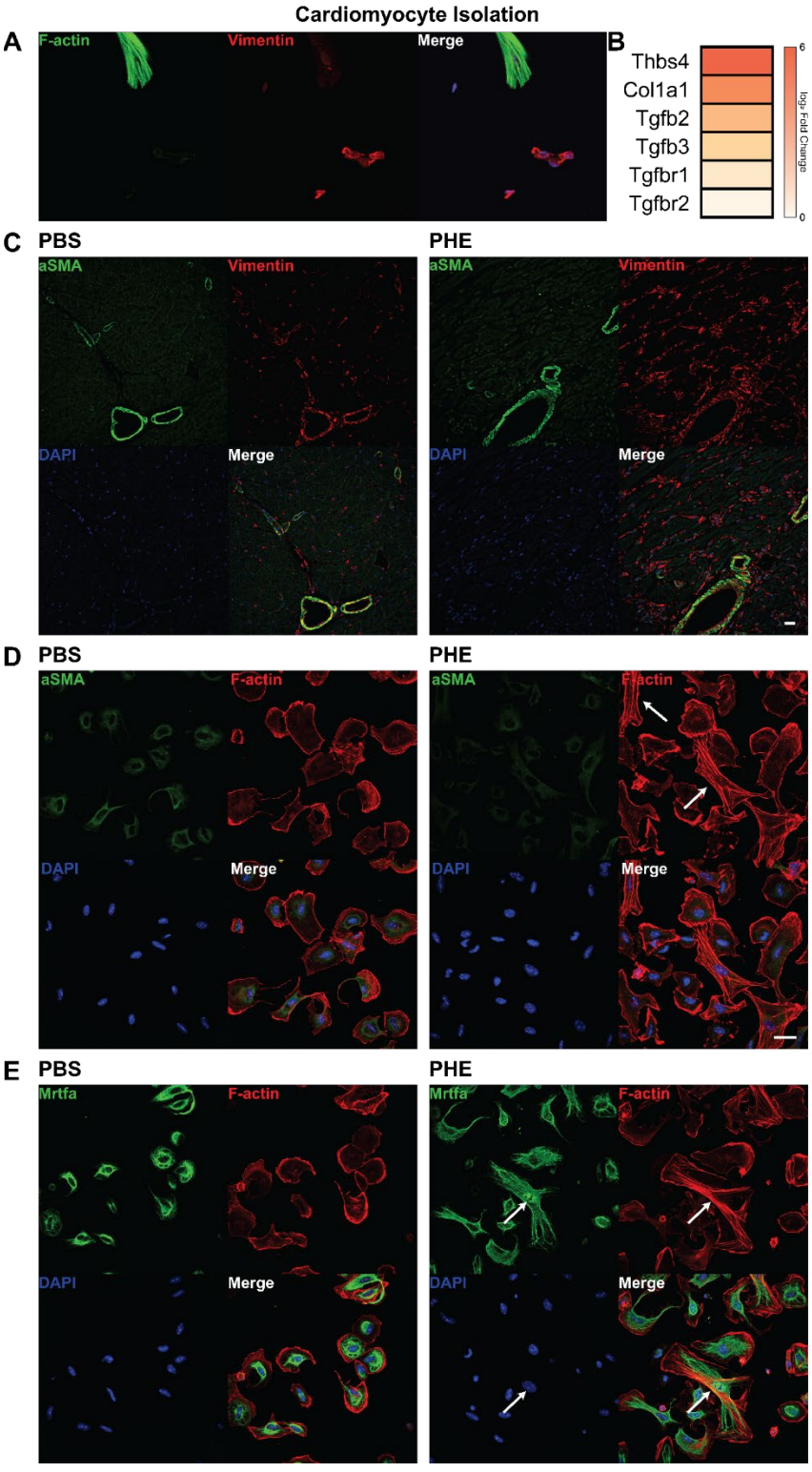
Cardiomyocyte Isolation
A
F-actin
Vimentin
Merge
B
Thbs4
Col1a1
Tgfb2
Tgfb3
Tgfbr1
Tgfbr2
log2 Fold Change
6
0
C
PBS
PHE
aSMA
Vimentin
DAPI
Merge
D
PBS
PHE
aSMA
F-actin
DAPI
Merge
E
PBS
PHE
Mrtfa
F-actin
DAPI
Merge

Figure 4-8. Fibrotic Response to Acute PHE Induce Hypertrophy. A. Cardiomyocyte isolation and staining for fibroblast specific marker Vimentin demonstrated fibroblast contamination in the cardiomyocyte isolation method. **B.** PHE RNA-seq heat map of fibroblast activation markers and signaling mechanisms for fibroblast activation. **C.** Confocal microscopy of whole tissue IHF for activated fibroblasts via positive α smooth muscle actin (αSMA, green) staining. PBS (left) and PHE (right) demonstrated positive αSMA staining around the vasculature (smooth muscle cells) but was absent in vimentin positive (red) interstitial fibroblasts. Vimentin positive fibroblasts occupied a much larger cellular density in PHE than PBS (scale = 25 μm). **D.** Isolated fibroblasts from PHE (right) were not positive for αSMA (same as PBS), but demonstrated increased F-actin stress fibers (red, marked by white arrows, scale = 25 μm). **E.** Absent of αSMA positive fibroblasts, but with PHE induced fibroblast proliferation and F-actin stress fibers (red), mechanosensitive Mrtfa (green), which translocates to the nucleus upon fibroblast exiting the quiescent state, was assessed. In PHE (right) Mrtfa was found in the nucleus (white arrow), this was not contingent on F-actin stress fiber formation.

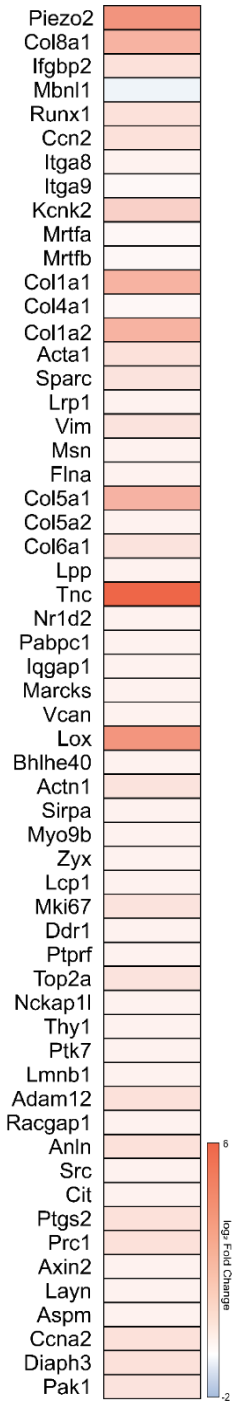
Piezo2
Col8a1
Ifgbp2
Mbnl1
Runx1
Ccn2
Itga8
Itga9
Kcnk2
Mrtfa
Mrtfb
Col1a1
Col4a1
Col1a2
Acta1
Sparc
Lrp1
Vim
Msn
Flna
Col5a1
Col5a2
Col6a1
Lpp
Tnc
Nr1d2
Pabpc1
Iqgap1
Marcks
Vcan
Lox
Bhlhe40
Actn1
Sirpa
Myo9b
Zyx
Lcp1
Mki67
Ddr1
Ptprf
Top2a
Nckap1l
Thy1
Ptk7
Lmnb1
Adam12
Racgap1
Anln
Src
Cit
Ptgs2
Prc1
Axin2
Layn
Aspm
Ccna2
Diaph3
Pak1
log2 Fold Change
2
-2

Figure 4-9. Mechanosensitive PHE Induced Gene Expression. Heat map of mechanosensitive genes mined by comparing the upregulated PHE RNA-seq data set with known mechanosensitive gene lists (Mechanome project and pre-printed data sets).

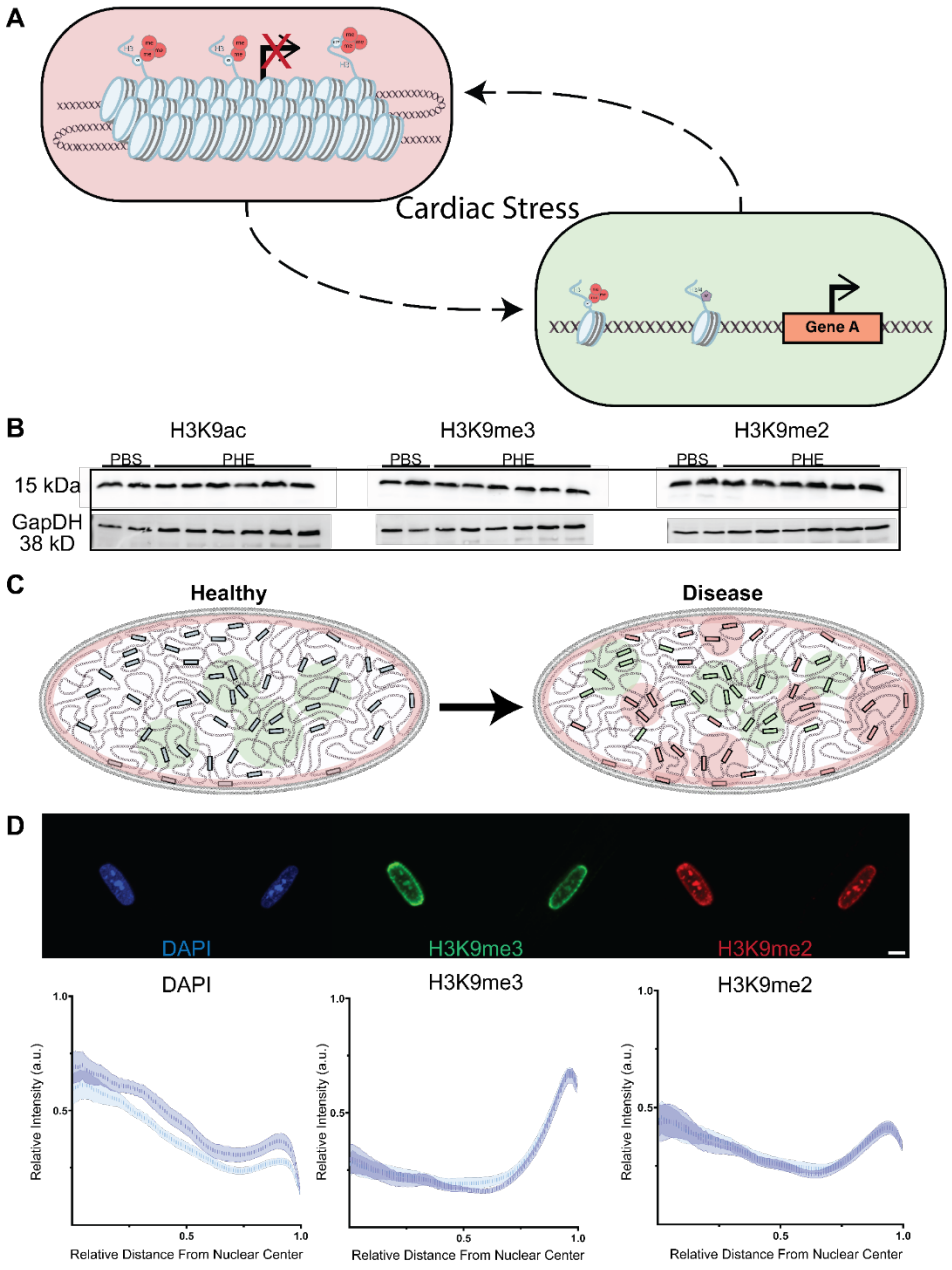

Figure 4-10. Acute PHE Does Not Alter Histone Post-Translational Modification Global Abundance or Localization. A. Schematic of the hypothesis that there are global switches of heterochromatic regions (red section, with H3K9me2 and H3K9me3) and euchromatic regions (green, H3K4me3 and H3/4K27ac) upon cardiac stress. **B.** Western blot of isolated cardiomyocytes for Histone post-translational modifications, showing no

observable differences between PBS and PHE. **C.** Schematic of the hypothesis that while global changes were not seen, it may be localized movement of chromatic regions, specifically heterochromatic regions (red) to the nuclear interior. **D.** Confocal imaging of DAPI, H3K9me3, and H3K9me2 of PBS and PHE group isolated cardiomyocytes. Quantification of nuclear localization of markers relative to the nuclear center graphed below (Matlab), no marker showed signs of differential localization.

Gene Name	Log_2 Fold Change	p_{adj}
Piezo2	3.834974	2.09E-29
Col8a1	3.288341	2.19E-34
Igfbp7	1.41956	5.77E-08
Mbnl1	-0.00381	0.979136
Ccn2	2.08322	1.07E-20
Itga8	1.232081	0.071361
Itga9	0.482265	0.023255
Kcnk2	1.442495	4.47E-05
Mrtfa	0.502297	0.056458
Mrtfb	0.287369	0.001485
Col1a1	3.427714	9.36E-39
Col4a1	0.676045	0.002157
Col1a2	3.118814	1.64E-31
Acta1	2.086904	5.84E-18
Sparc	1.486713	7.52E-08
Lrp1	0.809693	0.000868
Vim	1.419216	9.09E-10
Msn	0.742926	6.68E-09
Flna	0.728155	0.045314
Col5a1	2.014571	3.33E-17
Col6a1	1.664007	8.38E-11
Lpp	0.606378	5.10E-06
Tnc	6.385759	5.18E-47
Nr1d2	0.673675	1.05E-05
Pabpc1	0.600063	0.000289
Iqgap1	0.825655	0.000357
Marcks	0.715806	0.024775
Vcan	1.198296	7.62E-05
Lox	4.171236	1.48E-57
Bhlhe40	0.632706	0.000169
Actn1	1.324838	1.12E-19
Sirpa	0.644633	6.05E-08
Myo9b	0.738058	2.63E-09
Zyx	0.604703	0.000322
Lcp1	0.792906	0.0033
Mki67	1.784565	1.97E-06
Ddr1	0.680039	0.000432
Ptprf	0.664766	1.59E-07
Top2a	1.669348	3.72E-05
Nckap1l	0.977009	4.15E-05
Thy1	0.812199	0.028165
Ptk7	1.214081	5.31E-09

Table 4-1. RNA-seq Results of PHE-Activated Mechanosensitive Genes

Lmnb1	0.637471	0.032661
Adam12	1.987098	1.20E-08
Racgap1	1.117509	7.54E-06
Anln	2.12535	6.95E-15
Src	0.643653	0.001174
Cit	1.23443	4.64E-05
Ptgs2	2.197294	7.83E-06
Prc1	2.183378	7.19E-08
Axin2	0.644352	0.006154
Layn	0.943818	6.13E-05
Aspm	1.507107	6.25E-05
Ccna2	1.94687	3.68E-06
Diaph3	1.949731	1.97E-05
Pak1	1.534	1.47E-05

Table 4-1 (continued). RNA-seq Results of PHE-Activated Mechanosensitive Genes

Chapter 4 Bibliography

1 Kehat, I. & Molkentin, J. D. Molecular pathways underlying cardiac remodeling during pathophysiological stimulation. *Circulation* **122**, 2727-2735, doi:10.1161/CIRCULATIONAHA.110.942268 (2010).

2 Munch, J. & Abdelilah-Seyfried, S. Sensing and Responding of Cardiomyocytes to Changes of Tissue Stiffness in the Diseased Heart. *Front Cell Dev Biol* **9**, 642840, doi:10.3389/fcell.2021.642840 (2021).

3 Scarborough, E. A. *et al.* Microtubules orchestrate local translation to enable cardiac growth. *Nat Commun* **12**, 1547, doi:10.1038/s41467-021-21685-4 (2021).

4 Chapski, D. J. *et al.* Early adaptive chromatin remodeling events precede pathologic phenotypes and are reinforced in the failing heart. *J Mol Cell Cardiol* **160**, 73-86, doi:10.1016/j.yjmcc.2021.07.002 (2021).

5 Heineke, J. & Molkentin, J. D. Regulation of cardiac hypertrophy by intracellular signalling pathways. *Nat Rev Mol Cell Biol* **7**, 589-600, doi:10.1038/nrm1983 (2006).

6 Hieda, M. *et al.* Increased Myocardial Stiffness in Patients With High-Risk Left Ventricular Hypertrophy: The Hallmark of Stage-B Heart Failure With Preserved Ejection Fraction. *Circulation* **141**, 115-123, doi:10.1161/CIRCULATIONAHA.119.040332 (2020).

7 Hall, C., Gehmlich, K., Denning, C. & Pavlovic, D. Complex Relationship Between Cardiac Fibroblasts and Cardiomyocytes in Health and Disease. *J Am Heart Assoc* **10**, e019338, doi:10.1161/JAHA.120.019338 (2021).

8 Yamamoto, K. *et al.* Myocardial stiffness is determined by ventricular fibrosis, but not by compensatory or excessive hypertrophy in hypertensive heart. *Cardiovasc Res* **55**, 76-82, doi:10.1016/s0008-6363(02)00341-3 (2002).

9 Makarenko, I. *et al.* Passive stiffness changes caused by upregulation of compliant titin isoforms in human dilated cardiomyopathy hearts. *Circ Res* **95**, 708-716, doi:10.1161/01.RES.0000143901.37063.2f (2004).

10 LeWinter, M. M. Titin isoforms in heart failure: are there benefits to supersizing? *Circulation* **110**, 109-111, doi:10.1161/01.CIR.0000137284.17083.93 (2004).

11 Lyon, R. C., Zanella, F., Omens, J. H. & Sheikh, F. Mechanotransduction in cardiac hypertrophy and failure. *Circ Res* **116**, 1462-1476, doi:10.1161/CIRCRESAHA.116.304937 (2015).

12 Moulik, M. *et al.* ANKRD1, the gene encoding cardiac ankyrin repeat protein, is a novel dilated cardiomyopathy gene. *J Am Coll Cardiol* **54**, 325-333, doi:10.1016/j.jacc.2009.02.076 (2009).

13 Zhong, L. *et al.* Targeted inhibition of ANKRD1 disrupts sarcomeric ERK-GATA4 signal transduction and abrogates phenylephrine-induced cardiomyocyte hypertrophy. *Cardiovasc Res* **106**, 261-271, doi:10.1093/cvr/cvv108 (2015).

14 Remes, A. *et al.* Adapted clustering method for generic analysis of histological fibrosis staining as an open source tool. *Sci Rep* **13**, 4389, doi:10.1038/s41598-023-30196-9 (2023).

15 O'Connell, T. D., Rodrigo, M. C. & Simpson, P. C. Isolation and culture of adult mouse cardiac myocytes. *Methods Mol Biol* **357**, 271-296, doi:10.1385/1-59745-214-9:271 (2007).

16 Patro, R., Duggal, G., Love, M. I., Irizarry, R. A. & Kingsford, C. Salmon provides fast and bias-aware quantification of transcript expression. *Nat Methods* **14**, 417-419, doi:10.1038/nmeth.4197 (2017).

17 Yates, A. D. *et al.* Ensembl 2020. *Nucleic Acids Res* **48**, D682-D688, doi:10.1093/nar/gkz966 (2020).

18 Soneson, C., Love, M. I. & Robinson, M. D. Differential analyses for RNA-seq: transcript-level estimates improve gene-level inferences. *F1000Res* **4**, 1521, doi:10.12688/f1000research.7563.2 (2015).

19 Love, M. I., Huber, W. & Anders, S. Moderated estimation of fold change and dispersion for RNA-seq data with DESeq2. *Genome Biol* **15**, 550, doi:10.1186/s13059-014-0550-8 (2014).

20 Raudvere, U. *et al.* g:Profiler: a web server for functional enrichment analysis and conversions of gene lists (2019 update). *Nucleic Acids Res* **47**, W191-W198, doi:10.1093/nar/gkz369 (2019).

21 Seelbinder, B. *et al.* Nuclear deformation guides chromatin reorganization in cardiac development and disease. *Nat Biomed Eng* **5**, 1500-1516, doi:10.1038/s41551-021-00823-9 (2021).

22 Monte, E. *et al.* Systems proteomics of cardiac chromatin identifies nucleolin as a regulator of growth and cellular plasticity in cardiomyocytes. *Am J Physiol Heart Circ Physiol* **305**, H1624-1638, doi:10.1152/ajpheart.00529.2013 (2013).

23 Rosa-Garrido, M. *et al.* High-Resolution Mapping of Chromatin Conformation in Cardiac Myocytes Reveals Structural Remodeling of the Epigenome in Heart Failure. *Circulation* **136**, 1613-1625, doi:10.1161/CIRCULATIONAHA.117.029430 (2017).

24 Winick-Ng, W. *et al.* Cell-type specialization is encoded by specific chromatin topologies. *Nature* **599**, 684-691, doi:10.1038/s41586-021-04081-2 (2021).

25 Rolfe, M., McLeod, L. E., Pratt, P. F. & Proud, C. G. Activation of protein synthesis in cardiomyocytes by the hypertrophic agent phenylephrine requires the activation of ERK and involves phosphorylation of tuberous sclerosis complex 2 (TSC2). *Biochem J* **388**, 973-984, doi:10.1042/BJ20041888 (2005).

26 Mitter, S. S., Shah, S. J. & Thomas, J. D. A Test in Context: E/A and E/e' to Assess Diastolic Dysfunction and LV Filling Pressure. *J Am Coll Cardiol* **69**, 1451-1464, doi:10.1016/j.jacc.2016.12.037 (2017).

27 Cazorla, O. *et al.* Differential expression of cardiac titin isoforms and modulation of cellular stiffness. *Circ Res* **86**, 59-67, doi:10.1161/01.res.86.1.59 (2000).

28 Linke, W. A. & Hamdani, N. Gigantic business: titin properties and function through thick and thin. *Circ Res* **114**, 1052-1068, doi:10.1161/CIRCRESAHA.114.301286 (2014).

29 Herwig, M. *et al.* Modulation of Titin-Based Stiffness in Hypertrophic Cardiomyopathy via Protein Kinase D. *Front Physiol* **11**, 240, doi:10.3389/fphys.2020.00240 (2020).

30 Robison, P. *et al.* Detyrosinated microtubules buckle and bear load in contracting cardiomyocytes. *Science* **352**, aaf0659, doi:10.1126/science.aaf0659 (2016).

31 Chen, C. Y. *et al.* Suppression of detyrosinated microtubules improves cardiomyocyte function in human heart failure. *Nat Med* **24**, 1225-1233, doi:10.1038/s41591-018-0046-2 (2018).

32 LeWinter, M. M. & Granzier, H. Cardiac titin: a multifunctional giant. *Circulation* **121**, 2137-2145, doi:10.1161/CIRCULATIONAHA.109.860171 (2010).

33 Raskin, A. *et al.* A novel mechanism involving four-and-a-half LIM domain protein-1 and extracellular signal-regulated kinase-2 regulates titin phosphorylation and mechanics. *J Biol Chem* **287**, 29273-29284, doi:10.1074/jbc.M112.372839 (2012).

34 Ling, S. S. M., Chen, Y. T., Wang, J., Richards, A. M. & Liew, O. W. Ankyrin Repeat Domain 1 Protein: A Functionally Pleiotropic Protein with Cardiac Biomarker Potential. *Int J Mol Sci* **18**, doi:10.3390/ijms18071362 (2017).

35 Jeyaseelan, R. *et al.* A novel cardiac-restricted target for doxorubicin. CARP, a nuclear modulator of gene expression in cardiac progenitor cells and cardiomyocytes. *J Biol Chem* **272**, 22800-22808, doi:10.1074/jbc.272.36.22800 (1997).

36 Kojic, S. *et al.* A novel role for cardiac ankyrin repeat protein Ankrd1/CARP as a co-activator of the p53 tumor suppressor protein. *Arch Biochem Biophys* **502**, 60-67, doi:10.1016/j.abb.2010.06.029 (2010).

37 Miller, M. K. *et al.* The muscle ankyrin repeat proteins: CARP, ankrd2/Arpp and DARP as a family of titin filament-based stress response molecules. *J Mol Biol* **333**, 951-964, doi:10.1016/j.jmb.2003.09.012 (2003).

38 Song, Y. *et al.* Cardiac ankyrin repeat protein attenuates cardiac hypertrophy by inhibition of ERK1/2 and TGF-beta signaling pathways. *PLoS One* **7**, e50436, doi:10.1371/journal.pone.0050436 (2012).

39 Zhang, N. *et al.* Cardiac ankyrin repeat protein contributes to dilated cardiomyopathy and heart failure. *FASEB J* **35**, e21488, doi:10.1096/fj.201902802RR (2021).

40 Bang, M. L. *et al.* The muscle ankyrin repeat proteins CARP, Ankrd2, and DARP are not essential for normal cardiac development and function at basal conditions and in response to pressure overload. *PLoS One* **9**, e93638, doi:10.1371/journal.pone.0093638 (2014).

41 Wang, J. *et al.* Phenylephrine promotes cardiac fibroblast proliferation through calcineurin-NFAT pathway. *Front Biosci (Landmark Ed)* **21**, 502-513, doi:10.2741/4405 (2016).

42 Fu, X. *et al.* Specialized fibroblast differentiated states underlie scar formation in the infarcted mouse heart. *J Clin Invest* **128**, 2127-2143, doi:10.1172/JCI98215 (2018).

43 Small, E. M. *et al.* Myocardin-related transcription factor-a controls myofibroblast activation and fibrosis in response to myocardial infarction. *Circ Res* **107**, 294-304, doi:10.1161/CIRCRESAHA.110.223172 (2010).

44 Nava, M. M. *et al.* Heterochromatin-Driven Nuclear Softening Protects the Genome against Mechanical Stress-Induced Damage. *Cell* **181**, 800-817 e822, doi:10.1016/j.cell.2020.03.052 (2020).

45 Patten, R. D. & Hall-Porter, M. R. Small animal models of heart failure: development of novel therapies, past and present. *Circ Heart Fail* **2**, 138-144, doi:10.1161/CIRCHEARTFAILURE.108.839761 (2009).

46 Zolk, O. *et al.* Cardiac ankyrin repeat protein, a negative regulator of cardiac gene expression, is augmented in human heart failure. *Biochem Biophys Res Commun* **293**, 1377-1382, doi:10.1016/S0006-291X(02)00387-X (2002).

47 Kempton, A. *et al.* Altered regulation of cardiac ankyrin repeat protein in heart failure. *Heliyon* **4**, e00514, doi:10.1016/j.heliyon.2018.e00514 (2018).

48 Wei, Y. J. *et al.* Upregulated expression of cardiac ankyrin repeat protein in human failing hearts due to arrhythmogenic right ventricular cardiomyopathy. *Eur J Heart Fail* **11**, 559-566, doi:10.1093/eurjhf/hfp049 (2009).

49 Bisping, E. *et al.* Gata4 is required for maintenance of postnatal cardiac function and protection from pressure overload-induced heart failure. *Proc Natl Acad Sci U S A* **103**, 14471-14476, doi:10.1073/pnas.0602543103 (2006).

50 Almodovar-Garcia, K., Kwon, M., Samaras, S. E. & Davidson, J. M. ANKRD1 acts as a transcriptional repressor of MMP13 via the AP-1 site. *Mol Cell Biol* **34**, 1500-1511, doi:10.1128/MCB.01357-13 (2014).

51 Borbely, A. *et al.* Hypophosphorylation of the Stiff N2B titin isoform raises cardiomyocyte resting tension in failing human myocardium. *Circ Res* **104**, 780-786, doi:10.1161/CIRCRESAHA.108.193326 (2009).

52 Wang, X. & Robbins, J. Proteasomal and lysosomal protein degradation and heart disease. *J Mol Cell Cardiol* **71**, 16-24, doi:10.1016/j.yjmcc.2013.11.006 (2014).

53 Ren, Z. *et al.* Single-Cell Reconstruction of Progression Trajectory Reveals Intervention Principles in Pathological Cardiac Hypertrophy. *Circulation* **141**, 1704-1719, doi:10.1161/CIRCULATIONAHA.119.043053 (2020).

54 Bretherton, R. *et al.* Correcting dilated cardiomyopathy with fibroblast-targeted p38 deficiency. bioRxiv. doi: https://doi.org/10.1101/2023.01.23.523684 (2023)

FUTURE DIRECTIONS

The experiments, ideas, and investigation in this dissertation took years of thought and are simply laying the groundwork for further exploration into mechanosensitive mechanisms driving cardiac function and disease. Throughout this work, the focus has been forces outside the nucleus that upon disease phenotypes, directly affect gene transcription. What forces are felt at the nuclear level? The clear connection between sarcomeric organizing proteins to the nucleoskeleton to chromatin through the LINC complex[1] show the nucloskeletal structure is vital for force transmission.[2] In cardiomyocytes, the peripheral bound chromatin, bound at LADs, is a highly controlled mechanism, as mutations in Lamin A/C in iPSC-CMs minimally altered chromatin topological architecture and gene expression.[3] While cardiomyocyte chromatin may not be as responsive to changes in forces as other more plastic cell types (fibroblasts), the gene expression profile activated early in disease, which then perpetuates as time and heart disease progresses, suggests a chromatin, or gene expression memory.[4] Through the TAC model, we have detailed this early gene response, before a pathological phenotype, however, this timepoint coincides with the necessity of increased force generation to overcome increased afterload. It is my view that this is where mechanotransduction pathways and cardiac disease progression intersect. The question remains of which mechanosensors become initially activated and are sufficient to promote the pathological gene program and how they contribute to disease progression. The assumption would be, as many molecular mechanisms tend to be in cardiac disease, they serve to initially compensate for the new workload, yet overtime contribute to the maladaptive remodeling.

In our models of cardiac disease, the remodeling of the cardiac tissue during concentric hypertrophy involves two processes, increased sarcomeric protein production and organization for cardiomyocyte growth and fibrosis.[5] While there are other areas of the cardiomyocyte that are mechanosensitive hubs[6], the I-band region of the sarcomere remains of interest. The passive stiffness table setter titin[7] and the mechanosensing proteins bound to it, including transcriptional regulator Ankrd1.[8] The question remains in the PHE model: is the hypertrophic process causing a change in titin isoforms to make the cardiomyocyte stiffer and does a changing of isoforms dislocate Ankrd1 to become more of a gene regulator? Titin isoform N2BA:N2B ratios are decreased in dilated cardiomyopathies,[9] and this has been speculated to influence the mechanosensation of the fibroblast population. Fibroblasts have long been used as surrogates to identify mechanosensitive mechanism[10] because they are incredibly sensitive to environmental changes, and their response often contributes to disease progression. The interplay between cardiac fibroblast stress response and the cardiomyocyte hypertrophic mechanosignaling mechanisms are the crux of understanding disease progressions in heart failure.

The goal of this project was to connect cardiomyocyte cytoskeletal and nucleoskeletal organization to chromatin architecture in cardiac hypertrophy. Going into this project, the RNA-seq and chromatin capture data set allowed to take an inside of the nucleus to outside approach, identifying gene expression that restructured the cardiomyocyte nuclear lamin. The second half of my work, starting in Chapter 4, takes the opposite approach, and to me is the most exciting. Characterizing molecules and pathways that are first responders to changes in cardiac workload and identifying those

that influence pathological gene expression prior to a phenotype will lead to future mechanosensitive biomarkers of cardiac disease.

FUTURE DIRECTIONS: BIBLIOGRAPHY

1 Stroud, M. J., Banerjee, I., Veevers, J. & Chen, J. Linker of nucleoskeleton and cytoskeleton complex proteins in cardiac structure, function, and disease. *Circ Res* **114**, 538-548, doi:10.1161/CIRCRESAHA.114.301236 (2014).

2 Lombardi, M. L. *et al.* The interaction between nesprins and sun proteins at the nuclear envelope is critical for force transmission between the nucleus and cytoskeleton. *J Biol Chem* **286**, 26743-26753, doi:10.1074/jbc.M111.233700 (2011).

3 Bertero, A. *et al.* Chromatin compartment dynamics in a haploinsufficient model of cardiac laminopathy. *J Cell Biol* **218**, 2919-2944, doi:10.1083/jcb.201902117 (2019).

4 Chapski, D. J. *et al.* Early adaptive chromatin remodeling events precede pathologic phenotypes and are reinforced in the failing heart. *J Mol Cell Cardiol* **160**, 73-86, doi:10.1016/j.yjmcc.2021.07.002 (2021).

5 Rosa-Garrido, M. *et al.* High-Resolution Mapping of Chromatin Conformation in Cardiac Myocytes Reveals Structural Remodeling of the Epigenome in Heart Failure. *Circulation* **136**, 1613-1625, doi:10.1161/CIRCULATIONAHA.117.029430 (2017).

6 Lyon, R. C., Zanella, F., Omens, J. H. & Sheikh, F. Mechanotransduction in cardiac hypertrophy and failure. *Circ Res* **116**, 1462-1476, doi:10.1161/CIRCRESAHA.116.304937 (2015).

7 Herwig, M. *et al.* Modulation of Titin-Based Stiffness in Hypertrophic Cardiomyopathy via Protein Kinase D. *Front Physiol* **11**, 240, doi:10.3389/fphys.2020.00240 (2020).

8 Kojic, S. *et al.* A novel role for cardiac ankyrin repeat protein Ankrd1/CARP as a co-activator of the p53 tumor suppressor protein. *Arch Biochem Biophys* **502**, 60-67, doi:10.1016/j.abb.2010.06.029 (2010).

9 Borbely, A. *et al.* Hypophosphorylation of the Stiff N2B titin isoform raises cardiomyocyte resting tension in failing human myocardium. *Circ Res* **104**, 780-786, doi:10.1161/CIRCRESAHA.108.193326 (2009).

10 Walker, C. J. *et al.* Author Correction: Nuclear mechanosensing drives chromatin remodelling in persistently activated fibroblasts. *Nat Biomed Eng* **5**, 1517-1518, doi:10.1038/s41551-021-00748-3 (2021).